Probabilistic Estimation of River Discharge Considering Channel Characteristics Uncertainty with Particle Filters

by

Yeonsu KIM

2013

Probabilistic Estimation of River Discharge Considering Uncertain Channel Characteristics with Particle Filters

by

Yeonsu KIM

A dissertation submitted in partial fulfillment of the requirement

for the degree of Doctor of Philosophy

Dept. of Civil and Earth Resources Engineering

Kyoto University, Japan

2013

Abstract

A probabilistic approach is introduced to a 2D dynamic wave model to deal with the uncertain characteristics of a river channel. As a probabilistic approach, particle filters, which perform the sequential Monte Carlo (SMC) estimation based on a point mass representation of probability densities within Bayesian theorem, are introduced. Among the various uncertain factors, the inflow to the upstream end and Manning roughness coefficient are chosen to construct particles to consider all feasible conditions which induces significant errors in flood forecasting and estimation.

In addition, the proposed method provides an alternative to establish a rating curve. A simple rating curve, which is fitted to finite measured discharge and water stages at few locations within the rivers reach, is generally utilized for calculating discharge, but many efforts for continuous updating of the rating curve are required to reflect the continuous change of channel geomorphology and the vegetation distribution. Thus the proposed method can serve as the alternative because it considers the change of vegetation distribution by aerial photo and channel geomorphology.

Chapter 2 reviews this basic framework to combine a 2D dynamic wave model with particle filters and theoretical basis of the framework.

Chapter 3 proposes a short term prediction algorithm of water level based on the basic framework. At first, it is validated with a synthetic experiment. The synthetic experiment makes it possible to confirm the method without any exogenous disturbances using the artificial true values generated from a simulation. Then the prediction algorithm is applied to the Katsura River, located in Kyoto, Japan. With the sequentially updated water level at the upstream end, the given rating curve is corrected, and the composite Manning roughness coefficient is estimated. Based on the estimated results at every hour, short term water stage prediction is implemented. The prediction results are compared with the observed discharge and water stage. The 2D dynamic

wave model reflects well the variations of the water stage in the estimates of a flood event, and the water stage estimation results show good agreement with the observed one.

In terms of predicted water stage, a limitation of the method was found that a gap between the predicted water stage and the observed water stage became larger according to the increase in leading time. The reason why the gap is occurred is because it is assumed that the Manning roughness coefficient is uniform over the calculation domain and changes according to water level. Thus large errors have to be incorporated into the Manning roughness coefficient of each particle to track the Manning roughness coefficient changing according to water level. The large errors caused the uncertainties of predicted discharge and water stage.

Chapter 4 improves the limitations of Chapter 3 by considering the spatial distribution of the Manning roughness coefficient on the calculation domain and by introducing a variance reduction factor in the noise evolution equation. The calculation domain is separated into three sections: main channel, floodplain, and vegetation area, which are identified by the aerial photo. Then the noise scale is determined from the calculation of the variation at previous time step. The improved two factors could enhance the estimation capability, and show good reproducibility of other events as well.

Chapter 5 reviews the availability of the method with the hydrologic model's outputs to other catchment areas. Furthermore, it is utilized to estimate the peak discharge of the partially gauged flood event occurred in the Kumano River located in Japan in 2011. The sequential applications of the estimation method with hydrologic outputs are implemented to the previous three historic flood events to quantify the uncertainties of the Manning roughness coefficient of the subject river channel. Based on the optimized range of Manning's *n*, the ensemble simulations are implemented to estimate the largest peak discharge of the 2011 flood using the discharge estimated by a

hydrological model for the upper boundary condition. The possible range of the largest peak discharge was successfully evaluated through the comparison of the observed flood marks. Finally, a rating curve established by the estimation results at the Ouga station is examined.

Chapter 6 enhances the treatments of the upper boundary conditions used in the previous chapters. An upstream boundary condition is generated from an existing uncertain rating curve in chapters 3 and 4 and from a hydrologic model in chapter 5. These approaches involves limitations in applications to actual flood events because the measured discharge data is generally not enough to establish a rating curve, and the locations, where the rating curve is available, are also limited. Thus, the index exponent of a rating curve following a power function and Manning roughness coefficient are approximated with particle filters and a 2D dynamic wave model. for the sakes of extracting the reasonable values for whole time water stage from the results of particle filters, smoothing is implemented based on trajectory tracking in reverse time direction. The smoothing provides the rating curve within a reasonable range, and it shows good agreement with the observed data.

Declaration of authorship

I declare that this dissertation titled 'Probabilistic Estimation of River Discharge Considering Channel Characteristics Uncertainty with Particle Filters' is my own and has been generated by me as the result of my own original research. I confirm that this work was done wholly or mainly while in candidature for a research degree at Kyoto University. Any part of this dissertation has not been submitted for a degree or any other qualification at any other University or institution, and it has been clearly stated.

Yeonsu KIM

Acknowledgement

First of all, I would like to gratefully and sincerely thank Prof. Michiharu Shiiba, Prof. Yasuto Tachikawa, Prof. Kaoru Takara, Prof. Takashi Hosoda Hososa, and Dr. Sunmin Kim for their support, guidance, understanding and patience during my PhD course in Kyoto University. Without them and all who were around me, this dissertation would not have been completed.

These studies in this dissertation were carried out under the full-time PhD course in Hydrology and Water Resources Research Laboratory, Kyoto University, Japan. This dissertation has been more improved by the committee members, Prof. Kaoru Takara, Prof. Takashi Hosoda, and Prof. Yasuto Tachikawa. I really appreciate the committee members again for their valuable comments and guidance.

My supervisors, Prof. Michiharu Shiiba and Prof. Yasuto Tachikawa, showed me an attitude as a professor and a researcher by themselves, which always helped to wake me up inside. I have been really happy to have studied with my supervisors since October, 2010.

Then, I would like to express my deepest gratitude to Dr. Sunmin Kim, Prof. Kazuaki Yorozu, My seniors, Dr. Seong Jin Noh and Dr. Hyeonuk An for their valuable comments, scientific discussion, and technical support.

Next, I also thank my laboratory member and Ms. Iwasa. They help me kindly, and their help was so valuable to adjust to living in Japan. Moreover, I want to say that I could enjoy the life in Japan thanks to my friends, Dr. Hayeong Jung, Dr. Pedro Luiz Borges Chaffe, Dr. Maja Ostric, Dr. Duong Duc Toan and Dr. Supattana Wichakul.

After that, I was extraordinarily fortunate to meet Prof. Kwan Sue Jung as a supervisor in Chungnam national university, Korea. I could learn many things from his lessons and discussions. Then I also appreciate my seniors and juniors in Chungnam national university, Korea: Prof. Giha Lee, Prof. Chang Lae Jang, Dr. Jeong Yup Kim, Dr. Yongjung Choi, Daejin Jung, Jungsu Bok, Dr. Seung Soo Lee, Wansik Yu, Young A Shin, and Eunbi Kang.

Finally, I would like to thank my family for their love, support, and understanding during my life.

In addition, I could finish this course work thanks to the financial support from Japanese Government (Monbukagakusho: MEXT) Scholarship and from HSE program and GCOE program in Kyoto University.

Contents

List of figures

List of tables

Chapter 1. Introduction

1.1 Objectives of research

Discharge data is a prerequisite for most of the hydrologic analysis, and it is utilized for many purposes, including flood forecasting, water resource management, hydraulic structure design, and hydrologic parameter calibration. In spite of the many uses, it is generally converted from the water stage and the simple rating curve, which is established from fitting to the finite measured discharge samples. Thus, the uncertainties of the discharge estimated by a rating curve are quite large, as pointed out by Pelletier (1987) and Di Baldassarre and Montanari (2009). Moreover, a river flow is influenced by the conditions of the river channel. Thus the change of the channel geomorphology and vegetation distribution has to be considered to maintain the accuracy of discharge data.

In this respect, hydraulic simulations with various conditions have advantages in considering the feasible conditions, and sequential updating of the simulations makes it possible to reflect the change of conditions within a river channel. Therefore, particle filters are introduced to a 2D dynamic wave model. The main objectives of this thesis are as follows:

1) To develop a method to estimate river discharge and Manning roughness coefficient probabilistically by introducing a 2D dynamic wave model and particle filters.

2) To devise an appropriate noise generator based on the evaluation of noise scale and preliminary knowledge about open channels for the sake of drawing approximate distributions of inflow at upstream end and Manning roughness coefficient when implementing the proposed method.

3) To establish or adjust a rating curve based on the simulated discharge from the proposed method considering the change of conditions within a river channel with assessing the uncertainties of the rating curve.

4) To enhance the water stage predictability based on the updated Manning roughness coefficient of the subject river channel and the reasonable discharge information to improve the fundamental error sources of hydrologic parameters in flood forecasting system.

6) To confirm the applicability of the method to various types of open channels.

The features of each objective are closely related to each other and to the improvement of flood forecasting through improving discharge prediction by the establishment and/or correction of a rating curve for the calibration of hydrologic parameters and improving flood stage prediction by channel roughness estimation.

1.2 Background

Recurring floods are one of the most frequently occurring natural disasters (ARDC, 2002). To prevent and reduce the damage caused by floods, flood forecasting, which forecasts the flow rates or water levels for an interval period ranging from a few hours to days ahead based on a rainfall-runoff model and a flood routing model, is required. Although the models provide important information about floods, hydrologic modeling includes many uncertainties because of measurements, parameters, and structural uncertainties (Noh 2012; Smith et al., 2008). Among the various factors induced the uncertainties of hydrological prediction and/or estimation, the discharge data at the basin outlet generally play a key role in confirming the performance of the hydrologic modeling and calibrating the parameters of a hydrologic model.

A rating curve is a convenient tool in estimating discharge, so it is generally utilized by the inputs of a flood routing model, the reference data for the design of water-control

and conveyance structures, the basic data to estimate sediment volume, and the data for hydrologic parameter calibrations. Despite the numerous uses for the data, most hydrologists have realized that discharge data involves significant uncertainties. For example, Pelletier (1987) showed that the discharge estimated by a simple rating curve varies in the range from 8% to 20%, at the 95% confidence interval, and Di Baldassarre and Montanari (2009) showed that the discharge errors are from 6.2% to 42.8%, at the 95% confidence interval. In addition, even the studies related to the improvement and uncertainties assessment of a rating curve is able to be performed at certain locations where both of the measured discharge and water stage were available.

1.2.1 Uncertainty in flood routing

The uncertainties of the rating curve transfer to the hydrologic outputs (Tillaart, 2010). Then a flood routing model utilizes the both of the rating curve and the hydrologic outputs. Thus it is inevitable that the predicted discharge or water stage by the flood routing model include many uncertainties.

In addition, the Manning roughness coefficient represented by the uncertain characteristics of the river channel is another uncertain factor in flood routing. The Manning roughness coefficient estimated from the simple Manning equation using the measured discharge and cross sectional information or investigating bed materials of river bed involved errors and it is affected from vegetation distribution, bed material, bed forms, and so on (Chow, 1959; Barnes, 1967; Coon, 1998).

As described above, the Manning roughness coefficient and inflow remain as uncertain factors in utilizing a flood routing model.

1.2.2 Past research to assess uncertainty in flood routing

To improve uncertainties of Manning roughness coefficient, a hydraulic simulation

introduced with the calibration method using the water stage data and the measured discharge (Fread, 1989). Then it is showed that the predictability of water stages could be enhanced with the improvement of channel roughness (Ding et al., 2006; Hsu et al., 2006).

To deal with the discharge uncertainties, two types of studies have been done. One is focused on improving the rating curve directly (Schmidt 2002; Reitan and Petersen-Øverleir 2008; Reitan and Petersen-Øverleir 2009; Petersen-Øverleir 2004, 2005). The approaches, such as the dynamic rating curve (Jones 1916; Dottori et al. 2009; Reitan and Petersen-Øverleir, 2011), the multi-segment rating curve (Reitan and Petersen-Øverleir 2009), and the uncertainties analysis are implemented, but it requires much effort and a large budget. Moreover, the studies are limited to places where discharge and water stages are available.

Another study utilizes hydraulic simulation (Onda et al. 2006; Hosoda et al. 2008, 2010; Di Baldassarre and Montanari 2009; Domeneghetti, 2012). Onda et al. (2006) and Hosoda et al. (2008, 2010) derived the equation to estimate the boundary conditions at both ends from the Method of Characteristics (MOC) and reconstructed the hydrograph using the hydrograph located in the middle of the reach, but the time terms included in the equation limited the applications, as pointed out by Hosoda et al. (2010).

Unlike the difficulties in obtaining the discharge data, the water stage data is continuously measured, and the accuracy of the water stage data is better than the discharge data. Aricò et al. (2009) considered the uncertainties of inflow and channel roughness simultaneously with several cases. The numerical simulation approaches were only performed within the limited range because of the equifinality problem occurring in estimating the simultaneous inflow and channel roughness by the upstream water stage. As pointed out by Schmidt (2002), numerical flow simulation was not feasible for representing the open channel flow with only the given number of potential conditions and parameters particular to a certain site. In addition, the open channel flow is affected

by various factors, such as channel geomorphology, hydraulic structures, vegetation, and so on.

The alternatives are to consider various feasible conditions and to introduce appropriate constraints and control theory for the massive calculation of various conditions. Recent development of a measuring system and the calculation ability of the computer are providing solutions for the alternatives. First, aerial photos, channel geomorphology, and water stages became easy-to-use data, so we were able to identify the status of the river reach, like vegetation, and the hydraulic structure of the river reach using the aerial photo. We got information about the approximate discharge with the water stage and channel geomorphology because we were able to estimate roughly the flow volume. A massive calculation is possible with the parallelizing by Open-MP or Open-MPI with the development of the computer. Thus, the Monte Carlo method, which requires massive calculations, is extensively utilized.

In hydrologic modeling, a sequential Monte Carlo method has already been introduced to improve the uncertainties of the parameters and enhance the flood predictability (Noh 2012; Vrugt et al. 2008; Moradkhani et al. 2005). In hydraulic modeling, it has been introduced to estimate the discharge and to enhance the predictability of water stages, using a remote sensing-derived water stage and data assimilation scheme (Montanari et al. 2009; Matgen et al. 2010; Giustarini et al. 2011). However, they could not consider the various conditions of the river channel due to the inaccuracy of water stage data and the 1-dimensional model. Tachikawa et al. (2011) showed that the predictability of the river channel is improved with data assimilation, consideration of the various conditions, and the 1-dimensional dynamic wave model. Ricci et al. (2011) improved the inflow using the Kalman filter and hydraulic modeling. Tachikawa et al. (2011) and Di Baldassarre and Montanari (2009) pointed out that at least a 2-dimensional model is required to represent the channel geomorphologic effects and to utilize the water stage to update data. As described before, the sequential Monte Carlo method is one of the methods that improve flood predictability, and it is appropriate for

estimating discharge because the river channel continuously is evolving and the rating curve of the locations where water stages are available have to be updated continuously.

1.3 Outline of thesis

This thesis consists of 7 chapters, and each chapter is based on the basic framework utilizing 2D dynamic wave model and PFs. Thus the different simulation conditions and characteristics are briefly summarized in Table 1-1.

Chapter 2 reviews this basic framework to combine a 2D dynamic wave model with particle filters and theoretical basis of the framework.

Chapter 3 proposes a short term prediction algorithm of water level based on the basic framework. At first, it is validated with a synthetic experiment. The synthetic experiment makes it possible to confirm the method without any exogenous disturbances using the artificial true values generated from a simulation. Then the prediction algorithm is applied to the Katsura River, located in Kyoto, Japan. With the sequentially updated water level at the upstream end, the given rating curve are corrected, and the composite Manning roughness coefficient is estimated. Based on the estimated results at every hour, short term water stage prediction is implemented. The prediction results are compared with the observed discharge and water stage.

The 2D dynamic wave model reflects well the variations of the water stage in the estimates of a flood event, and the water stage estimation results show good agreement with the observed one. A limitation of the method was found that a gap between the predicted water stage and the observed water stage became larger according to the increase in leading time due to the uniform Manning roughness coefficient over the calculation domain. The uncertainties of Manning roughness coefficient has to be maintained to track the Manning roughness coefficient changing according to water level.

Chapter 4 improves the problems of Chapter 3 by considering the spatial distribution of the Manning roughness coefficient on the calculation domain and by introducing a variance reduction factor in the noise evolution equation. The calculation domain is separated into three sections: main channel, floodplain, and vegetation area, which are identified by the aerial photo. Then the noise scale is determined from the calculation of the variation at previous time step. Through the two factors could enhance the estimation capability, and show good reproducibility of other events as well.

This approach is implemented based on the given rating curve, so the applications are limited to the locations where both of discharge and water stage are available.

Chapter 5 reviews the availability of the method with the hydrologic model's outputs to other catchment areas to solve the limitations of Chapter 4. Furthermore, it is utilized to estimate the peak discharge of the partially gauged flood event occurred in the Kumano River located in Japan in 2011. The sequential applications of the estimation method with hydrologic outputs are implemented to the previous three historic flood events to quantify the uncertainties of the Manning roughness coefficient of the subject river channel. Based on the optimized range of Manning's n, the ensemble simulations are implemented to estimate the largest peak discharge of the 2011 flood using the discharge estimated by a hydrological model for the upper boundary condition. The possible range of the largest peak discharge was successfully evaluated through the comparison of the observed flood marks. Finally, a rating curve established by the estimation results at the Ouga station is examined.

Chapter 6 enhances the treatments of the upper boundary conditions used in the previous chapters. An upstream boundary condition is generated from an existing uncertain rating curve in chapters 3 and 4 and from a hydrologic model in chapter 5. These approaches involves limitations in applications to actual flood events because the measured discharge data is generally not enough to establish a rating curve, and the locations, where the rating curve is available, are also limited. Thus, the index exponent

of a rating curve following a power function and Manning roughness coefficient are approximated with particle filters and a 2D dynamic wave model. Then, to extract the reasonable values from the results of particle filters, smoothing is implemented based on trajectory tracking in reverse time direction. The smoothing provides the rating curve within a reasonable range, and it shows good agreement with the observed data.

Finally, Chapter 7 presents the conclusions.

Table 1-1 Different simulation conditions and characteristics in each chapter

	Chapter 3	**Chapter 4**	**Chapter 5**	**Chapter 6**
Classification of Manning's *n*	1	3	3	3
Reference discharge	Existing rating	Existing rating	Outputs of a hydrologic model	–
Influence factors to rating curve	Channel control	Channel control	Channel control	Section control + Channel control
Filter	SIR	SIR	SIR	Generic PFs (SIS+SIR) + Smoothing
Result	Prediction + estimation	Estimation	Estimation	Estimation

Chapter 2. Basic framework to combine a 2D dynamic wave model and particle filters

This chapter reviews the basic framework to combine a 2D dynamic wave model with particle filters. A mathematical system model is not perfect because it depicts only its characteristics of direct interest (Maybeck, 1982), so a deterministic simulation with pre-determined parameters and uncertain inputs occasionally cause errors in estimation or prediction. Thus it is necessary to control the inputs or parameters to enhance the outputs of the simulation. In this respect, a 2D dynamic wave model, which is able to reproduce flood events with consideration of channel geomorphology, vegetation distribution within the river channel, results in errors due to the uncertainties of input data, parameters and system. Thus particle filters, which have advantages in dealing with non-linear and non-Gaussian problems, are introduced to deal with uncertainties of them. In addition, the theoretical basis is of a 2D dynamic wave model and particle filters are reviewed.

2.1 Basic framework

The basic framework to combine a 2D dynamic wave model and particle filters is the basis of each chapter (Fig. 2-1). It consists of 2D dynamic wave model (Nagata, 2002) that reproduces a flood event considering the geomorphologic effects of a river channel and particle filters, which consider the uncertainties of non-linear and non-Gaussian problems. As shown in Fig. 2-1, the steps of the basic framework are as follows:

1) The framework is based on several assumptions: all errors are caused by only inputs, parameters, and observed data, and the initial stage of the simulation is in a steady flow condition.
2) Before starting with “stabilization step”, the boundary conditions and Manning roughness coefficient of each particle are disturbed independently. At “steady sim.” step, parallel of particles with various feasible conditions are implemented by multiple threads until the calculated flow condition of each particle reaches steady state conditions using MPI or Open-MP. The parallelizing and serializing locations in the flow chart are marked by a distributor ⊕ and connector ⊗, respectively in Fig. 2-1.
3) After finishing “steady sim.” step, the parallelized calculations are again serialized to update the upstream water stage at the connector ⓞ. With the updated water stage, the likelihood of each particle is calculated. According to the likelihood, the normalized weight of each particle is calculated.
4) At the “resampling” step, the lighter particles are removed, and the heavier particles are duplicated with some noise to avoid degeneracy of particles.
5) After finishing “stabilization step”, the calculated velocity, water depth, and so on in the calculation domain are transferred to the “main calculation step” at the connector Ⓐ.
6) Thus all particles include the different simulation conditions. Each particle is

calculated again within the boundary conditions of next time step.

7) From here, the same procedure with "Stabilization step" is repeated with time marching from t to t+1.

Through the whole procedure, the approximate distributions of inflow and the Manning roughness coefficient of the objective river channel are calculated.

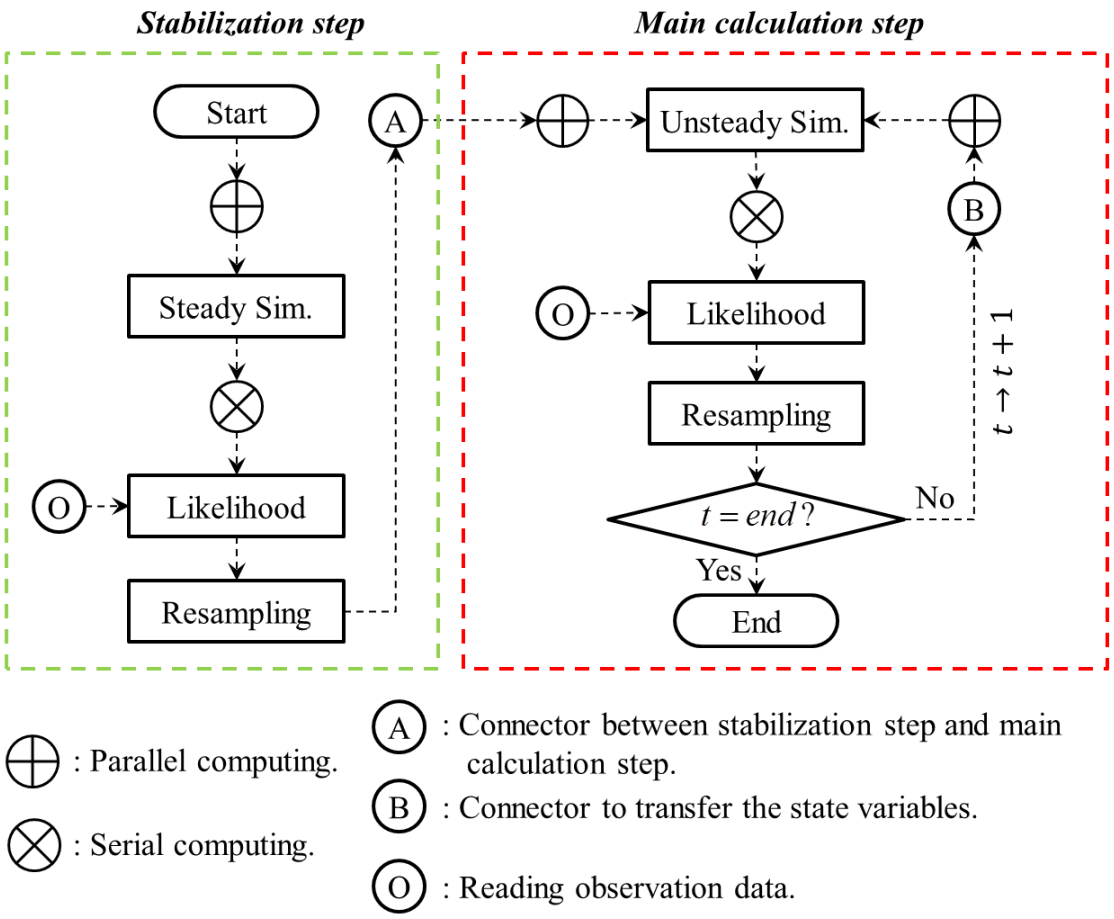

Figure 2-1 Flow chart of the basic framework.

2.2 2D dynamic wave model

The 2D dynamic wave model (Nagata, 2002) consisted of a continuity equation and a momentum equation as follows:

$$\frac{\partial h}{\partial t}+\frac{\partial M}{\partial x}+\frac{\partial N}{\partial y}=0 \tag{2-1}$$

$$\frac{\partial M}{\partial t}+\frac{\partial uM}{\partial x}+\frac{\partial vM}{\partial y}=-gh\frac{\partial z_s}{\partial x}-\frac{\tau_{bx}}{\rho}+\frac{\partial}{\partial x}\left(-\overline{u'^2}h\right)+\frac{\partial}{\partial y}\left(-\overline{u'v'}h\right) \tag{2-2}$$

$$\frac{\partial N}{\partial t}+\frac{\partial uN}{\partial x}+\frac{\partial vN}{\partial y}=-gh\frac{\partial z_s}{\partial x}-\frac{\tau_{by}}{\rho}+\frac{\partial}{\partial x}\left(-\overline{u'v'}h\right)+\frac{\partial}{\partial y}\left(-\overline{v'^2}h\right) \tag{2-3}$$

where h is water depth, M and N represent discharge fluxes in the x-direction and the y-direction, respectively. u and v are average velocities of the x-direction and the y-direction, respectively. τ_{bx} and τ_{by} are the bed shear stresses, ρ is water density, and g is gravity. $\overline{u'^2}$, $\overline{v'^2}$ and $\overline{u'v'}$ are the depth averaged Reynolds stress on $x-y$ coordinate. The depth averaged Reynolds stress was calculated as follows:

$$-\overline{u'^2}=2D_h\left(\frac{\partial u}{\partial x}\right)-\frac{2}{3}k \tag{2-4}$$

$$-\overline{u'v'}=D_h\left(\frac{\partial u}{\partial y}+\frac{\partial v}{\partial x}\right) \tag{2-5}$$

$$-\overline{v'^2}=2D_h\left(\frac{\partial v}{\partial y}\right)-\frac{2}{3}k \tag{2-6}$$

$$D_h=\alpha h u_* \tag{2-7}$$

where D_h is the eddy viscosity coefficient. Then k is depth-averaged turbulence energy. α is the constant number. u_* is the friction velocity ($u_*=\sqrt{\tau/\rho}$).

k is determined by the empirical equation proposed by Nezu and Nakagawa (1993) as follows:

$$\frac{k}{u_*^2} = 4.78 \exp\left(-2\frac{z}{h}\right) \tag{2-8}$$

where z is the water depth from the bottom($z = 0$) to water surface($z = h$).

The equation was integrated against the water depth as follows:

$$k = 2.09 u_*^2 \tag{2-9}$$

The shear stress was converted by the Manning's equation as follows:

$$\tau_{bx} = \frac{\rho g n^2 u \sqrt{u^2 + v^2}}{h^{1/3}} \tag{2-10}$$

$$\tau_{by} = \frac{\rho g n^2 v \sqrt{u^2 + v^2}}{h^{1/3}} \tag{2-11}$$

where n is the relative roughness.

The equations were numerically solved using Finite Volume Method (FVM) on a structure grid. In dealing with the convection term, the simple first-order upwind scheme was utilized. Then, the Adams-Bashforth method was introduced for the time integration.

2.3 Particle filters

Particle filters (PFs) performed the sequential Monte Carlo (SMC) estimation based on a point mass representation of probability densities within Bayesian theorem (Ristic et al., 2004). The sequential process of particles in time using the nonlinear model is preceded up to the next available measurement (Salamon and Feyen, 2010). Among various implementations of the PFs, this study introduces the Sequential Importance Resampling (SIR) method to reflect current state more similarly as time passes. We briefly reviewed the state space model for a nonlinear system, the typical method (Sequential Importance Sampling (SIS) method), and the selected SIR method in sequence. Then, the sampling constraints were described.

2.3.1 State space model for non-linear system

A non-linear system can be represented using the state equation and the observation equation as follows:

$$x_t = f(x_{t-1}, v_t) \tag{2-12}$$

$$Z_t = g(x_t, w_t) \tag{2-13}$$

where the functions f and g represent the state equation and the observation equation, respectively. The state variable(x_t) evolves with noise(v_t) based on the state equation. v_t and w_t indicate process noise and observation noise, respectively.

The state variable can be represented as a set of samples (“particles”) at time(t), and each particle consists of a variable and a weight that define the contribution of the particle. Eqs. (2-12) and (2-13) can be represented by probability as follows:

$$p(x_t|x_{t-1}) \tag{2-14}$$

$$p(Z_t|x_t) \tag{2-15}$$

According to Bayes theorem and the Markovian property, the posterior density ($p(x_t|Z_t)$) can be estimated from the likelihood ($p(z_t|x_t)$) and the prior density ($p(x_t|x_{t-1})$) as follows:

$$p(x_t|Z_t) = \frac{p(z_t|x_t)}{p(z_t|Z_{t-1})} p(x_t|Z_{k-1}) \propto p(z_t|x_t)p(x_t|Z_{k-1}) \tag{2-16}$$

where the normalising constant($p(z_t|Z_{t-1})$) depends on the likelihood.

The optimal solution was introduced by the above posterior density, which represents the recursive propagation as time passes.

2.3.2 Sequential Importance Sampling(SIS) method

The SIS algorithm consists of the recursive propagation of the weights, and the process proceeded with the sequentially updated observation data (Arulampalam et al., 2002). Sampling from the state posterior density Eq. (2-17) was impossible, as pointed out by Doucet et al.(2000); therefore, the weights were normalised using. $\sum_{i=0}^{n} w_t^i = 1$. Then, the posterior density at time t can be approximated as follows:

$$p(X_t|Y_t) = \sum_{i=0}^{n} w_t^i \delta(X_t - X_t^i) \tag{2-17}$$

The weight, which is a discrete weighted approximation of the posterior density, was chosen using the principle of importance sampling (Arulampalam et al., 2002). If the sample (X_t^i) is drawn from an importance density ($q(X_t|Z_t)$), then the weight can be

represented as follows:

$$w_t^i \propto \frac{p\left(x_t^i|z_t\right)}{q\left(x_t^i|z_t\right)} \tag{2-18}$$

In terms of the sequential case $p(X_t|Z_t)$ for new samples were derived from approximations of $p\left(X_{t-1}\middle|Z_{t-1}\right)$ and measurement . If the importance density is chosen to factorise:

$$q\left(X_t|Z_t\right) = q\left(x_t|X_{t-1}, Z_t\right)q\left(X_{t-1}|Z_{t-1}\right) \tag{2-19}$$

Then the sample (X_t^i) can be obtained from the argument of the previous sample (X_{t-1}^i). Thus, the updated equation becomes (Ristic et al., 2004):

$$p\left(X_t|Z_t\right) \propto p\left(z_t|x_t\right)p\left(x_t|x_{t-1}\right)p\left(X_{t-1}|Z_{t-1}\right) \tag{2-20}$$

Using Eqs. (2-20) and (2-18), the weight was modified as follows:

$$w_t^i \propto w_{t-1}^i \frac{p\left(z_t\middle|x_t^i\right)p\left(x_t^i\middle|x_{t-1}^i\right)}{q\left(x_t^i\middle|X_{t-1}^i, Z_t\right)} \tag{2-21}$$

Finally, the posterior density ($p(x_t|Z_t)$) can be approximated as:

$$p\left(x_t\middle|Z_t\right) \approx \sum_{i=1}^{N} w_t^i \delta\left(x_k - x_k^i\right) \tag{2-22}$$

As N approaches infinity, the approximation approaches the true posterior density.

2.3.3 Sequential Importance Resampling (SIR) method

The SIR algorithm is one version of the PFs. It is derived from the typical SIS

algorithm by choosing the importance density to be the transitional prior density and performing the resampling for every time step (Ristic et al., 2004). The advantage of the SIR algorithm is that it avoids the degeneracy problem in the SIS algorithm. In addition, the evaluation of the importance weight and sampling from the importance density becomes easy. Then, resampling at every time step means that we did not need to calculate the importance weight from the current time step to the next time step and that the weights were given by the proportionality, as pointed out by Ristic et al. (2004).

$$w_t^i \propto p\left(Z_t \middle| x_t^i\right) \tag{2-23}$$

They state that the SIR algorithm can be inefficient and result in a rapid loss of diversity in particles. However, if a hidden target has no measurement data and changes sharply as time passes, adequate errors must be incorporated continuously. Moreover, a process with enough freedom with respect to the particles is helpful when considering the interrelationship between inflow, channel roughness, and water stage.

One of the important points is how to incorporate the errors in each particle because the abrupt change of each value of particles induced the errors in calculation. To avoid the problems, each value of particles is evolved from time *t* to *t*+1 like Fig. 2-2. Resampling at time *t* just duplicates the chosen particles according to weight. Then the a duplicated value at time *t* and a perturbed sample, which is incorporated some noise to a duplicated value at time *t*, at time *t*+1 are interpolated, and the interpolated value($v_{t+\Delta t}^i$) is applied to the calculation as Manning roughness coefficient and inflow like Eq. (2-24).

$$v_{t+\Delta t}^i = \frac{v_t^i - v_{t+1}^i}{\Delta t} \tag{2-24}$$

where, v_t^i indicates the duplicated value at time *t* of particle *i*; Δt means the time step utilized in the 2D dynamic wave model.

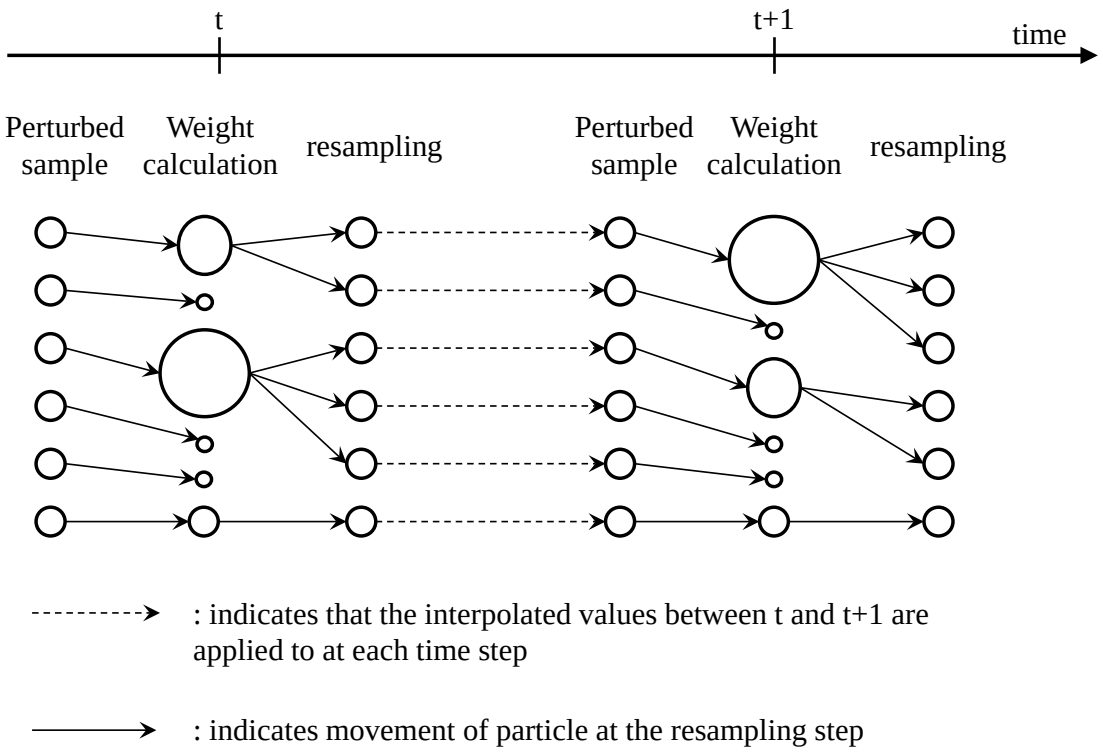

Figure 2-2 Schematic view of the evolved particles.

2.3.4 Likelihood calculation and perturbation method

The Gaussian likelihood of each particle was calculated against the observed water stage to reduce the variations resulting from the interaction between parameters and state variables.

$$w_t^i = p\left(Z_t \middle| x_t^i\right) = \frac{1}{\sigma\sqrt{2\pi}} e^{\frac{-\left(x_t^i - z_t\right)^2}{2\sigma^2}} \tag{2-25}$$

where σ is the standard deviation associated with the observed water stage(z_t), and x_t^i is the state variable that represents the simulated water stage at certain cross-sections within the result of particle i.

Then, the normalised weight was calculated by the likelihood as follows:

$$W_t^i = \frac{w_t^i}{\sum_{j=1}^{N} w_t^j} \tag{2-26}$$

where w_t^i indicates the likelihood of the i th particle at time t. W_t^i denotes the normalised weight of each particle at time t, and N represents the number of particles.

Each particle was resampled depending on its own normalized weight using the systematic resampling method, and noise was added to duplicated particles. This sequential updating procedure made it possible to consider the time-variant state variables and parameters with some constraints.

During the initial stage, the noise drawn from the uniform distribution was added to inflow and Manning's *n* because we do not have prior information about both of them. In the sequential updating stage, the perturbation method and the variance of the particles directly affect the accuracy of the results. Thus, the efficiency of the methodology is also related to the perturbation method. Reflecting previous experience of the changed pattern to improve accuracy and efficiency would be ideal, but the pattern of Manning's *n* is variable based on the river channel situation. The detailed descriptions of the perturbation method is in each chapter because it is continuously improved for the estimation of Manning's *n* and the inflow together causing equifinality problems against matching the water stage at every time step.

Chapter 3. Synthetic experiment with updating a rating curve and estimating Manning's *n*

This chapter focuses on two topics: one is to verify the developed method using a 2D dynamic wave model and particle filters through the synthetic experiment. Another is to investigate the applicability of the method to a short-term flood prediction with a real event. Then the contents are based on Kim et al. (2012(a)).

The method is designed to consider the uncertainties of inflow and channel roughness in an estimation process. Based on the estimated results, short term flood forecasting is implemented. At the estimation process, a hidden state variable (inflow) is continuously estimated by the sequentially updated observation (water stage at an upstream end) using particle filters. The estimation process is applied to the Katsura River located in Kyoto, Japan, and it was verified first through a synthetic experiment, which take advantages of uncertain measurements and parameters because we are able to assume true measurement and parameters for analyzing the proposed method. The synthetic experimental result shows that the algorithm successfully traces the hidden true values on a real-time basis. In addition, the prediction results were also compared with observed water stages.

3.1 Introduction

Flood forecasting is crucial information for mitigating and/or protecting the damages induced by flood to our properties and human lives. In general, a hydrological model is utilized to predict the volume and peak time of flood, based on a given rainfall information. Then, a hydraulic model calculates water stage profile for a specific river channel to provide more detailed flood information.

The most successful method of accurate flood forecasting may need precise rainfall information and a well-organized hydrologic model, as well as hydraulic models. However, it is not avoidable to suffer much erroneous forecasting information through a series of conversion, which is from rainfall to discharge and from discharge to water stage. Thus, we are still lacking in our forecasting methods, not only in accurate rainfall forecasting but also in proper hydrologic and hydraulic modeling.

Among many error sources of forecasting in the above mentioned processes, this study focuses on data assimilation into a hydraulic model to properly convert uncertain river discharge information into correct water stage information on a specific river channel. Generally, input data into a hydraulic model, such as inflow from the upper boundary, already include a certain amount of error, and additional system error that comes from a hydraulic model will be added during simulations. To avoid these conventional error sources, this study proposes a new method of hydraulic model utilization, which considers the input error, system error, and observation error using a recursive Monte Carlo simulation algorithm.

Real-time updating of model state variables has already been adopted in many researches with stochastic approaches like the Kalman filter and particle filters. Kalman filter is introduced into the 1D dynamic wave model to improve forecasting accuracy considering observed water stage and discharges (Shiiba et al., 2000). Hsu et al. (2006) showed that updating of the channel roughness coefficient during a simulation

considering observed water stage improves prediction capability, and a fixed channel roughness coefficient results in an inaccurate prediction. Discharge also includes uncertainties, as pointed out by Dottori et al. (2009) and Di Baldassarre and Montanari (2009) even observed that discharge data include many uncertainties. In addition, discharge data converted by a rating curve from observed water stages includes many uncertainties.

Aricò et al. (2009) presented a simultaneous estimation method for discharge and channel roughness, and proved that it is essential to consider heterogeneous channel roughness. It is obvious that channel roughness, inlet flow, and the interaction of these factors are critical items for accurate water stage estimation. A stochastic model or a real-time based calibration seems necessary for considering many errors during hydrologic and hydraulic model simulations.

Recent researches have introduced a new type of recursive updating scheme, called particle filters (PFs), into 1D hydraulic models to consider the non-linearity of system models (Montanari et al., 2009; Giustarini et al., 2011; Matgen et al., 2010). Tachikawa et al. (2011) also introduced PFs into the 1D hydraulic model, and they improved the predictability of water stages by using the sequentially updated water stages. However, the 1D model was not able to fully consider the geomorphologic characteristics of channel, and the tracking ability of water stage in their study was limited. In terms of the method incorporating noise, the conventional Kalman filter algorithm has limitations in its application to unknown non-normal variances in the state or observational equation (Bradely, 1992). However, PFs are applicable in the non-linear system without any Gaussian assumption.

In this chapter, we introduce an improved prediction algorithm that is based on a 2D dynamic wave model and particle filters considering input, parameters and observation errors. To verify the proposed algorithm, we tested our method on a short reach on the Katsura River in Kyoto, Japan. A 2D dynamic wave model is adopted in this study to

reproduce the relation of water stage, discharge, and parameters on a complex river bed more precisely. This chapter is composed of the following sections. Section 3-2 describes the proposed methodology. Section 3-3 explains about the particle filtering system. Then, the design of the synthetic experiment (Bentley, 1900) and the verification of the algorithm with a synthetic experiment are presented in section 3-4. Next, in section 3-5, we implement the performance analysis of the prediction method with a real event data. Finally, section 3-6 summarizes this chapter.

3.2 Methodology

3.2.1 Prediction algorithm

The prediction algorithm largely consists of a particle filtering system (estimation system) and a prediction system (Fig. 3-1). The prediction algorithm runs on results arrived at through an estimation process. As was presented in chapter 2-1, the estimation system, which is based on SIR algorithm and a 2D dynamic wave model, is composed of a perturbation step, an update simulation step, and a resampling step. First, a boundary condition, such as the upstream discharge, the downstream water stage, and model parameter values (channel roughness) are disturbed to consider their uncertainties at the perturbation step. Then, the state variables, which are calculated by the 2D dynamic wave model, and parameter values are sequentially updated in the resampling step according to the weight calculated in comparison with the sequentially updated water stage. Next, the state variables and parameter values are transferred to the prediction process to reflect the current state more accurately after the updating. The prediction process is calculated for up to 6 hours, with the updated state variables and parameter values every hour. The connection between the prediction system and the estimation system are represented by the connector Ⓒ in Fig. 3-1. Before implementing the prediction process, ensemble conditions are generated. Manning's roughness coefficient is fixed as the value chosen in the resampling step at the current time step, and

the predicted inlet flows up to 6 hours are determined by the proportions of the particle's inlet discharge against the given discharge at the current time step. Thus the prediction algorithm is rigorously a hindcast simulation to confirm the methodology.

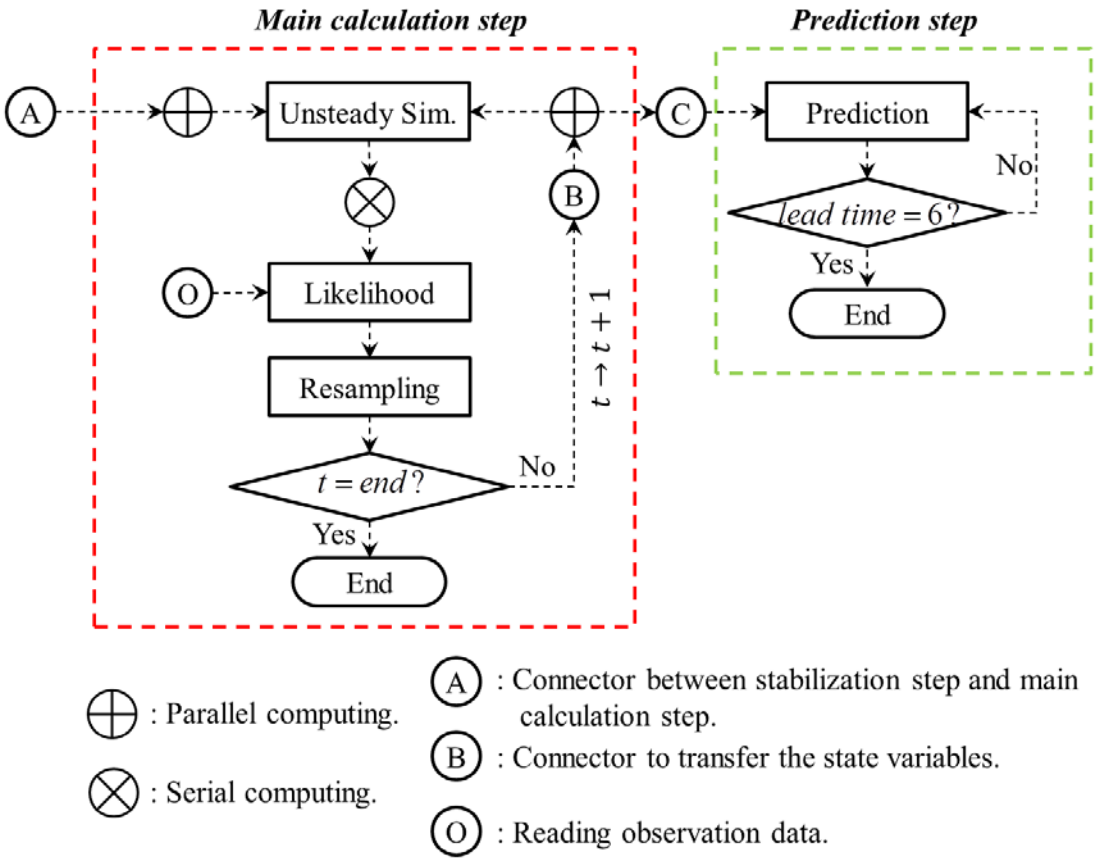

Figure 3-1 Water stage prediction algorithm.

3.2.2 Study area

The proposed method is applied the Katsura River located in Kyoto, Japan (Fig. 3-2). The watershed area is 1090 km^2 at the Hazukashi station. The targeted reach length is about 2km from Hazukashi station to Nosou station, and the calculation domain is composed of 500 structured grids (Fig. 3-3). There are two water stage stations at both ends without tributaries, so the characteristics of the reach are good for application of the method since we neglect the lateral flow in consideration of discharge uncertainties.

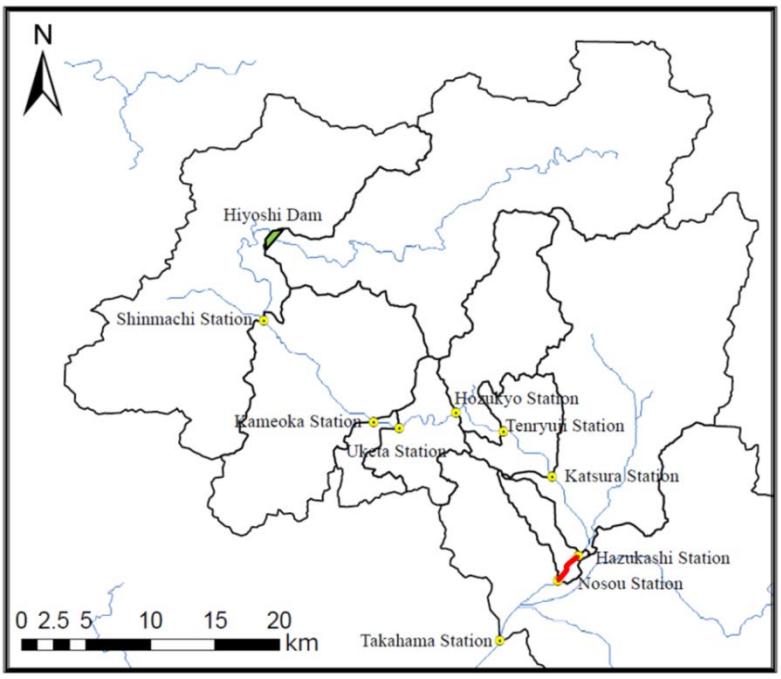

Figure 3-2 Watershed area of the Katsura river located in Kyoto, Japan.

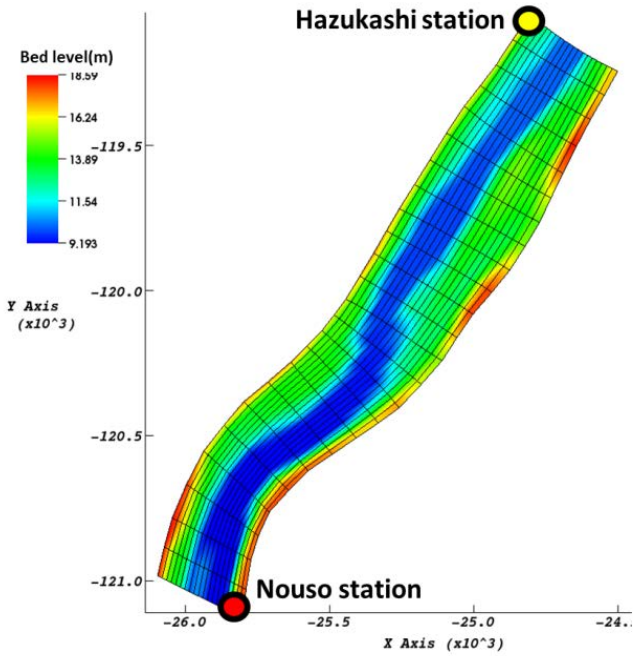

Figure 3-3 Calculation domain from Hazukashi station to Nosou station of the Katsura river.

3.2.3 Procedure for verification and application

We will firstly verify our proposed method with a synthetic experiment, which is based on artificial true values. Then the method is going to be tested on a natural river channel with the observed data to confirm its predictability.

3.3 Particle filtering system

PFs perform the sequential Monte Carlo (SMC) estimation based on particle representations of probability densities within Bayesian theorem (Ristic et al., 2004). The sequential process of particles in time using the nonlinear model is preceded up to the next available measurement (Salamon and Feyen, 2010). Among the various PFs, the sequential importance resampling (SIR) method is introduced in this study since the SIR can reduce the meaningless calculations and estimate current state more exactly.

3.3.1 Perturbation equation of estimation process

From the assumption that all errors come from uncertainties of channel roughness, inlet inflow and measured water stage at downstream, we incorporate some errors to Manning's roughness coefficient, inflow, and downstream water stage.

The general method, which adds white noise to the chosen particles like Eq. (3-4), shows the limitations in tracking rapidly changing parameter values and state variables. Therefore, the modified extrapolation method, which showed appropriate ability when tracking abruptly changed channel roughness with Kalman filter in the study of Crissman et al. (1994), is introduced to generate the noise of Manning roughness coefficient and inlet flow, as in Eq. (3-3) and Eq. (3-1), respectively.

The polynomial extrapolation method reduces the variation of particles, but it shows the weakness in inflection points, such as peak time of discharge hydrograph. As an alternative to these problems, we introduced the two types of perturbation equations to generate noise of Manning's roughness coefficient. In order to choose the perturbation equation, the discharge ratio (Eq. (3-2)), where $q\left(H_t^{obs,up}\right)$ is the discharge converted from the existing rating curve and the observed water stage at the current time, is introduced. Several cases were tested to determine the criteria to choose the perturbation equation, and it has been confirmed that a 20% discharge variation ratio is the proper value in our subject river channel. In the case when the ratio is less than 20%, Eq. (3-4) is applied, and Eq. (3-3) is applied when the ratio is more than 20%. It should be noted that this value is not a general index for other river channels.

$$Q_{t+1}^{i} = Q_t^{i} + (q(H_{t+1}^{obs,up}) - q(H_t^{obs,up})) + \varepsilon_{Q,t+1}^{i},\ \varepsilon_{Q,t+1}^{i} \sim \mathrm{N}\left(0, (0.1q(H_{t+1}^{obs,up}))^2\right) \quad (3\text{-}1)$$

$$Q_{t+1}^{ratio} = \frac{\left|q(H_{t+1}^{obs,up}) - q(H_t^{obs,up})\right|}{q(H_{t+1}^{obs,up})} \quad (3\text{-}2)$$

In case that $Q_{t+1}^{ratio} > 0.2$, $n_{t+1}^{i} = n_t^{re} + (\hat{n}_t - \hat{n}_{t-1}) + \varepsilon_{n,t+1}^{i}$, $\varepsilon_{n,t+1}^{i} \sim \mathrm{N}(0, 0.005^2)$ (3-3)

In case that $Q_{t+1}^{ratio} \le 0.2$, $n_{t+1}^{i} = n_t^{re} + \varepsilon_{n,t+1}^{i}$, $\varepsilon_{n,t+1}^{i} \sim \mathrm{N}(0, 0.01^2)$ (3-4)

$$H_{t+1}^{i} = H_{t+1}^{obs,down} + \varepsilon_{H,t+1}^{i}, \qquad \varepsilon_{H,t+1}^{i} \sim \mathrm{N}(0, 0.1^2) \quad (3\text{-}5)$$

where, Q_t^i, n_t^i and $H_t^{i,down}$ indicate the discharge, Manning roughness n, and downstream water stage of i-th particle at time t, respectively. $\varepsilon_{Q,t+1}^{i}$, $\varepsilon_{n,t+1}^{i}$, and $\varepsilon_{H,t+1}^{i}$ indicate the errors drawn from the normal distribution. $H_{t+1}^{obs,up}$ and $H_{t+1}^{obs,down}$ indicate the observed water stage at upstream and downstream, respectively. $q(H_t^{obs,up})$ is the discharge converted from an existing rating curve and the time series observed

upstream water stage. $\hat{n}_t$ indicates the weight averaged roughness coefficient in each time step according to the normalized weight by Eq. (2-25).

3.3.2 Resampling process

The key idea in the particle filters is to represent the posterior pdf $p(x_t|Z_t)$ with a set of random draws, called particles (Salamon and Feyen, 2010). The posterior density at time t is approximated as Eq. (2-17) and the updated equation can be shown as Eq. (2-18). At each updating step, the weight, which is calculated by Eq. (2-18), is calculated against the observed water stage at upstream. Then, the likelihood of each particle was normalized as Eq. (2-26). According to the normalized weight, the particles are removed or multiplied in the resampling step. The systematic resampling method (Kitagawa, 1996) is introduced among various resampling methods.

3.3.3 Constraints on noise generation

This method considers various cases with the disturbed channel roughness and inflow, but particles are controlled by only the normalized weight calculated against the updated water stage. Therefore, it is not enough to control the two randomly generated variables—the Manning roughness and inlet discharge—with only the weight calculated against updated water stage. In order to reduce the meaningless calculation, we assume the errors of observed discharge are fewer than 35%.

3.4 Evaluation of the proposed method with synthetic experiment

3.4.1 Synthetic experimental design

The key idea of the synthetic experiment is to confirm whether the method estimates inflow and channel roughness reasonably with the updated water stage at upstream

without any exogenous disturbances or not. The synthetic experiment consists of two steps. First step is to generate synthetic truth by the simulation with given conditions: downstream water stage, upstream inflow, and channel roughness. In terms of given conditions, the time series upstream discharge and downstream water stage of the real event, which occurs from 6:00 on October 20, 2004, to 15:00 on October 21, 2004, are utilized by the boundary conditions. In addition, the flood plain exists on both sides of the main channel. The Kamo River joins at the upstream of the reach and the Uji River joins at the downstream of the reach. Although they do not join inside the study reach, the effect of the tributaries and flood plain makes flow conditions very complex. Thus we simply assume that Manning's roughness coefficient (n_t) is linearly inverse proportional to water stage ($H_t^{obs,up}$) at time t as follows:

$$n_t = (18 - H_t^{obs,up}) / 250 + 0.02 \tag{3-6}$$

The simulation provides time-series upstream water stage as a by-product. The given conditions and the by-product are the synthetic true data.

At the second step of the synthetic experiment, the upstream water stage among synthetic true data serves as the sequential updating data of the implementation of the proposed method. Then downstream water stage and upstream inflow, which are same with observed data, are utilized by downstream boundary condition and the reference discharge of the upstream boundary condition, respectively. Thus the inflow and channel roughness are tracked by the proposed method. In addition, the synthetic data composed of the observed time series upstream discharge, downstream water stage, the generated upstream water stage, and the relationship equation about Manning's *n* are utilized as verification data and marked as "TRUE" in the following graphs.

3.4.2 Evaluation of the estimation results with synthetic data

In this section, the test for the particle filter algorithm—namely, whether or not the algorithm successfully traces the hidden "True" is implemented. In this testing step, upstream discharges and downstream water stage, including a certain level of error like Eq. 3-1 and 3-5, respectively, are used as the boundary condition. Then some errors were considered in Manning roughness coefficient as well like Eq. 3-3 and 3-4. Based on this condition, the particle filter algorithm with the correct water stage information was updated to trace the correct discharges and proper Manning roughness coefficient on a real-time basis.

It is believed that a large number of particles improve the accuracy of the estimation and prediction. The algorithm proposed in this study has been tested with different particle numbers, such as 100, 300, and 500 particles. We have determined that 100 particles in our algorithm are sufficient in the sense of calculation time and simulation accuracy in the Figs. 3-4, 3-4, and 3-5. In addition, the water stage of synthetic truth is utilized as updating data for the second step of the synthetic experiment.

In Figs. 3-3, 4, and 5, the weight averaged values, the values of each particle, and the true values of water stage, inlet discharge, and Manning's roughness coefficient are marked as a black line, red points and blue points, respectively. According to the graphs, the range of perturbed particles covers the true values, and particularly, the initial errors of Manning's roughness were also corrected during the tracking procedure by the learning process of particle filters. Root mean square error (RMSE) is utilized to compare the averaged values with synthetic truth. The RMSE for water stage and discharge are 0.11m and 31.75 m^3/s, respectively. Thus the results show that sequential evolution of each particle makes it possible to correct the channel roughness with considering the uncertainties of the inflow. In addition, the graphs in Figs. 3-4 ~ 3-6 show the approximate values Manning's *n* could be obtained.

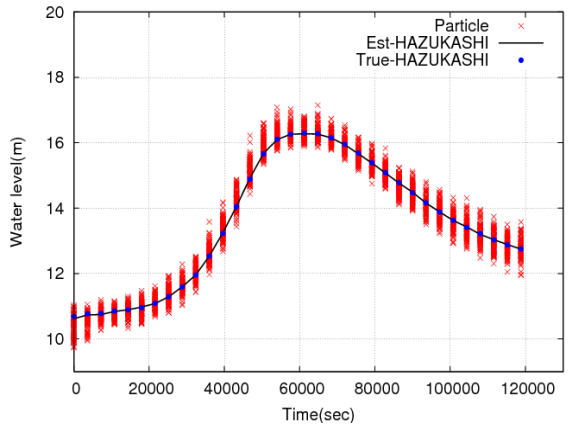

Figure 3-4 The comparison of averaged water stage in the synthetic experiment.

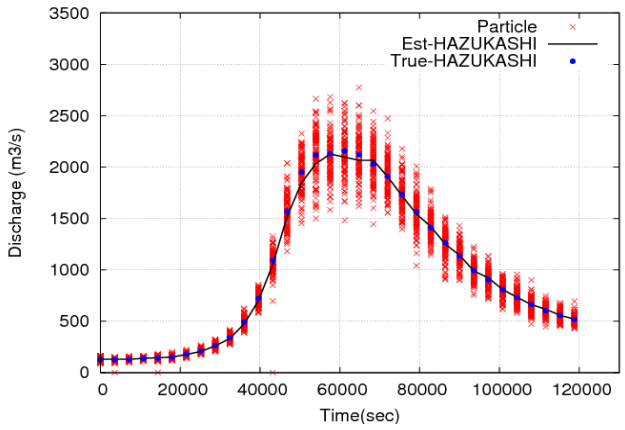

Figure 3-5 The comparison of inlet discharge in the synthetic experiment.

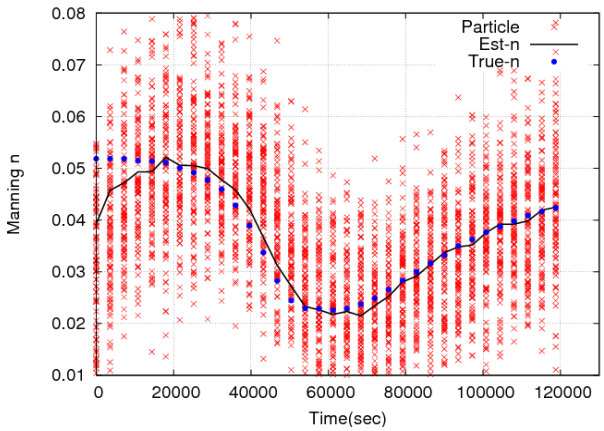

Figure 3-6 The comparison of Manning roughness coefficient in the synthetic experiment.

3.5 Prediction results and analysis using observed data

In this section, the predictability of the algorithm with observed data is presented. Most of the applied conditions for this simulation are the same with synthetic experiment, but the simulation is different in that this test utilizes real observed water stage for updating and true values for Manning's *n* do not exist.

In the prediction process, Manning's roughness coefficient is fixed as the value chosen in the resampling step at the current time step, and the predicted inlet flows up to 6 hours are determined by the proportions of particle's inlet discharge against the given discharge at the current time step. The prediction process performs up to 6 hours. Then the results at 1 hour (1HR), 3 hours (3HR), and 6 hours (6HR) are compared with the observed water stage and discharge (OBS) at Hazukashi station (Figs. 3-7 and 3-8). EST indicates the average values with the weight, while the prediction results are averaged with even weight. Table 3-1 shows the comparison results of the estimation and prediction of the water stage.

The estimated water stage and 1 hour ahead water stage shows good agreement with the observed one. With increased lead time, the accuracy of the prediction result is less than the 1 hour ahead prediction result due to the fixed roughness coefficient chosen in the resampling step, while the real channel roughness varies according to time.

In addition, the estimated Manning's roughness coefficient is plotted in Fig. 3-9 with the values of each particle. Manning's roughness coefficient is so varied due to the flood plain and backwater increasing the channel roughness when flooding occurs. Then Fig. 3-8 also shows that the estimated discharges are similar to the observed discharges, even though there is some discrepancy at the peak point and the recession limb of the hydrograph. However, the discrepancy in Fig. 3-8 may come from the rating curve conversion because the discharge is converted from the observed water stage.

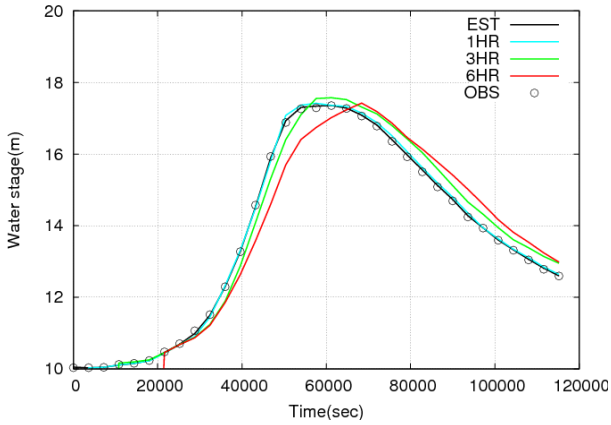

Figure 3-7 The comparison of prediction water stage at the Hazukashi station.

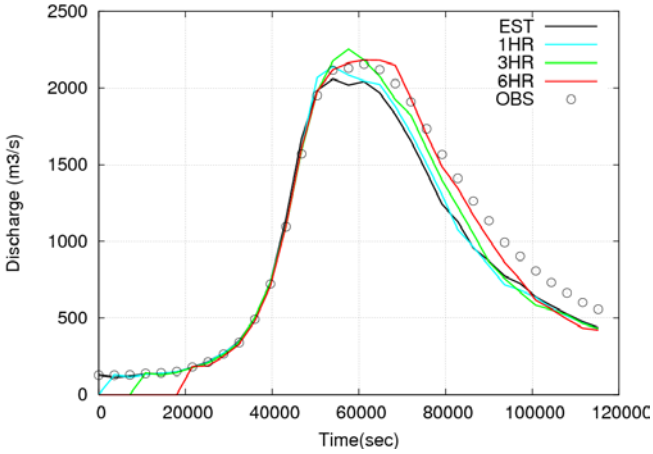

Figure 3-8 The comparison of prediction discharge at the Hazukashi station.

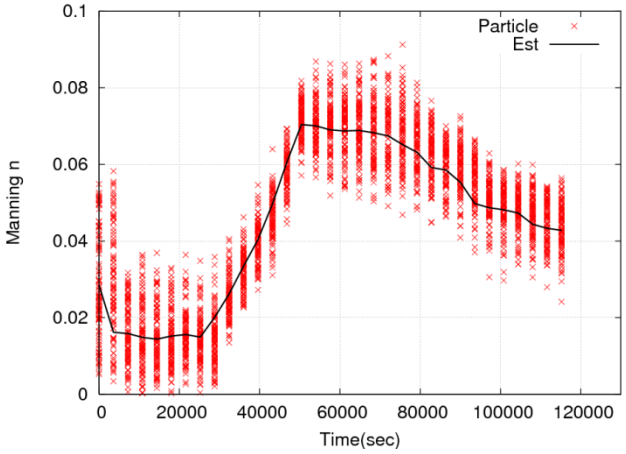

Figure 3-9 The estimated tendency of Manning roughness.

Table 3-1 Water stage comparison of the estimation and prediction at Hazukashi station.

Classification	RMSE of water stage (m)	Maximum absolute error (m)
Estimation	0.024	0.075
1hr prediction	0.097	0.258
3hr prediction	0.291	0.758
6hr prediction	0.565	1.376

3.6 Summary

Stochastic approaches are introduced to the 2D dynamic wave model to incorporate errors to consider the uncertainties of inflow and Manning roughness coefficient. As a stochastic approach, particle filters are utilized to deal with non-linear and non-Gaussian problems. In addition, the point mass representations in particle filters make it possible to consider all feasible conditions together. First, the proposed method is verified with the synthetic experiment to prevent unexpected exogenous disturbances. The estimated inflow and Manning roughness coefficient show good agreements with the artificial true value generated in the synthetic experiment. The availability as a water stage prediction model for a real event is checked. The estimated inflow show consistency with the observed discharge, but the gap between the predicted water stage and observed value becomes lager according to the increase in leading time. Although the method showed good estimation capability, the consideration of Manning roughness coefficient as an uniform value limit the water stage predictability. In addition, the large variation of Manning's n in tracking the Manning's n changed according to the change of water depth induce the large variation in estimated water stage and upstream inflow.

Chapter 4. Experiment to a real event considering the spatial distribution of Manning's *n* in a calculation domain

In this chapter, we tried to improve the weak points of the chapter 3 by introducing a spatially distributed Manning's n because the Manning's n changed according to the variation of the water depth is very difficult to apply in prediction algorithm based on the contents of Kim et al.(2012(b)).

Thus only the estimation process is focused in this chapter and the estimated results are compared with the observed discharge data for the verification. In the estimation system, Sequential Importance Resampling (SIR) method is introduced to a 2D hydraulic model to simultaneously estimate inflow and Manning roughness coefficient (Manning's n). The equifinality problem between the Manning's n and the inflow is considered using the proposed method. To solve the problem, we introduced the variance reduction factor and the correction factor in the perturbation step of the proposed method. The perturbed inflow and Manning's n were updated according to the observed water stage with state variables. The result of the proposed method shows good agreement with the observed discharge, which enabled us to estimate the Manning's n and inflow discharge at the same time considering the uncertainties of the existing rating curve. Finally, it showed that the methodology not only estimates the appropriate Manning's n but also improves the existing rating curve.

4. 1 Introduction

Discharge data at the basin outlet are utilized in water resource management, hydrological model calibration, flood prediction, and so on. These data are obtained by measuring the flow velocity or constructing a rating curve, or through the installation of a specific gauging station such as a flume. Among them, a general method uses a rating curve, which depicts the relationship between stage and discharge at the section based on occasional measurements. Even if a rating curve is based on measurement data, it assumes that the flow is steady state and the channel bed does not change as time passes; this means a dynamic river flow estimation with a rating curve has limitations. Therefore, the accuracy of the discharge obtained by transforming a time-series observed water stage to discharge using the rating curve is uncertain. Di Baldassarre and Montanari (2009) investigated the uncertainties of the discharge using a 1D hydraulic model and classified the uncertainty into three categories: One is due to the interpolation and extrapolation of a rating curve; another is due to the presence of unsteady flow conditions; and the last one is generated by the seasonal change in the channel roughness. They showed that using a rating curve might generate significant errors when estimating discharge from the stage measurements, and the errors may be more than 15% of the true discharge.

As an alternative to these traditional discharge estimation methods, in recent years, a hydraulic routing model has been considered as a tool for flood prediction or estimation. Such a hydraulic model introduces a stochastic approach to dealing with the uncertainties of the model structure, state variables, and the model parameters. In addition, because the water stage is more accurate than the discharge data, it serves as reference data for updating state variables. Shiiba et al. (2000) applied a Kalman filter to the one-dimensional dynamic wave model. They considered the uncertainties from imperfect parameters and boundary conditions. The stochastic approach showed that the estimation errors – due to parameter calibration uncertainty, input uncertainty, and error

propagation systems involved in a deterministic model – could be reduced.

Such a stochastic approach using a hydraulic model primarily focuses on channel roughness or uncertain inflow. Originally, the particle filters (PFs) are applied to a one-dimensional hydraulic model (Montanari, et al., 2009; Matgen, et al., 2010; Giustarini, et al., 2011), and showed that the PFs could reduce the uncertainties of the discharge and water stage by updating the water stage using satellite imagery. However, Manning's *n* was determined using the trial-and-error method with a certain discharge. In other words, the uncertainties of the Manning's *n* were not considered.

Because channel roughness is included in the friction factor for river flow, it affects the relationship between water stage and discharge. Therefore, Fread (1989), Hsu, et al. (2006), and Ding, et al. (2006) showed that the consideration of Manning's *n* improves the prediction ability of the water stage in flood prediction. Kim, et al. (1995) showed that an uncertain Manning's *n* could generate different discharges for the same water stage when using a 1D hydraulic model.

Using this approach, we confirmed that channel roughness and inflow are important factors for simulation, and the interrelationship of discharge, water stage, and channel roughness is very complex. Therefore, usually only channel roughness or discharge are estimated because estimating both variables at the same time is difficult. As an alternative, Aricò et al. (2009) estimated discharge and Manning's *n* simultaneously, but they focused simply on estimating the peak discharge and finding a representative Manning's *n* – but not a Manning's *n* changed according to flow conditions. Tachikawa et al. (2011) introduced PFs to the 1D dynamic wave model, showing that the parameters and boundary conditions could be estimated well by updating the water level using PFs. Because the embedded system model is a one-dimensional dynamic wave model, limitations exist in utilising updated water stage data; the model cannot consider the geomorphologic effect. Kim et al. (2012) introduced PFs to the 2D hydraulic model, but they did not solve the problem between the Manning's *n* and discharge clearly since

they considered Manning's *n* as the uniform values for all calculation domains of the river.

Therefore, this chapter aimed to present a simultaneous estimation method that considered an uncertain Manning's *n* with spatial distributions and an uncertain inflow. We used the 2D dynamic wave model, which can reflect the effect of river geomorphology and is sensitive to variations in the water stage. The Monte Carlo sequential data assimilation scheme – the so-called Particle Filters – is applicable for non-linear and non-Gaussian systems and was combined with the 2D dynamic wave model. The proposed method was verified through real observed discharge, and the applicability of the proposed method was confirmed with another flood event.

4.2 Methodology

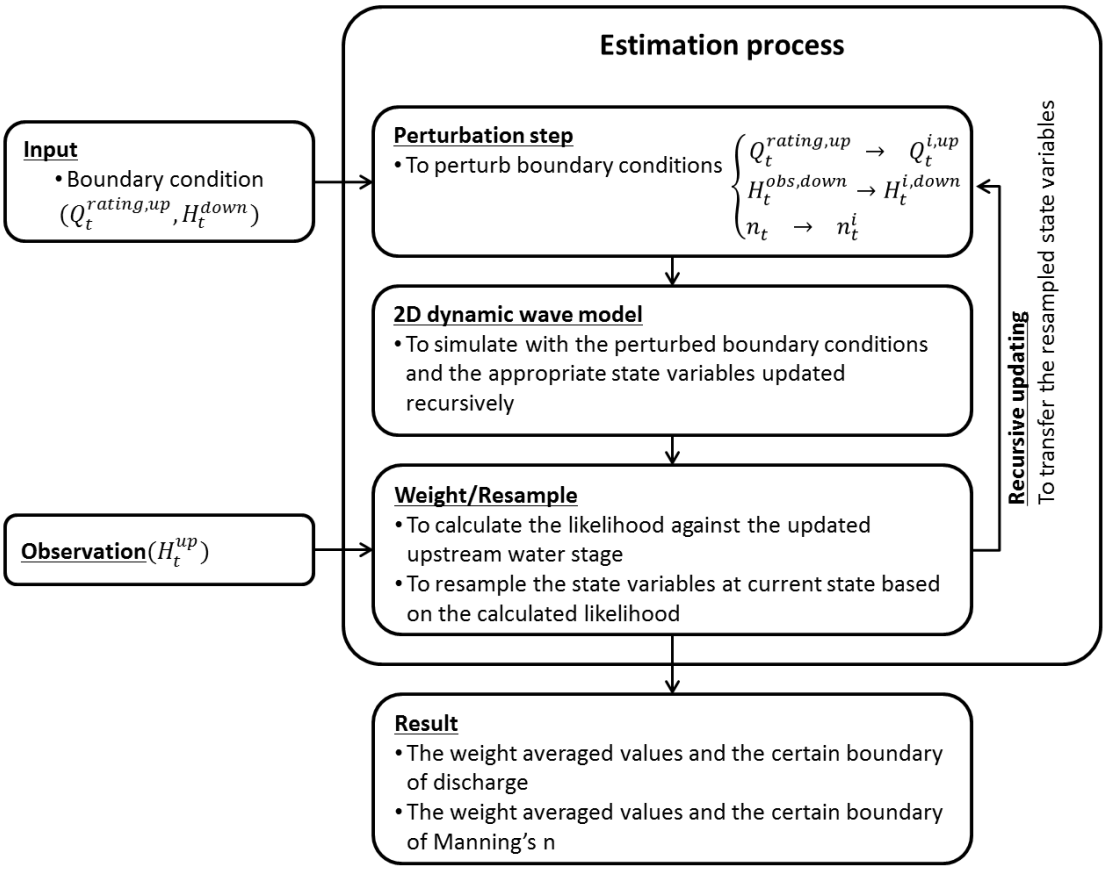

Figure 4-1 Procedure of the proposed estimation process.

The proposed method was built on the assumption that a rating curve and the Manning's *n* include uncertainties and sequential updating of the observed water stage reduces these uncertainties. To understand that framework in regard to the proposed method, we needed to consider the sequential procedure (shown in Fig. 4-1) and the structure of it. With regard to the structure, it consisted of a two-dimensional dynamic wave model (2D model) and a particle filters (PFs). The 2D dynamic wave model calculated variables inside the calculation domain. The particle filter incorporated noise to the boundary conditions of each 2D model at the perturbation step before

implementing the 2D model and compared the results against the observed water stage at the weight calculation step. Concerning the sequential procedure, the estimation process repeated every hour because we utilized the hourly observed data. At first, the boundary conditions of inflow and the roughness coefficient, including uncertainties, were incorporated with some errors at the perturbation step, so the 2D model ran with the various boundary conditions, so-called particles. The 2D model was a deterministic model unless many similar systems run simultaneously and independently, and the result of each particle was evaluated by the updated water stage every updating step. The 2D model was parallelised by Open Multi Processing (OpenMP), which supports shared memory multiprocessing programming for efficient calculation during the estimation process. The weight of each particle was calculated against the observed water stage for every updating step, and the weight recursively updated the state variables consecutively.

In terms of using a 2D model, channel roughness, inflow, and water stage have the closest connections with each other for estimating one of them. Manning's *n* was determined by the engineer on the basis of the small number of investigations of the bed material, vegetation, channel shape, and so on. In addition, the inflow obtained from a rating curve or a hydrological model involved many uncertainties, and the 2D model is highly nonlinear. Thus, we selected the Sequential Importance Resampling (SIR) method for this approach since the resampling step – which entails removing particles with low weights and duplicating particles with heavier weights with a brief process – makes the system reflect variables more accurately than the typical PFs, Sequential Importance Sampling (SIS).

To verify the proposed method, we applied the method to the Katsura River located in Kyoto, Japan. Because natural flood event data are affected by many anonymous factors, we designed experiments based on the natural river reach instead of using experiments implemented in a laboratory. The experiment implemented with two events: One event from October 2004 was utilized to estimate inflow and a spatial distribution

of the Manning roughness coefficient. Another event occurred in September 2004 and was utilized to confirm the applicability of the proposed method. The results – which are the Manning's *n* and the modified rating curve – estimated from the proposed method were validated for the simulation using the deterministic model.

4.2.1 Likelihood calculation

The Gaussian likelihood of each particle (Eq. (2-25)) was calculated against the observed water stage to reduce the variations resulting from the interaction between parameters and state variables. The standard deviation is determined by 0.1 m. Then, the normalised weight was calculated by the likelihood as Eq. (2-26). Each particle was resampled depending on its own normalised weight using the systematic resampling method, and noise was added to duplicated particles. This sequential updating procedure made it possible to consider the time-variant state variables and parameters with some constraints.

4.2.2 Perturbation equation of the method

During the initial stage, the noise drawn from the uniform distribution on was added to inflow and Manning's *n*. In terms of inflow, the errors were determined as -20% and 20% of a given discharge in considering the maximum error rate derived from Fig. 4-2, respectively.

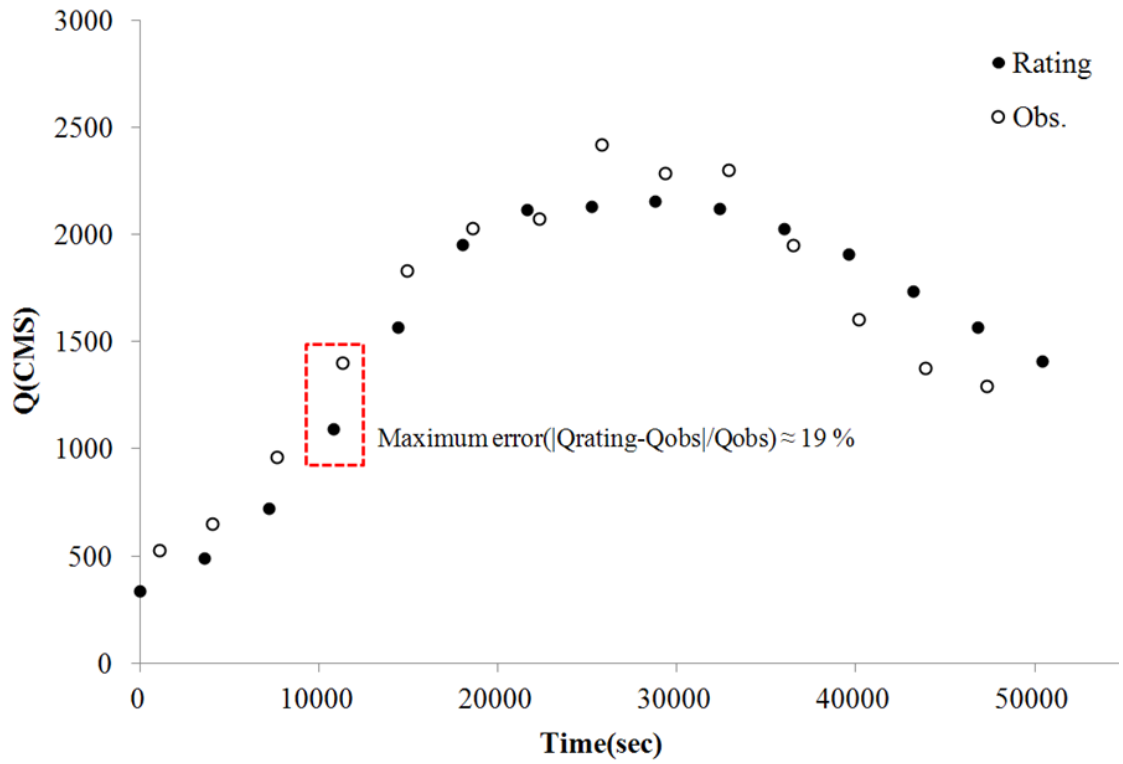

Figure 4-2 Comparison between the discharge converted from a rating curve and the observed discharge at Hazukashi station within the Katsura river located in Kyoto, Japan.

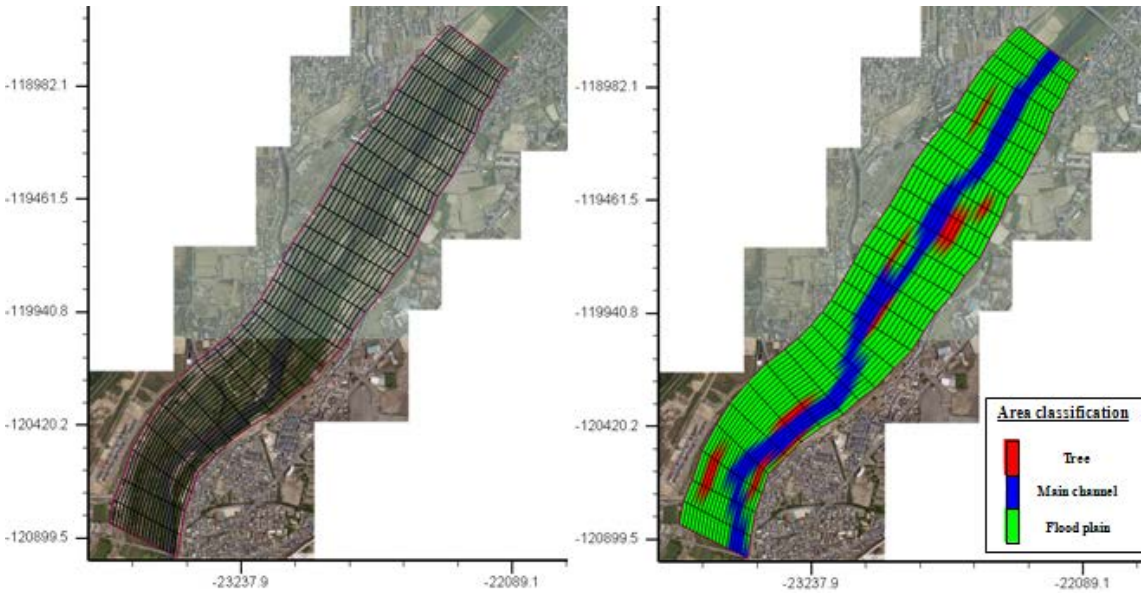

Figure 4-3 Area classification of the study area from the aerial photo.

In terms of Manning's *n*, the study area was separated into 3 categories, which were main channel, flood plain, and the area densely colonised by trees (see Fig. 4-3). On each area, and were determined as 0.02 and 0.05, 0.04 and 0.1, and 0.08 and 0.14 based on DEFRA/EA (2003), respectively.

In the sequential updating stage, the perturbation method and the variance of the particles directly affect the accuracy of the results. Thus, the efficiency of the methodology is also related to parameters. Reflecting previous experience of the changed pattern to improve accuracy and efficiency would be ideal. However, the pattern of Manning's *n* is variable based on the river channel situation, and we can assume that the Manning's *n* is determined by the certain fixed value in each section (Fig. 4-3). In addition, we assume that the discharge transformed from a rating curve with the water stage has a certain pattern. We considered these assumptions in designing the perturbation step. Because the large variances of Manning's *n* and the inflow cause equifinality problems against matching the water stage at every time step, the variance reduction factor was introduced in tracking the Manning's *n*, and the correction factor was introduced in tracking the discharge.

In total, five variables – which are water stage at outlet, inflow, and Manning's *n* in each separated zone – were evolved independently in the perturbation step. Water stage at outlet was disturbed with normal distribution, considering the observational errors as Eq. (3-5)

Concerning the inflow involving some uncertainties obtained from the existing rating curve, the perturbation method for the inflow was defined as follows:

$$Q_t^i = Q_{t-1}^i + a_t(q(H_t^{obs,up}) - q(H_{t-1}^{obs,up})) + \varepsilon_{Q,t}^i, \tag{4-1}$$

$$\varepsilon_{Q,t}^i \sim N\left(0, (0.1q(H_t^{obs,up}))^2\right)$$

$$a_t = (\widehat{Q}_{t-1}^i / q(H_{t-1}^{obs,up}) + \widehat{Q}_t^i / q(H_t^{obs,up}))/2$$

where, Q_t^i is the inflow of particle i at the time step t; $q(H_t^{obs,up})$ is the inflow converted from the rating curve and water stage at the time step t; a_t^i is the recursive correction factor for the correction of $q(H_t^{obs,up})$, and $\hat{Q}_t^i$ is the average inflow according to weight. a_t^i indicates the noise drawn from the normal distribution.

The input data (inflow) are continuously corrected with a correction factor(a_t^i). The first term (Q_{t-1}^i) of the right hand side of the Eq. (4-1) maintains the distribution of the particles. The discrepancy between the 2nd and 3rd terms include the errors of the existing rating curve, so it was corrected by a_t^i because the ratio of the weighted averaged discharge and the converted discharge at previous time showed a pattern of errors. However, the error pattern of a rating curve using the rating curve has a different pattern between a rising limb and a decreasing limb.

a_t^i is only applied when the signals of $q(H_t^{obs,up}) - q(H_{t-1}^{obs,up})$ and $\left(q(H_t^{obs,up}) - q(H_{t-1}^{obs,up})\right) - \left(q(H_{t-1}^{obs,up}) - q(H_{t-2}^{obs,up})\right)$ are the same. If the signal was different, Eq. (4-1) was applied without a_t for the artificial evolution.

In terms of Manning's *n*, we utilized two methods for each separated zone: For the main channel, we used a variance reduction method according to the variance of the previous time step as follows:

$$\text{In the case } Var_{t-1}^n \geq (0.001^2): \; n_t^i = n_{t-1}^i + (\hat{n}_{t-1} - \hat{n}_{t-2}) + \varepsilon_{n,t}^i \;, \qquad (4\text{-}2)$$

$$\varepsilon_{n,t}^i \sim N(0, s^2 Var_{t-1}^n)$$

Another method maintained the variance of Manning's *n* to consider the uncertainties of Manning's *n* as follows:

$$\text{In the case } Var_{t-1}^{n} \geq (0.001^2): \quad n_t^i = n_{t-1}^{re} + \varepsilon_{n,t}^i \quad , \varepsilon_{n,t}^i \sim N(0, 0.001^2) \qquad (4\text{-}3)$$

where, n_t^i is Manning's n of particle i at the t time step, $\varepsilon_{n,t}^i$ represents noise drawn from the normal distribution, n_{t-1}^{re} is the resampled value at the t time step, is the tuning factor introduced by Moradkhani et al. (2005) to reduce the variance of the particles, and Var_{t-1}^{n} is the variance of Manning's n of main channel at the $t-1$ time step.

For flood plain and the area colonised by trees, the same method was utilized.

4.3 Verification and applications

The proposed method was applied to the Kastura River located in Kyoto, Japan (Fig. 3-2). The reach length was about 2.5 km from the Hazukashi water stage station (inlet) to the Nosou water stage station (outlet). The flow of the study area was inclined to be affected by vegetation, but the type of vegetation varied from grass to tall trees, and the density of the vegetation was also different, according to the location. Thus, the predetermined Manning's n included many uncertainties to represent the channel resistance. In terms of calculation domain, river channel was composed of 500 grids: The number of the cross-section point was 20, and the number of the cross-section was 25.

The experiments were designed to verify and confirm the reproducibility of the proposed method. Although the experimental results in the laboratory are generally utilized to verify hydraulic problems, it cannot consider the effect of the uncertainties of the natural river channel. In addition, it was not certain that the verification using the experimental results would assure the applicability to the natural river channel because channel roughness coefficient is related to the various anonymous factors. Therefore, the verification step was based on the comparison to the observed discharge. The proposed method was performed with various boundary conditions, which were the

downstream water stage observed at the Nosou station and the upstream inflow discharge converted from a rating curve with observed water stage, perturbed through the perturbation step. Using the observed water stage of the inlet, the state variables – including the inflow and the Manning's *n* – were continuously updated. Finally, the estimated Manning's *n* was tested with another event to confirm the reproducibility of the results estimated from the proposed method.

4.4 Simultaneous estimation of Manning's *n* and inflow and verification of the method

Manning's *n* and inflow were simultaneously estimated by the proposed method. The five parameters – three roughness values, inflow, and downstream water stage, which were essential and sensitive factors for hydraulic modeling – construct one particle. Each particle was disturbed with some errors through the perturbation step. With various particles, the simulations were implemented. For the verification, the flood event from 6:00 on October 20 to 14:00 on October 21, 2004, was utilized. The simulation was implemented with 300 particles, as 300 particles are enough to present the stabilised results.

Fig. 4-4 shows the estimated result of Manning's *n*, inflow, and upstream water stage. The weight averaged values are identified by a black line, and the red points indicate the value of particles. The cyan-coloured area and the yellow-coloured area indicate the 90% and 70% interval, respectively. In addition, the black points indicate the observed water stage or observed discharge.

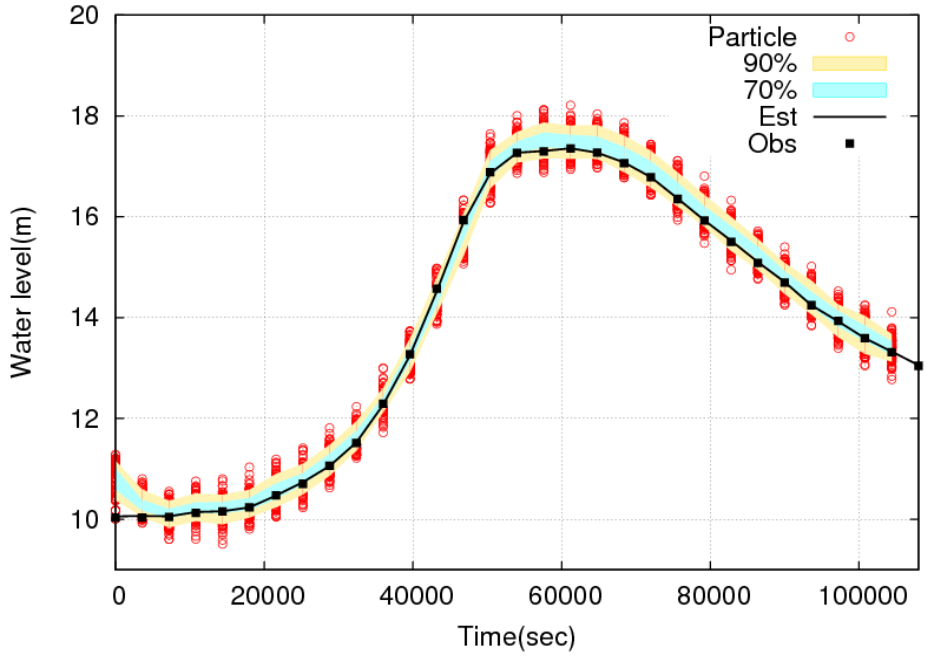

(a) Water Stage at Inlet

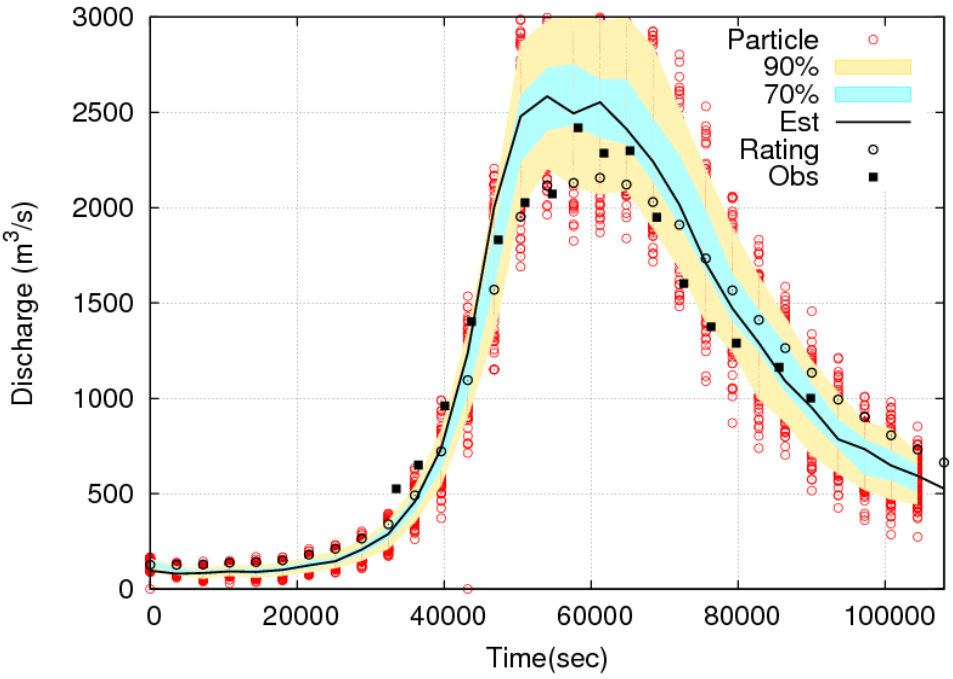

(b) Discharge at inlet.

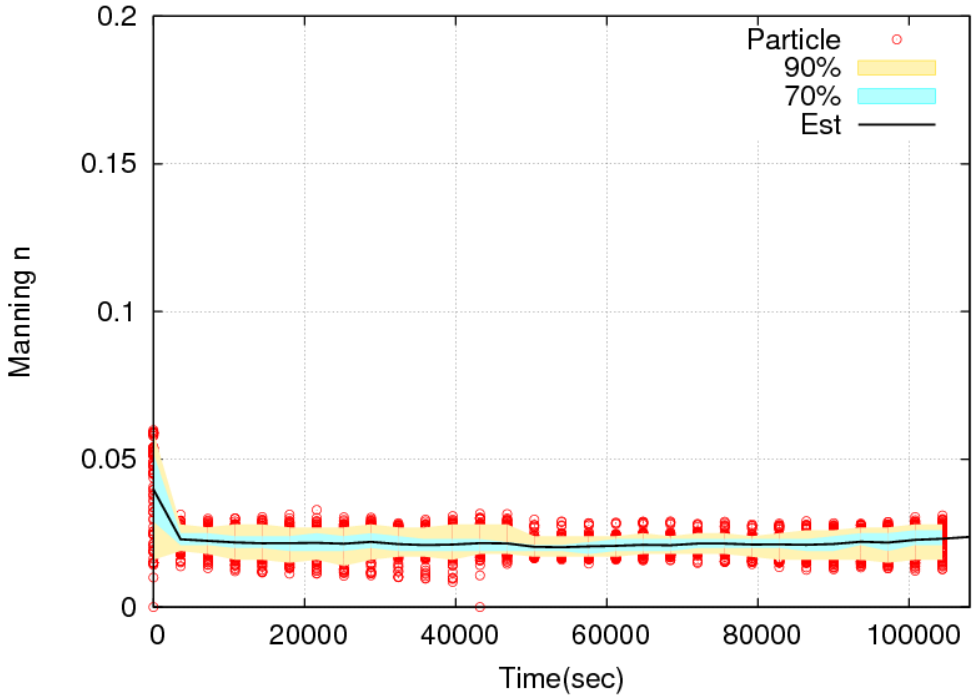

(c) Manning's *n* on the main channel.

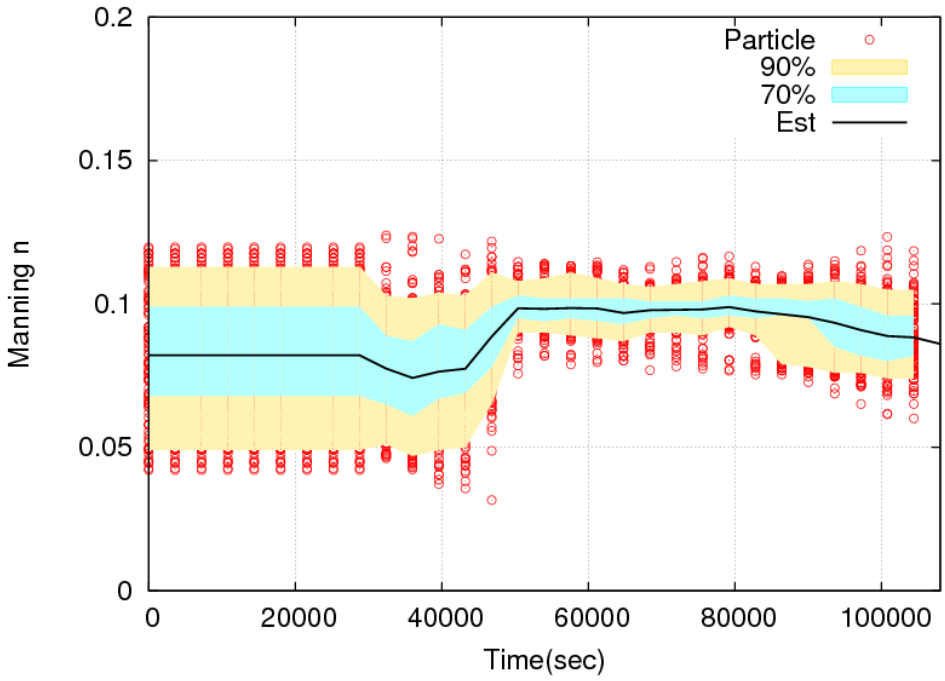

(d) Manning's *n* on the flood plain.

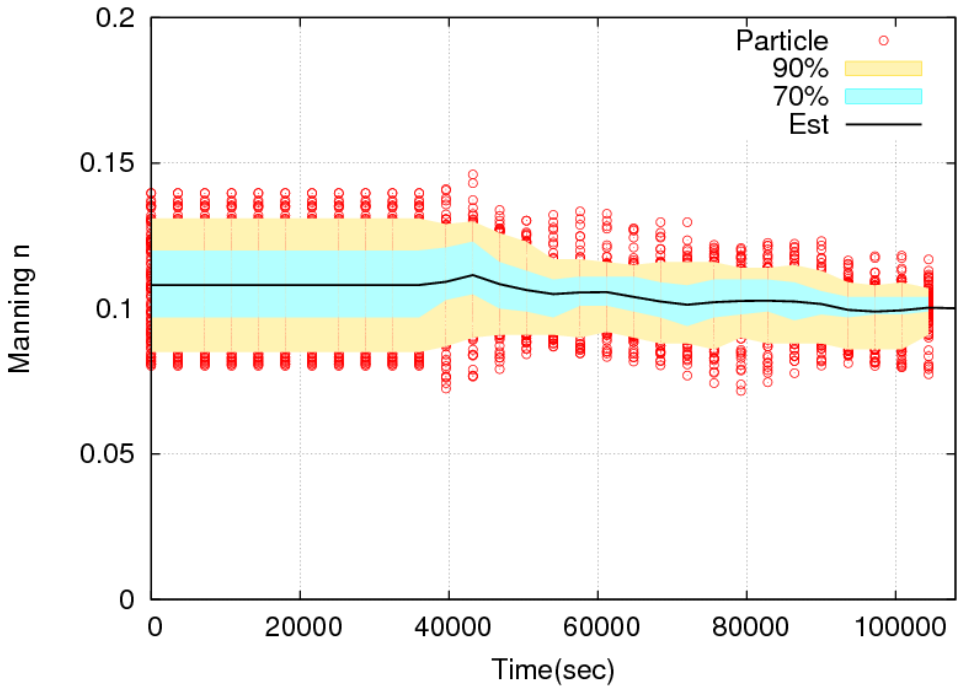

(e) Manning's *n* on the area colonised by trees

Figure 4-4 Estimated results through the proposed method.

In Fig. 4-4 (a), the estimated water stage is compared with the observed water stage. We judged that estimated water stage was higher than the observed water stage at the initial stage because a rating curve included uncertainties more than initial assumptions, 20% of a given discharge. This discrepancy was sequentially corrected by updating procedure. Excepting the initial stage, the water stage at upstream showed good agreement with the observed water stage. The method provided enough tracking ability of the water stage as reference data.

In terms of discharge at inlet (Fig. 4-4 (b)), the discharge converted from a rating curve marked by white point was higher than the estimated result in the initial part as with the graph of the water stage. Around peak time, an observed discharge marked by black points was compared with the estimated discharge and the converted discharge.

The comparison between the observed and converted ones is shown in Fig. 4-2 and 4-4(b); the converted one included many uncertainties. The simulation of incorporating errors can reflect the current flow state in dealing with flow magnitude. In addition, almost observed discharge was within the 90% interval, and the pattern of the observed discharge was reflected in the weight averaged discharge.

The Manning's *n* was estimated for each separated zone as shown in Fig. 4-4 (c)–(e). From the initial range, the variance was sequentially reduced by the variance reduction factor described in the perturbation method. During the proceedings, the estimated values were gradually approaching the converged value in each separated zone. In Fig. 4-4 (d) and (e), the beginning of the time series was the low flow period, which was not related to the Manning's *n* of the flood plain and the area colonised by trees. In other words, it did not update because it was not related to the flow calculation.

The verification step was confirmed with the measured discharge and the observed water stage upstream. Then it showed that the method was able to provide the ability to search the proper Manning's *n* and corrected the inflow for this event.

4.5 Evaluation of reproducibility of the proposed method through application to the other event

This evaluation was implemented with another event to confirm the validity of the estimated Manning's *n* and discharge by the proposed method. The weight averaged Manning's *n* at the final step of the previous experiment was utilized by the Manning's *n* of this simulation. They were 0.03680 (main channel), 0.08972 (flood plain), and 0.12222 (the area colonised by trees) for each separated zone. This simulation was implemented without updating, so it was the simulation using a deterministic 2D model. The evaluations were performed with 5 cases. Three cases utilized the same event of the previous experiment, and the others utilized the event from 16:00 on September 29 to

24:00 on September 30, 2004. The three cases using the same event from the previous experiment utilized a different inflow discharge. Each case utilized the discharge converted from an existing rating curve, the discharge converted from the modified rating curve obtained from the previous experiment results, and the time series discharge estimated from the proposed method, respectively. The relationship between the estimated discharge and the water stage is shown in Fig. 4-5. We introduced the modified rating curve with power function to compare the existing rating curve. Two cases using the event of September 2004 also utilized two different input discharges converted from the existing rating curve and the modified rating curve.

In the application of the event of October 2004, the estimated upstream water stage of each case was compared to the observed water stage in Fig. 4-6. The green line indicates the simulation result using the discharge converted from an existing rating curve as an upstream boundary condition. The red line indicates the simulation result using the discharge converted from the modified rating curve as an upstream boundary condition. Finally, the black line indicates the simulation result using the discharge estimated from the proposed method. The estimated upstream water stage of the second and third cases showed good agreement with the observed water stage. The performance of the method was also evaluated using the root mean square error (RMSE), which is included in Fig. 4-6 It means the proposed method provided the proper function to estimate the Manning's *n* and the inflow simultaneously.

$$RMSE = \sqrt{\frac{\sum_{t=1}^{N}\left(H_t^{obs} - H_t^{est}\right)^2}{N}} \tag{4-4}$$

To confirm the reproducibility of another event, the procedure was applied to another event of September 2004. Fig. 4-7 shows the results of the application. As we have seen from the result and the RMSE against the observed water stage, using the Manning's *n* and the modified rating curve obtained from the proposed method improved the estimated water stage using the existing rating curve.

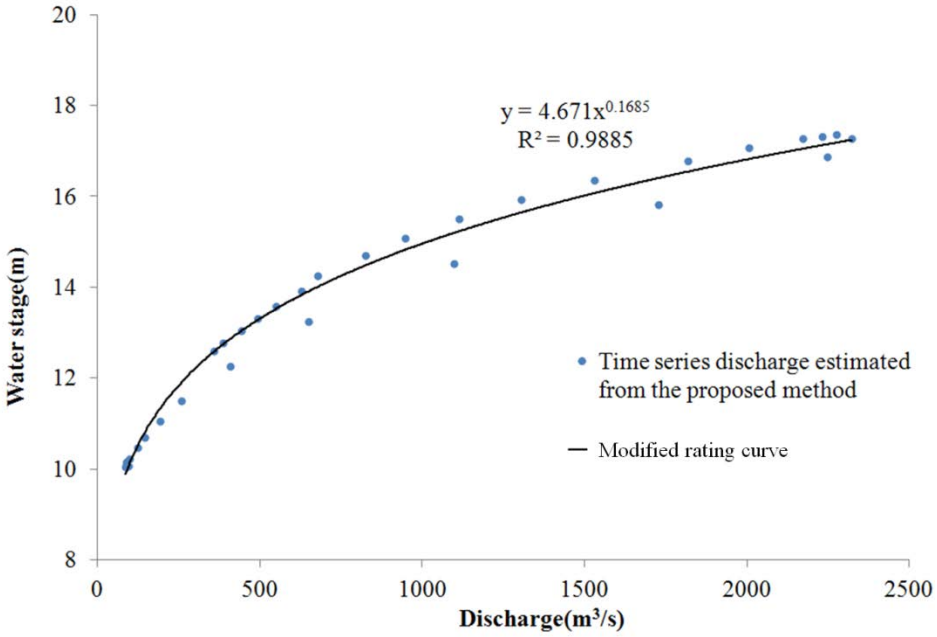

Figure 4-5 Modified rating curve using the discharge estimated from the proposed method.

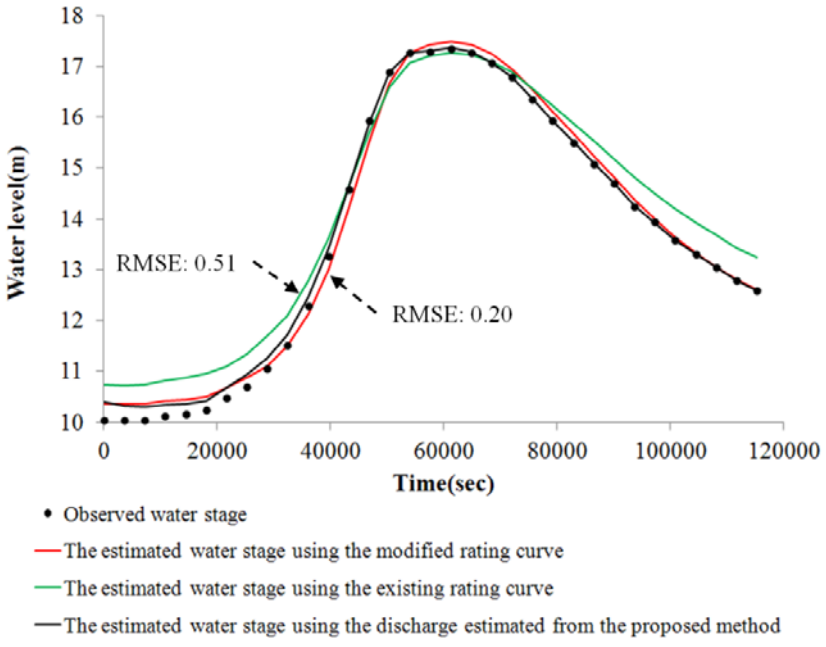

Figure 4-6 Comparison of the water stage at Hazukashi station from each deterministic simulation using the event in Oct., 2004.

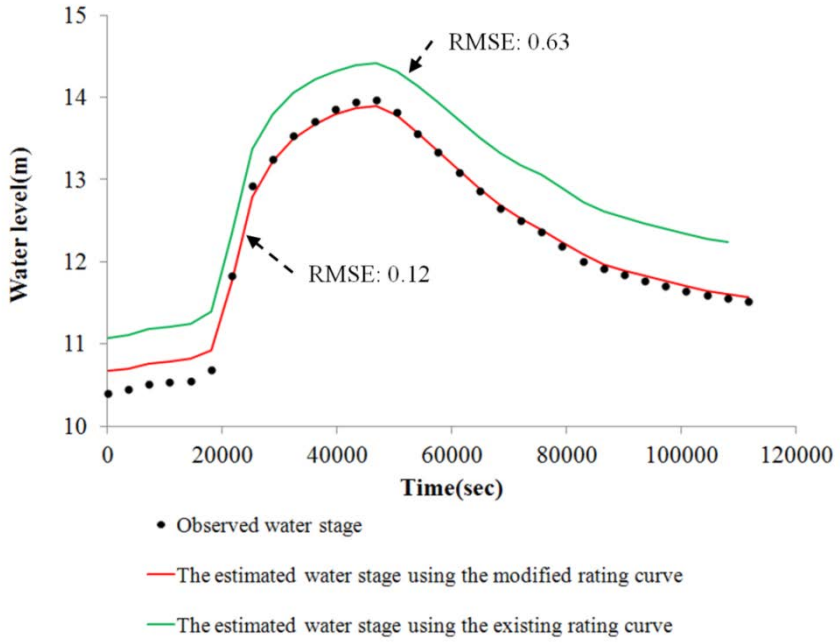

Figure 4-7 Comparison of the water stage at Hazukashi station from each deterministic simulation using the event occurred in Sep., 2004.

4.6 Summary

The two problems in chapter 3 are improved, and the availability to other events of the estimated inflow and Manning roughness coefficient from the proposed method is confirmed. One is the consideration of Manning roughness coefficient by a unique value all over the calculation domain. It degrades the predictability of water stage. As an alternative, the spatial distribution of Manning roughness coefficient is considered, and it is classified by the aerial photo. Another problem is large variation of the Manning roughness coefficient to track the Manning's n changed according to the water level. It induced too many uncertainties in the estimated water level and discharge. Thus a variation reduction factor is considered together with considering the spatial distribution of Manning's *n*. Then equifinality problems, which were induced by the combination of the Manning's *n* and the inflow in the resampling step, were solved by considering the variance reduction factor and the correction factor, an adequate number of particles and proper classification of the study area.

The proposed method was verified through an observed water stage and discharge data set. The proposed method enables the estimation of the inflow and the Manning's *n* simultaneously. Using the provided results from the method, the relationship between the water stage and the discharge at the water stage station can be constructed. The modified rating curve and Manning's *n* of each separated zone obtained from the proposed method was applied to another event to confirm the reproducibility. Through these verifications and application of the method, we confirm that it is a feasible alternative to the traditional method, in which the Manning's *n* estimated empirically and the discharge converted from an existing curve are utilized.

Chapter 5. Estimation of the partially gauged 2011 largest flood discharge at the Kumano River using particle filters

In this chapter, the ensemble estimation method is proposed to estimate the unmeasured largest flood event. The contents are based on Kim et al. (2013).

The largest-ever flood event was recorded at the Kumano River in the Kii peninsula of Japan from August 31 to September 4, 2011. Water level data exceeded the observation range in many places except in the Ouga water stage station at downstream. This study aimed to estimate the peak discharge of the event by using the estimation method, which is a 2D dynamic wave model combined with particle filters, and by considering the water level observed at the Hitari and Ouga stations and a river discharge estimated by a hydrological model. The estimation method was applied to the three historic flood events for quantifying the uncertainties of the Manning roughness coefficient (Manning's n) of the subject river channel. Based on the optimized range of Manning's n, the filtering method was applied to estimate the largest peak discharge of the 2011 flood using the discharge estimated by a hydrological model. The possible range of the largest peak discharge was successfully evaluated through the comparison of the observed flood marks. Finally, a rating curve established by the estimation results at the Ouga station is examined.

5.1 Introduction

From August 31 to September 4, 2011, the largest ever flood event occurred in the Kii peninsula, Japan due to the 12th typhoon in 2011. Although the peak discharge was able to be estimated using a rating curve or a hydrological model (Meno et al., 2012), its accuracy is controversial because of the uncertainties in the rating curve at the Ouga station, and prediction uncertainties of a hydrologic model for the largest flood we have ever experienced. Historic flood events utilized in the hydrologic model calibration (Meno et al., 2012) are all located in the extrapolation ranges in the rating curve.

Prediction uncertainties of discharge come from the various characteristics of the open channel flow such as channel geomorphology, channel roughness, initial and boundary conditions and so on. Considering such factors properly, it makes sense that a hydraulic model and a hydrologic model should be fully utilized to estimate river discharge combined with filtering techniques and all available observed information.

To estimate river discharge using the hydraulic model, one essential prerequisite is the boundary condition such as inflow from the upper reach. The upper boundary inflow is possible to estimate using a hydrologic model; however, the uncertainty included in the estimated boundary inflow should be treated properly with filtering techniques. To consider the uncertainties of the boundary conditions, Tachikawa, et al. (2011) and Kim, et al.(2012(a)) introduced particle filters (PFs) into 1-dimensional and 2-dimensional hydraulic models, respectively, and successfully provided reliable river stages and discharges within the uncertain upstream inflow data. In the estimation methods to deal with the uncertainties of the discharge, available information such as water level was used as reference data to evaluate the uncertainties and update the state variables. Kim, et al.(2012(a)) adopted a 2D hydraulic model to consider the channel geomorphology more precisely, which incorporated reference water level data more effectively than a 1D model.

Simultaneous estimation of two variables such as channel roughness and upper boundary inflow discharge is a delicate problem because their combination can be almost unlimited for a given observed water level. Thus Hsu, et al.(2006), Ding, et al.(2006), and Kim, et al.(1995) only focused on one of two factors: either channel roughness or boundary inflow. However, the boundary inflow and the channel roughness should be estimated simultaneously considering that the channel roughness is affected continuously by the evolving channel geomorphology and the vegetation distribution of the flood plain.

In our previous study (Kim, et al., 2012(b)), it was shown that boundary inflow and channel roughness were able to be estimated simultaneously in a reasonable range using a 2-D hydraulic model combined with particle filters. Based on several historic flood events, the uncertain ranges of channel roughness can be identified and the most reasonable boundary inflow can be estimated. By utilizing this information, it is possible to estimate the proper river discharge of the following event, even though it has the largest ever flood peak.

In September 2011, the largest flood happened at the Kumano River basin resulting in an exceeded observation range at various water stage stations with the exception of the Ouga station. The rating curve at the Ouga station could have large uncertainties because the observed water level in the 2011 flood far exceeds the applicable range of the existing rating curve.

Therefore, this chapter aimed to estimate the discharge of the flood event in September, 2011 by fully utilizing a 2D hydraulic model, a distributed hydrologic model and filtering techniques with all available information. A sequential uncertainties analysis based on the previous study (Kim, et al., 2012(b))is applied first to quantify a proper range of channel roughness of the study river using the events occurring in August, 2003, August, 2004 and September, 2004. Based on the optimized model parameters, a distributed hydrologic model (Meno, et al., 2012) and a 2D hydraulic

model are fully utilized with limited water level information and flood marks to estimate the discharge of the largest flood in 2011.

5.2 Application process

As shown in Fig. 5-1, the whole process is composed of two parts: a 2D hydraulic model and particle filters. The connector “A” and “B” indicate reading boundary conditions and reading reference data, respectively. The basic frame shown in Fig. 5-1 is the method proposed by Kim et al.(2012(b)), which is used to estimate the spatial distribution of the channel roughness and the upper boundary inflow discharge at the same time. Kim et al.(2012(b)) applied the method to estimate channel roughness using discharge converted from a rating curve adding noise as the upper boundary condition. At the upper boundary of the channel reach in this subject area, the Hitari station, water level data is observed, although a rating curve is not established. Therefore, the upper boundary inflow discharge was estimated by a distributed hydrological model (Meno et al., 2012) as an alternative.

The initial range of Manning’s *n* is sequentially updated as the process progresses. The analysis process consists of three applications for the different events in August 2003, August 2004, and September 2004, respectively. At the first application for the August 2003 flood, the initial range of Manning’s *n* is set by certain values for the main channel, flood plain, and inundation area. Then, from the second application for the August 2004 flood, the initial range of Manning’s *n* is set by the 90% interval estimated at the final step of the previous application.

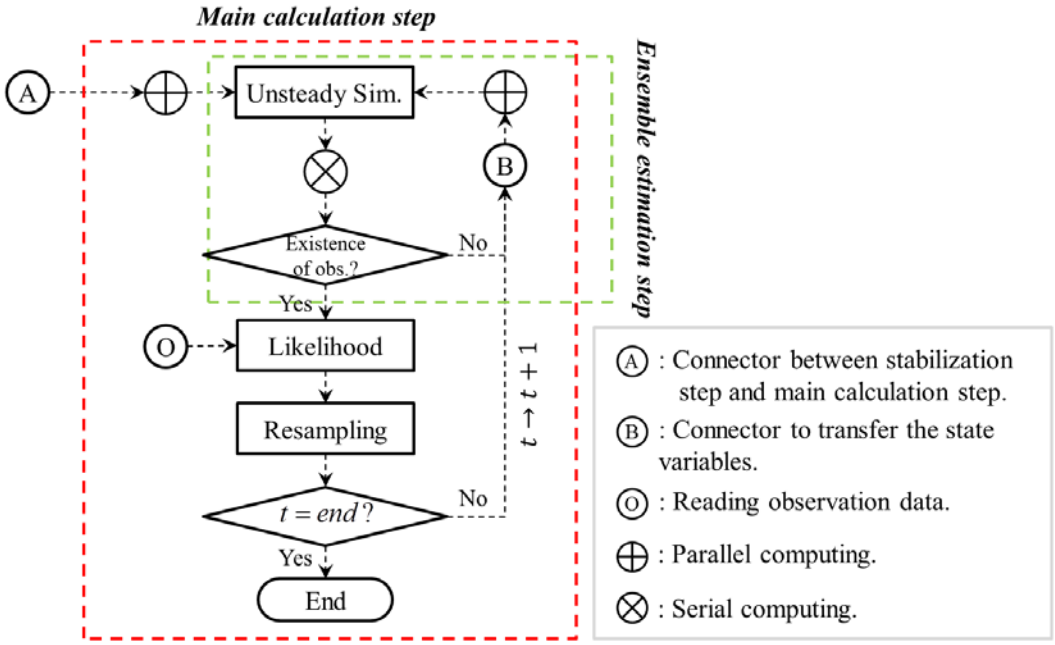

Figure 5-1 Flow chart of the estimation process.

Fig. 5-1 also shows the process to estimate the discharge of 2011 flood. The estimation method is the same as that applied to the three historic floods. However, the resampling step stops after the upstream water level used as the reference data does not exist due to exceed the observation range. In case of no data as a reference data of the estimation process, the process proceeds without resampling. The distribution of the inflow boundary discharge and Manning's *n* follow the distribution of the final step result when there is resampling.

For the application of the method to the largest flood in 2011, an upper boundary inflow is used as an averaged hydrograph estimated by a distributed hydrological model with different parameter sets optimized for different events (Meno, et al., 2012). A noise term is added to the inflow, and it is used for the upper boundary condition. Manning's *n* is used for the finally estimated value from the third event occurring in September 2004, which is used for the initial range of the channel roughness to estimate the discharge of the largest event in 2011.

5.3 Simultaneous estimation of discharge and channel roughness

5.3.1 Study area

The study area is the Kumano River located in the Kii peninsula, Japan. The total reach length is about 11km from the Hitari water stage station to the Ouga water stage station, which are located at upstream and downstream boundaries, respectively. The calculation domain is composed of 212 longitudinal points and 88 cross sectional points for a 2D hydraulic model (Fig. 5-2). The channel roughness is classified into three parts: main channel, flood plain, and inundation area. These parts are classified by the aerial photo. As upper boundary inflow conditions, the upstream discharge from the tributary (the Akagi River) and the main channel (the Kumano River) are considered. The lateral inflow to the channel reach is disregarded because the largest volume per second is smaller than 600m^3/s even in the largest flood in 2011 as estimated by the distributed hydrologic model.

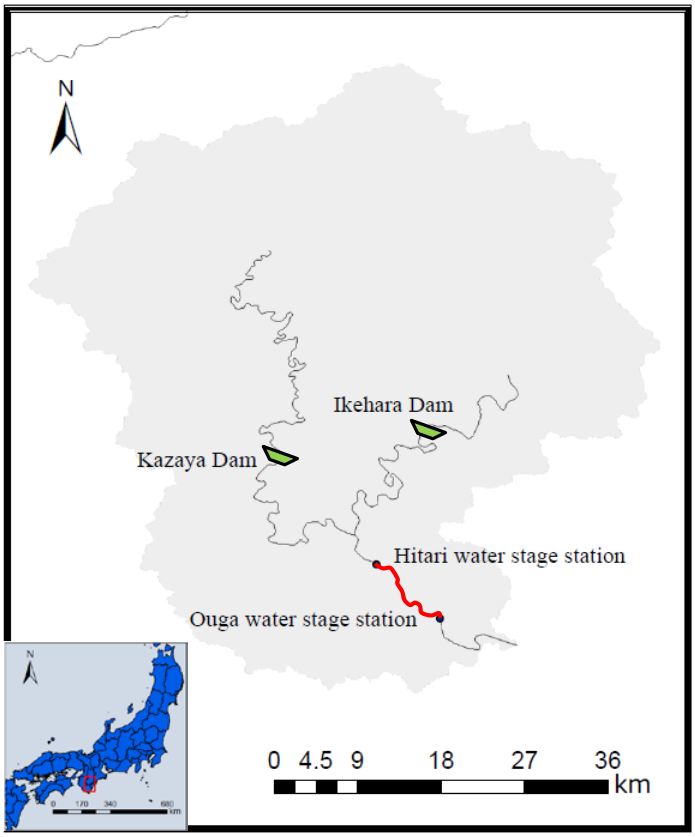

Figure 5-2 Watershed area of the Kumano river located in Kii Peninsula, Japan.

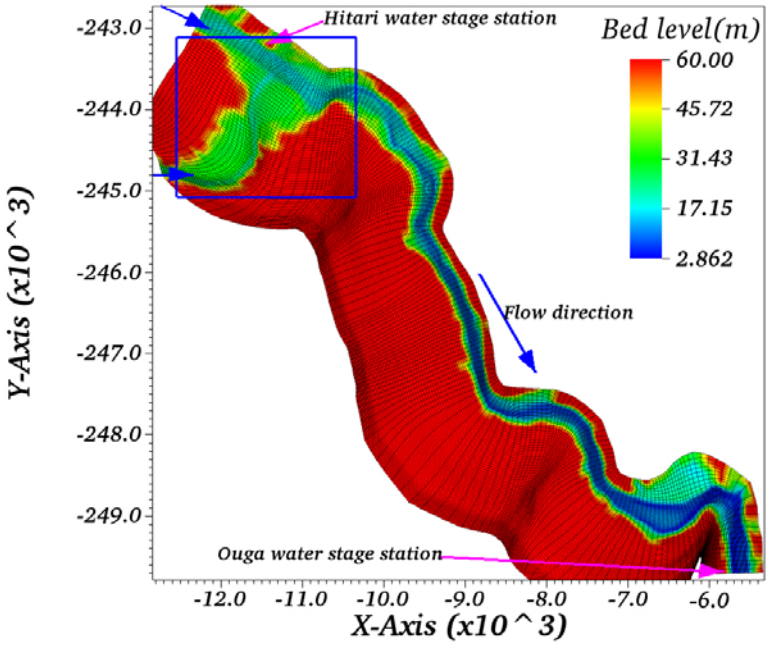

Figure 5-3 Calculation domain of the 2D hydraulic model.

5.3.2 Perturbation equation of the method

PFs perform the Sequential Monte Carlo (SMC) estimation based on particle representations of probability densities within Bayesian theorem (Ristic et al., 2004). The main purpose of PFs is to track a target variable as it evolves over time, typically with a non-Gaussian and multi-modal probability density function (Rekleitis, 2004). Particularly, PFs have special advantages in dealing with non-linear systems. Among the various PFs, Sequential Importance Resampling (SIR) is introduced in this study (Ristic et al., 2004).

In general, PFs require a number of particles for estimation and prediction, which sometimes causes equifinality problems. Kim et al.(2012(b)) introduced the reduction factor and the variance tuition factor into the perturbation step to reduce the effect of the equifinality problems which are induced by the interaction of the variables(e.g., discharge and Manning's *n*) when utilizing the water level data as reference data. The perturbation step consists of two steps: one is at the initial stage and another is at the updating stage. At the initial stage, the perturbation equations for each variable are as below:

$$H_0^i = H_0^{obs,down} + \varepsilon_{H,0}^i, \qquad \varepsilon_{H,0}^i \sim \mathrm{N}(0,0.1^2) \tag{5-1}$$

$$Q_0^i = Q_0^{hydro,up} + \varepsilon_{Q,0}^i, \qquad \varepsilon_{Q,0}^i \sim \mathrm{U}\left(0.7Q_1^{hydro,up}, 1.3Q_1^{hydro,up}\right) \tag{5-2}$$

$$n_0^i = \varepsilon_{n,0}^i, \qquad \varepsilon_{n,0}^i \sim \mathrm{U}(\alpha,\beta) \tag{5-3}$$

where $H_{0,1}^i$ and $H_1^{obs,down}$ are the downstream water level of each particle and the observed water level at downstream, respectively; Q_0^i and $Q_0^{hydro,up}$ are the upstream discharge of particle i and the discharge obtained from a hydrological model, respectively; n_0^i is the Manning's n of particle i at time t for the main channel; and

α and β are determined by 0.02 to 0.06, 0.02 to 0.08, and 0.04 to 0.1 to the main channel, flood plain, and inundation area, respectively.

At the updating stage the perturbation equations for each variable are as follows:

$$H_t^i = H_t^{obs,down} + \varepsilon_{H,t}^i, \qquad \varepsilon_{H,t}^i \sim \mathrm{N}(0,0.1^2) \tag{5-4}$$

$$Q_t^i = Q_{t-1}^{re,up} + c_t^i(Q_{t-1}^{hydro,up} - Q_{t-2}^{hydro,up}) + \varepsilon_{Q,t}^i, \quad \varepsilon_{Q,t}^i \sim \mathrm{N}\left(0,(0.1Q_{t+1}^{hydro,up})^2\right) \tag{5-5}$$

$$c_t^i = \left(\frac{\hat{Q}_{t-2}^{in}}{Q_{t-2}^{hydro,in}} + \frac{\hat{Q}_{t-1}^{in}}{Q_{t-1}^{hydro,in}}\right) \times 0.5$$

$$\text{In case} \quad \mathrm{Var}_{t-1}^{n} \geq 0.002^2, \qquad n_t^i = n_{t-1}^i + \varepsilon_{n,t}^i, \qquad \varepsilon_{n,t}^i \sim \mathrm{N}(0, s^2\mathrm{Var}_t^n) \tag{5-6}$$

$$\text{In case} \quad \mathrm{Var}_{t-1}^{n} < 0.002^2, \qquad n_t^i = n_{t-1}^i + \varepsilon_{n,t}^i, \qquad \varepsilon_{n,t}^i \sim \mathrm{N}(0,0.002^2) \tag{5-7}$$

where N indicate normal distribution; s is the tuition factor for the variance reduction proposed by Moradkhani et al. (2005); and Var_{t-1}^n is the variance calculated at the current step for the weight averaged values; c_t^i is the recursive correction factor, which is determined by relationship between the weight averaged values of particle and the discharge obtained from a hydrologic model at time *t*-1 and *t*-2.

In case that Var_{t-1}^n is smaller than the 0.002^2, Eq. (5-6) is applied to maintain the minimum tracking ability and to consider the change of Manning's *n* as the channel evolves. In addition, the same equation is applied to the flood plain and inundation area. Manning's *n* for the specific area is excluded from the filtering target when the number of wetted grids is smaller than 10% of the number of total grids of each classified zone.

At the resampling step, the likelihood of each particle against the observed water stage is calculated using the Gaussian function as Eq. (2-25). The standard deviation(σ)

associated with the observed stage (H_t^{obs}) and determined by 0.2m. Then, the normalized weight(W_t^i) is calculated by Eq. (2-26).

5.3.3 Estimation results

For the purpose of identifying the channel roughness of the river channel, the method was applied sequentially to the flood events in August 2003, August 2004, and September 2004. Through the sequential applications with 120 particles, Manning's *n* is continuously quantified. Figs. 5-4, 5-5, 5-6 and 5-7 show estimated upstream water levels, upstream discharge, and Manning's *n* for the main channel and flood plain, respectively. Figs. (a), (b), and (c) in each graph indicate the events occurring in August 2003, August 2004, and September 2004, respectively. In each figure, the cyan and the yellow color area indicate the 70% and 90% intervals of the particles. The black line means weight averaged values, and red points indicate the value of each particle. The black points in Fig. 5-4 are the observed water level used for reference data in the estimation process to calculate the weight of each particle. The estimated water level follows the observed water level as the process progresses as shown in Fig. 5-4.

In terms of Manning's *n*, the initial range at main channel, flood plain and inundation area is set at 0.02 to 0.06, 0.02 to 0.08 and 0.04 to 0.1, respectively. From the second application, the initial range of Manning's *n* is set by the 90% interval of the final step in the previous application (Fig. 5-5 and 5-6). As shown in Fig. 5-6 and 5-7, the variation of Manning's *n* is continuously reduced, but the minimum errors are maintained to keep the tracking ability.

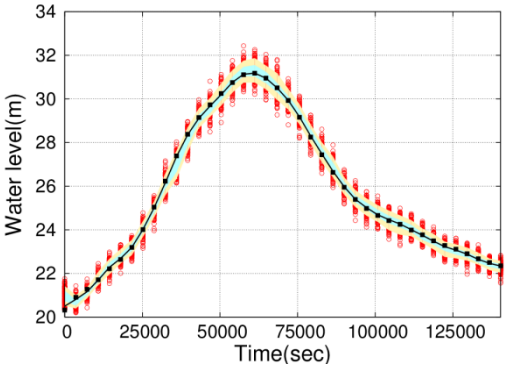

(a) Ev_2003(1)

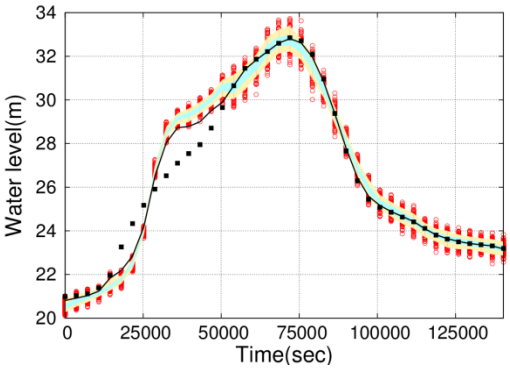

(b) Ev_2004A(2)

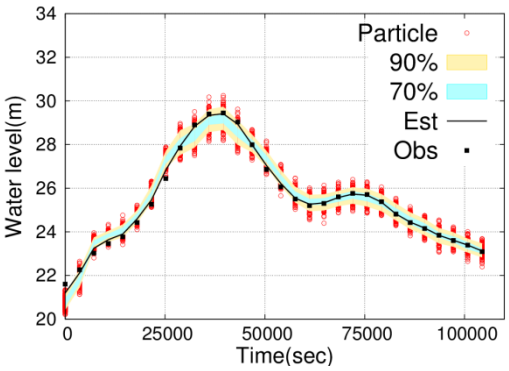

(c) Ev_2004B(3)

Figure 5-4 The comparison between the estimated water level and the observed water level at upstream.

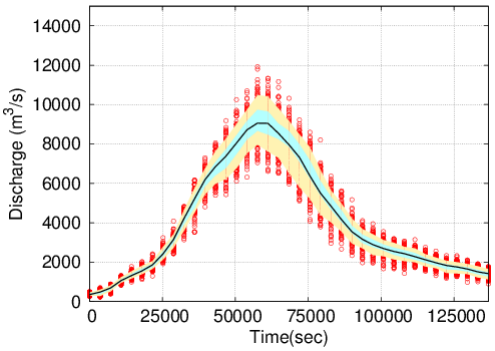

(a) Ev_2003(1)

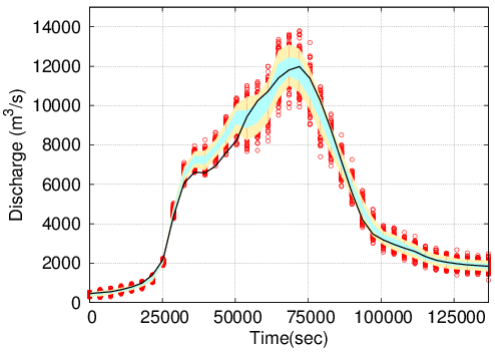

(b) Ev_2004A(2)

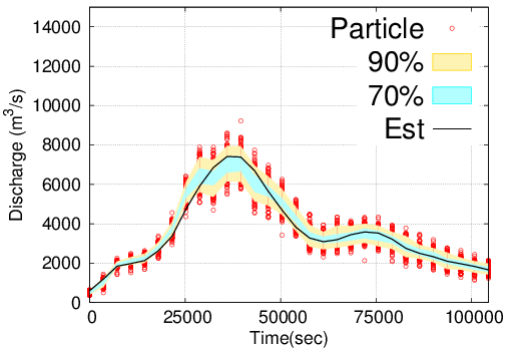

(c) Ev_2004B(3)

Figure 5-5 Estimated discharge from the proposed method.

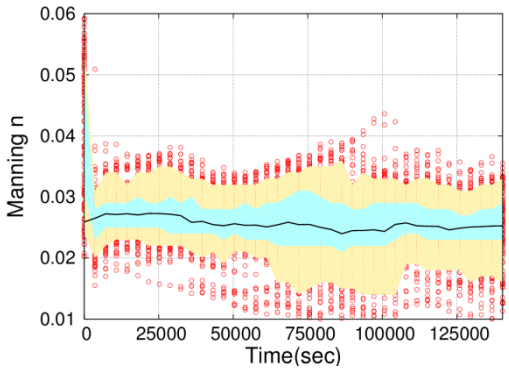

(a) Ev_2003(1)

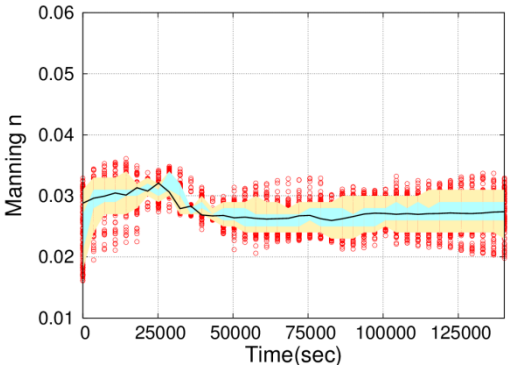

(b) Ev_2004A(2)

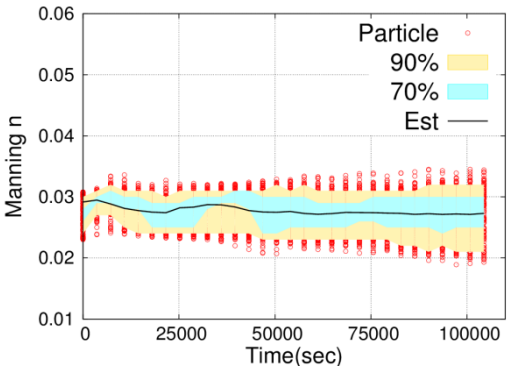

(c) Ev_2004B(3)

Figure 5-6 The estimated Manning's *n* at the main channel.

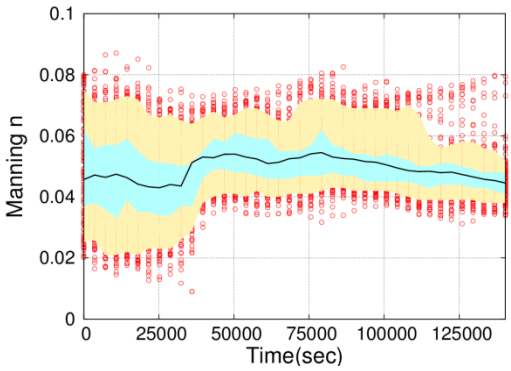

(a) Ev_2003(1)

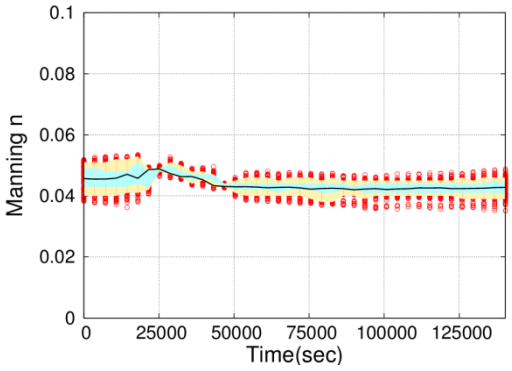

(b) Ev_2004A(2)

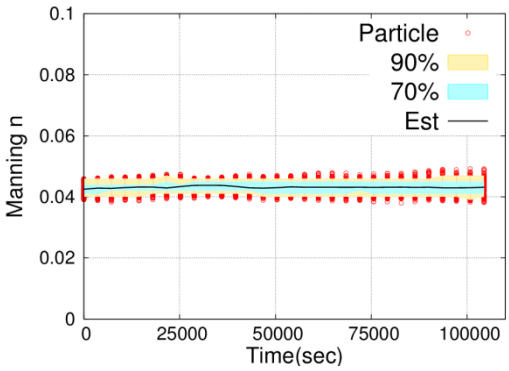

(c) Ev_2004B(3)

Figure 5-7 The estimated Manning's *n* at the flood plain.

5.4 Estimating 2011 flood discharge

The method shown in Fig. 5-1 is applied to estimate the discharge of the event occurring in September, 2011. The observed water level at upstream exists until 5am on September 3, which is roughly 24 hours before flood peak. Then the water level at upstream exceeds the measurable range of the station. Therefore the estimation process is proceeding by the method proposed by Kim et al., (2012(b)) before 5am September 3. The initial range of Manning's *n* is set by the values, which are 0.021~0.033, 0.040~0.047, and 0.057~0.08 at the main channel, flood plain, and inundation area, respectively, from the previous analysis process. After 6am on September 3, there is no reference data, so the weight of each particle is fixed by the values at the last time step of the update estimation, and is maintained for the subsequent simulation.

In terms of an upstream boundary condition, an averaged hydrograph for the main channel and the tributary (the Akagi River) from the hydrological model with different optimized model parameters (Meno et al., 2012) are considered. The difference between each hydrograph is smaller than 15% of the given discharge at each time step.

The estimated discharge at Ouga is plotted in Fig. 5-8. The updating procedure is implemented in the section where the percentile interval is located. For the verification of the peak discharge in 2011 flood, we utilized the observed flood marks provided by Wakayama prefecture. The flood marks are compared with the highest water level in each particle of the estimation process in Fig. 5-9. As shown in Fig. 5-9, almost all of the flood marks are within the lower parts of the highest water level of particles. This tendency is induced by the effect of the hydrological model outputs because there is a limitation to predicting discharge uncertainties from the time without updating. The level of flood marks at the Hitari station is about 41.4m, and the particles including the highest water level within 0.5m from 41.4m are tracked. From the corresponding particles, the peak discharge at the Ouga station is estimated in the range from

22500m^3/s to 25500m^3/s when considering errors by ±0.5m from the flood marks (Fig. 5-8). Then the inundation areas estimated by the 2D hydraulic model to have the highest water surface profile similar with flood marks in Fig. 5-9 are compared with the inundation map provided by Wakayama prefecture. The red broken line indicates the inundation area, and it shows good agreement with the simulated results (Fig. 5-10).

In addition, the discharge estimated from the estimation process and the observed water level at downstream are utilized to examine the rating curve at Ouga station. The rating curve is treated as the following power function:

$$Q = a(H_t^{up,obs} - H_0)^b \tag{5-8}$$

where a and H_0 are the constants, and b is an exponent. They define the unique relation between discharge and water level of the open channel.

The rating curves ((1), (2) and (3) in Fig. 5-11) are established from the estimated results of the three events. Then the rating curve considering the estimated results of 2011 flood and the three events, the old rating curve and the current rating curve developed by MLIT are compared. Through the comparison, it is confirmed that the rating curve established from the estimated results is similar to the currently used rating curve. It shows that sequential applications of the estimation process are able to establish a rating curve comparable with the current rating curve. Using the established rating curve and the observed water level, the peak discharge at Ouga station is estimated by about 25,300m^3/s.

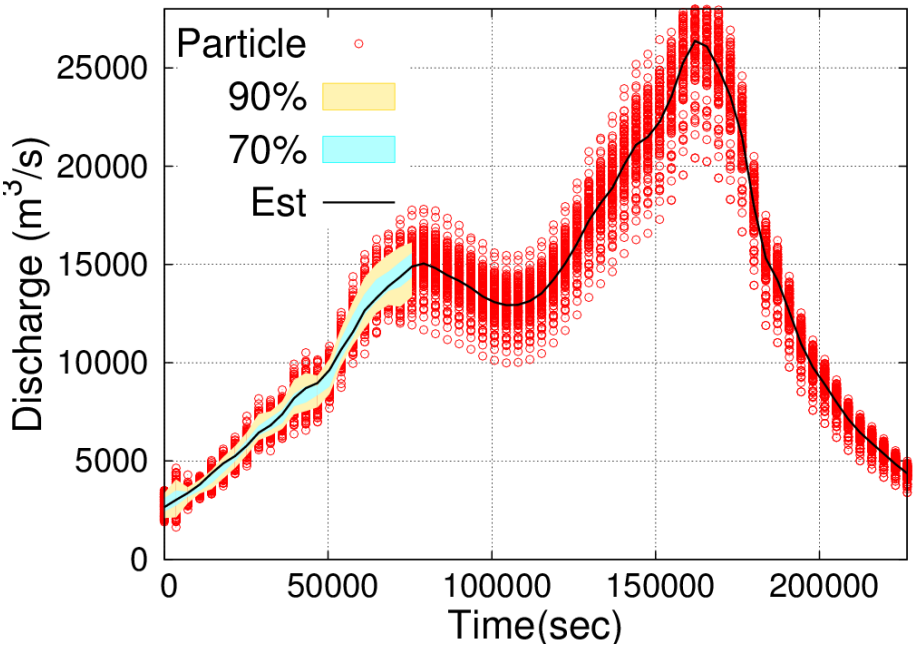

Figure 5-8 Discharge estimated from the estimation process at the Ouga station.

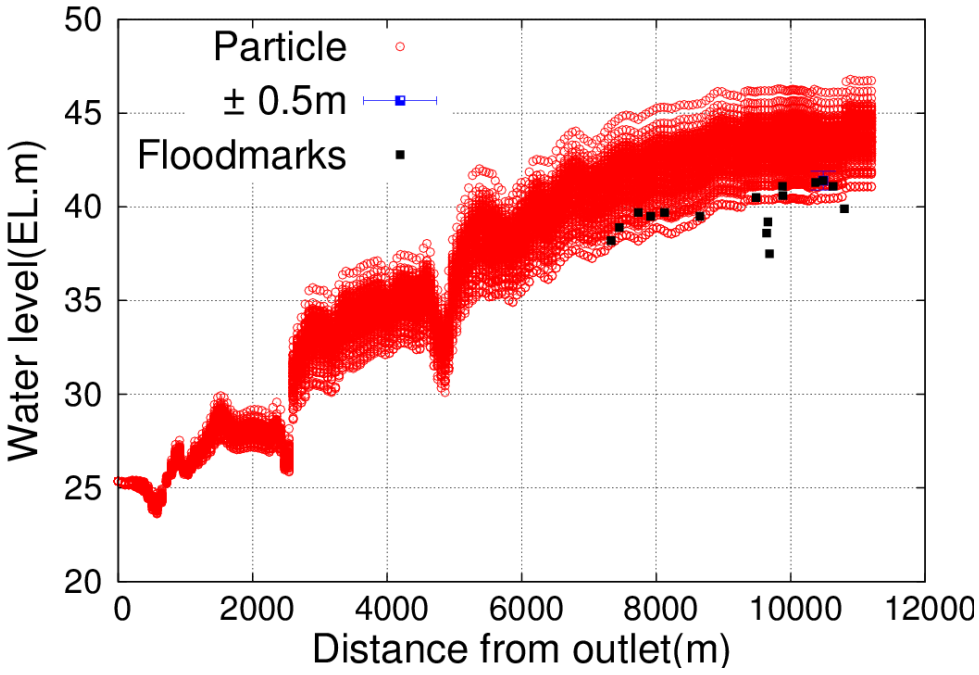

Figure 5-9 Comparison between the flood marks and the highest water level estimated from the estimation method.

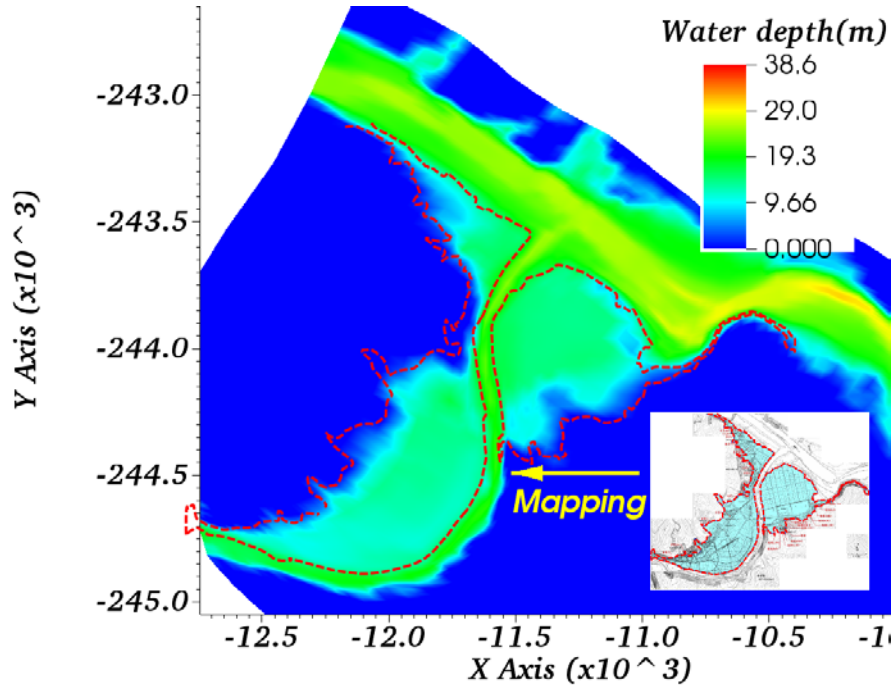

Figure 5-10 Comparison of an inundation area, which is the upper part of the study area(as shown in Fig. 2 by a blue line) and is marked by a red broken line to compare a simulated inundation area with an observed inundation area(bottom right).

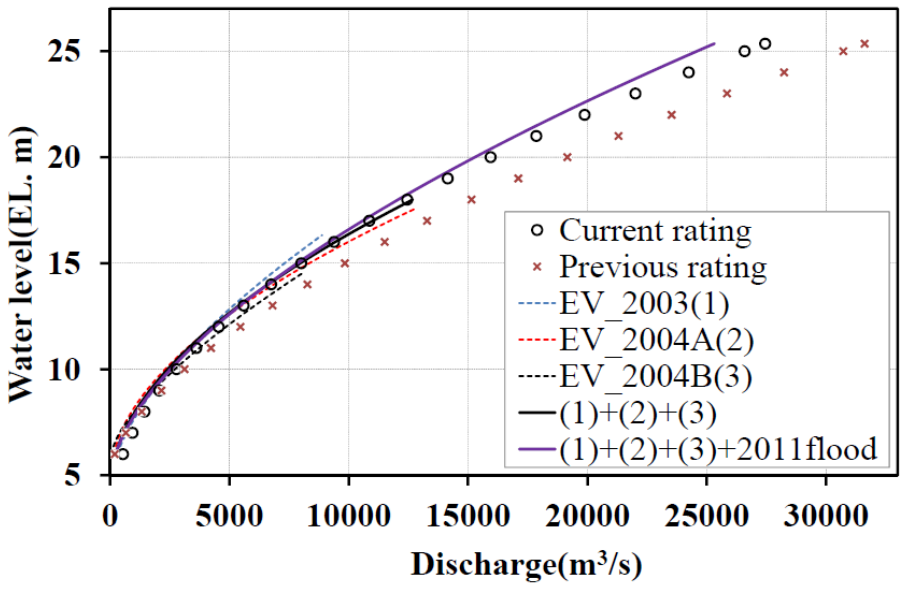

Figure 5-11 Comparison between an estiablished rating curve and the existing rating curve at the Ouga station.

5.5 Summary

An estimation method using a 2D dynamic wave model and particles filters are introduced to estimate the discharge of the event occurring in September, 2011. Before estimating the discharge of the event, the uncertainties of the channel roughness for the main channel, flood plain, and inundation area are quantified by the sequential application of the method. With the quantified channel roughness, inflow to the upper boundary is also estimated from distributed hydrological model outputs. The discharge of the largest event is estimated by considering the uncertainties of roughness coefficients and upper boundary inflows. For the verification of the peak discharge, the highest water level of each particle is compared with flood marks. By the comparison to the flood marks, the peak discharge is estimated in the range from 22500m^3/s to 25500m^3/s. In addition, the rating curve established from the estimation process is compared to the currently updated rating curve.

In further research, the estimation process would be combined with a hydrological model to improve the predictability of the water stage and the uncertainties of the hydrologic parameters.

Chapter 6. Establishing a rating curve with consideration of uncertain characteristics of river channel using particle filters and smoothing without discharge measurement

This chapter enhances the treatments of the upper boundary conditions used in the previous chapters. An upstream boundary condition is generated from an existing uncertain rating curve in chapters 3 and 4 and from a hydrologic model in chapter 5. The former method is only available at the locations where both of discharge and water stage are available. Then the latter one has the limitations in dealing with unexpected errors caused by a hydrologic model.

For the sake of improving the above mentioned problems, the linearized power function is introduced in the resampling process. Moreover, to avoid degeneracy caused by SIS and impoverishment caused by SIR, generic particle filters are introduced. Using the filtering, the approximate distributions of the Manning's n and index of the power function are estimated. Then to estimate the reasonable reference values from the filtering results for the practical use, smoothing is implemented based on trajectory tracking in reverse time direction. The method is applied to the Katsura River located in Kyoto, Japan. The river reach is about 5.4km from Tenryuji water stage gauging station to Katsura water stage gauging station. To verify the method, the estimated results are compared with the discharge observed at the upstream gauging stations.

6.1 Introduction

Stage-discharge relations using a power function or quadratic equation have been utilized for a century due to their efficiency and availability when using the one-to-one relationship between stage and discharge. They are generally established based on finite measured samples composed of discharge and water stage. Thus, their one-to-one relationships include a number of uncertainties, as pointed out by Pelletier(1987) and Di Baldassarre and Montanari(2009), as they do not reflect the unsteadiness of flood flow. The discharge data, which is converted from the relationship equation with the continuously observed water stage, is often utilized because of its simplicity in calibrating the parameters of hydrologic models and utilizing it by the boundary conditions of a hydraulic model. Thus, their uncertainties are propagated to the results of hydrologic and hydraulic simulation (Tillaart, 2010).

To improve or quantify the discharge uncertainties, field investigations are mainly performed. Although the direct measurement of discharge is the best way to deal with uncertainties, the accuracy of discharge measurement changes according to the observers' competence, and requires a great deal of efforts and a large budget. As an alternative, several indirect approaches are taken to improve the uncertainties of a rating curve using the continuously measured water stage contrary to the rarely measured discharge.

First, the simple slope-area method based on Manning equation enables the calculation of the discharge roughly from the bed slope, channel roughness, and cross section of the river reach. The method estimates the discharge based on the uniform flow assumption, so it can not consider backwater effect or geomorphological effect.

Then, the one dimensional dynamic wave model (1D model), which solves Saint Venant's equation, is introduced to consider the unsteadiness of the flood and its geomorphologic effect (Schaffranek et al., 1981; Rantz, 1982). These methods have

improved the discharge using simulation, but the simulations are generally affected from the sets of boundary conditions and parameters. Thus it is necessary to consider all feasible potential conditions, as pointed out by Schmidt(2002). In the various conditions, errors are caused from inputs, parameters, and system such as numerical stability, accuracy, diffusion, and dissipation (Schmidt, 2002; Gonzalez-Castro and Yen, 2000), and these have to be considered together because they are able to result in unpredictable errors.

Next, studies about boundary conditions using a dynamic wave model are performed to reconstruct the flood hydrograph at both ends of the river reach (Onda et al., 2006; Hosoda et al., 2008; Hosoda et al., 2010). They introduced the quadratic equation driven from the method of characteristics (MOC). The parameters of the equation were calibrated against the time series water stage of the gauging station located in the middle of the river reach. Their reconstructed hydrographs at both ends of the river reach show good agreements with the observed hydrographs. It shows that a dynamic wave model can be used to estimate boundary conditions with several assumptions. However, the time term coefficient included in the equation to generate boundary conditions limited the applications because the parameters varied according to the change in time.

After that, studies dealing with the discharge uncertainties are implemented. Thirel et al.(2010(a)) and Thirel et al. (2010(b)) proposed a method to estimate the discharge using a coupled model (hydrologic model and hydraulic model) with a satellite image. To deal with the uncertainties of image and discharge, Best Linear Uncertainties Estimation (BLUE) method is utilized. In addition, Particle Filters (PFs) are applied to a one-dimensional hydraulic model (Montanari et al., 2009; Matgen et al., 2010; Giustarini et al., 2011), and show that PFs can reduce the uncertainties of the discharge and water stage by updating the water stage using satellite imagery. However, Manning's *n* was determined using the trial-and-error method with a certain discharge. In other words, the uncertainties of Manning's *n* were not considered.

Finally, Tachikawa et al.(2011), Kim et al. (2012(a)), Kim et al. (2012(b)), and Kim et al. (2013) combined the particle filters with a dynamic wave model to incooperated the errors into parameters and inflow. The one dimensional dynamic wave model showed limitations in estimating inflow using the water stage (Tachikawa et al., 2011; Di Baldassarre and Montanari, 2009). Thus, the approaches using a 2D dynamic wave model are implemented to enhace the availability of the water stage as an observation data considerting the geomorphologic effects of a river reach (Kim et al., 2012(a); Kim et al., 2012(b); Kim et al., 2013). These method have limitations in that they require the reference discharge for an estimation.

Therefore, this chapter focused on dealing with the results approximated by the particle filters to estimate the inflow and Manning's roughness coefficient, which is appropriate for the whole time history. Smoothing is implemented on the basis of trajectory tracking in a time-reversed direction to estimate a reasonable range for the targeted values, and to evaluate their uncertainties. The results are verified with the observed discharge at the upstream end.

6.2 Method

The key idea of the proposed method is to estimate discharge and channel roughness from the approximated distributions of them obtained from particle filters using a smoothing. Particle filters are rigorously validated as tools for tracking the distribution of, and estimating the values of a hidden state as time progresses. Smoothing focused on obtaining sample realizations from the entire smoothing density (Godsill et al., 2004). The proposed method is largely composed of a series of filtering step and smoothing step combinations. At the filtering step, the distributions of Manning's *n* and the index exponent of the rating curve following power function are approximated using particle filters and a 2D dynamic wave model. The simulation conditions for the 2D dynamic wave model are set by the given information, such as channel geomorphology, aerial

photo, and time-series water stage. The aerial photo is used to identify the conditions of a river channel such as their vegetation distribution and a hydraulic structure, and the measured cross sections of the river channel and time series water stage are utilized to confirm the volumetric capacity of the river channel using a 2D dynamic wave model.

As boundary conditions of 2D dynamic wave model, upstream discharge and downstream water stage were used. The simulations were only implemented after the water stage is available at both ends of the river reach. Using the upstream water stage, an upstream discharge is generated from the simple simultaneous equation derived from the artificial relationship between the water stage and discharge. Then we assume that the lateral inflow within the channel reach is proportional to the ratio of the watershed at the gauging station by 10% of upstream inflow.

Based on the filtering results, the trajectories of the particles are tracked in time reversed direction and smoothing is implemented to confirm whether the results are fitted for the whole time series water stage or not. Finally, to verify the method, the rating curve established from the results of smoothing is compared with observed data.

6.2.1 Particle filters

Among various particle filters, generic particle filters are introduced. In this section, the generic particle filters, noise scale, and perturbation equations will be explained.

(1) Generic particle filters

Fig. 6-1 shows the flow chart of generic particle filters (Ristic et al., 2004), which is composed of Sequential Importance Sampling(SIS) and SIR(Sequential Importance Resampling), is introduced to avoid the effect of degeneracy, which means that one particle has negligible weight after several recursive steps, caused by SIS and the sample impoverishment, which leads to a loss of diversity of particles caused from SIR. Then the implementation of SIS or SIR is determined by the number of effective

particles, which in turn is calculated from the weight at the updating step, such as in Eq. (6-1).

$$\hat{N}_t^{eff} = \frac{1}{\sum_{i=1}^{N} \left(w_t^i\right)^2} \tag{6-1}$$

where, $\hat{N}_t^{eff}$ is the number of effective particle; w_t^i is the normalized weight at time t of particle i.

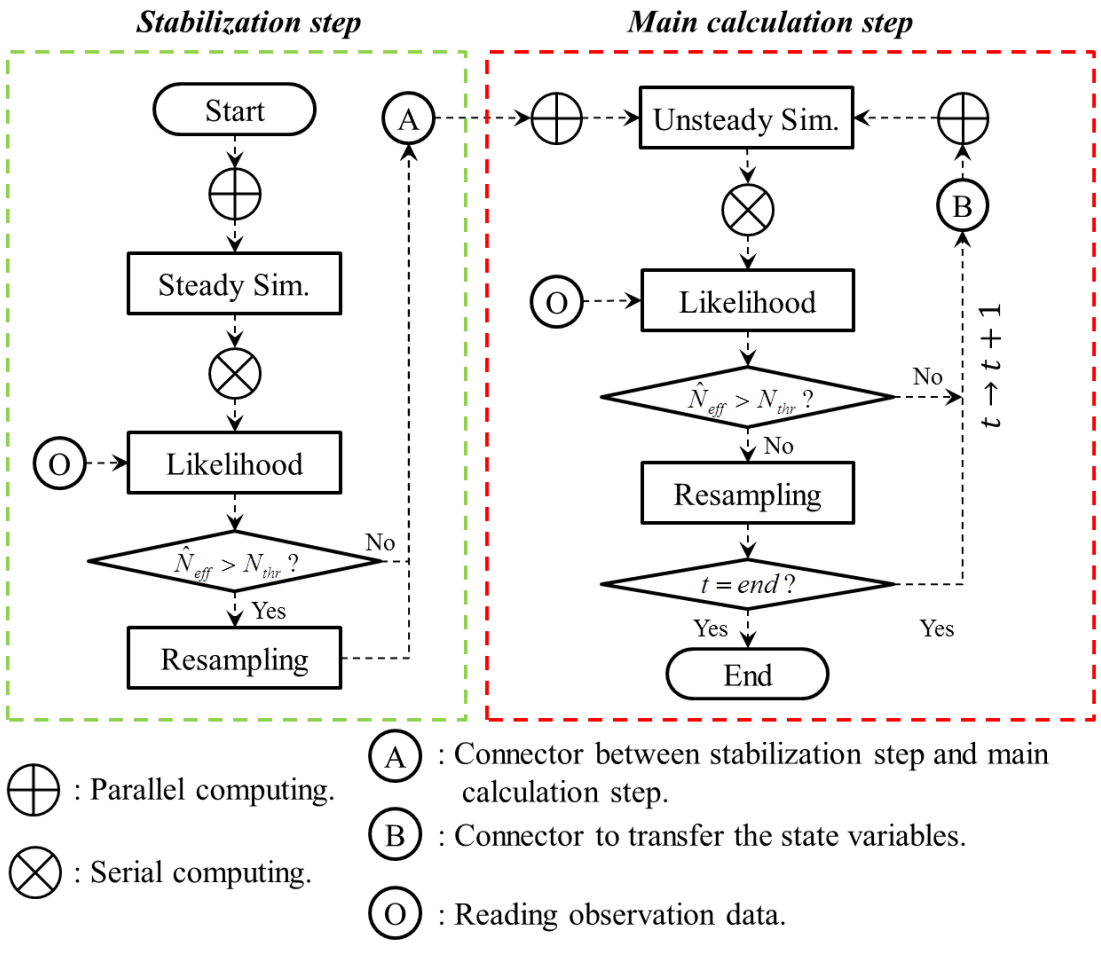

Figure 6-1 Flow chart of the method using 2D dynamic wave model and generic particle filters.

Although Kim, et al. (2012(a)) and Kim, et al. (2012(b)) showed that SIR provides reasonable results in estimating Manning's *n* and inflow simultaneously, their study area is only influenced by the channel control. Unlike these study areas, the method of this chapter is applied to the area influenced by section control and channel control at low flows and high flows, respectively. Thus rapidly reduced diversities of particles by introducing SIR induced the failures of tracking the targeted values in simulations.

(2) Determination of noise scale

The noise scale is important factors to determine the variations of particles and the tracking ability. Thus the noise scale of inflow, Manning's *n*, and water stage will be described in this section.

At first, observational errors(ε_H) of water stage are assumed to be results of gauging errors, channel measurement errors, grid generation errors, and independence from each other. Then the measurement error of the pressure gauging station is set by the normal distribution drawn from $N\left(0,0.05^2\right)$ (Boiten, 2000). Next, channel geomorphologic errors in surveying is determined by the normal distribution drawn from $N\left(0,0.045^2\right)$, which is calculated by the equation ($\sigma_{\varepsilon_H^2} = s\sqrt{L(km)}$) and s is utilized in leveling by 2~5mm per kilometer in level and L is the measured distance. Finally, the grid generation error is determined by the normal distribution drawn from $N\left(0,0.123^2\right)$, which is calculated by the comparison between the investigated cross section at Tenryuji station and Katsura station and the generated cross section for both cross sections. Therefore, the variation of errors at the water stage can be determined by the law of error propagation as follows:

$$\sigma_H{}^2 = (\sigma_H^1)^2 + (\sigma_H^2)^2 + (\sigma_H^3)^2 \approx (0.14m)^2 \qquad (6\text{-}2)$$

Second, the discharge errors(ε_Q) converted from a rating curve and water stage are determined by 10% (Boiten, 2000) and by 45.8% at 95% confidence interval (Di Baldassarre and Montanari, 2009). Then according to some studies (Henderson, 1966), the effect of slope term at the equation of motion is dominant, and the effect of local acceleration term, convective acceleration term, and pressure term is less than 10% of the discharge. It is very complex to consider the terms described above, so the discharge errors are determined by the uncertainties of an index of the power function. At the initial stage, the error range of the index is determined by the index supposed by Reitan and Petersen-Øverleir, 2008.

Finally, Manning's *n* is continuously changed according to the change of vegetation, evolution of channel geomorphology and so on. In this method, the application target is just one event, so Manning's *n* is considered by a fixed parameter for each section classified by a main channel, flood plain, vegetated area. Thus the minimum errors are determined by the normal distributions drawn by $N(0,0.001^2)$.

(3) Perturbation equation of particle filters

The basic concept of the sampling is already introduced by Fig. 2-2. Then magnitude of error of each variable is also determined already. Thus in this part, we will describe how to generated noise to evolve the particles when resampling in the initial and updating stage.

At first, resampling is based on the calculation of the particle's weight. The calculated upstream water stage of each particle is compared against the observed one. The likelihood is calculated by the equation (Eq. 2-25). Then the normalized weight was calculated by the likelihood as Eq. (2-26). Each particle was resampled depending on its own normalized weight using the systematic resampling method (Kitagawa, 1996; Ristic, et al., 2004).

According to the calculated weight, three parameters, which are Manning's *n* of main

channel, flood plain, and vegetated area, and two input variables, which are upstream inflow and lateral inflow, are perturbed. These are based on two assumptions: upstream inflow is generated from the artificial rating curve, and lateral inflow is proportional to upstream inflow with the ratio of the watershed area.

The perturbation method consists of two methods: one at the initial stage is based on the errors drawn from the uniform distribution, and another one at the updating stage is based on the errors drawn from normal distribution.

At the initial stage, upstream discharge, lateral inflow, and Manning's *n* for each section are perturbed with uniform distribution because of no prior information. Then the downstream water stage is disturbed by the noise drawn from the normal distribution.

$$H_0^{i,down} = H_0^{obs,down} + \varepsilon_{H,0}^{i} \qquad \varepsilon_{H,0}^{i} \sim \mathrm{N}(0,\ \ 0.05\mathrm{m}^2) \tag{6-3}$$

$$Q_0^{i,in} = q_0(H_0^{obs}) + \varepsilon_{Q,0}^{i} \qquad \varepsilon_{Q,0}^{i} \sim \mathrm{U}(0.5q_0(H_0^{obs}),\ \ 1.5q_0(H_0^{obs})) \tag{6-4}$$

$$Q_0^{i,lateral} = 0.1q_0(H_0^{obs}) + \varepsilon_{lat,0}^{i} \qquad \varepsilon_{lat,0}^{i} \sim \mathrm{U}(0.05q_0(H_0^{obs}),\ \ 0.15q_0(H_0^{obs})) \tag{6-5}$$

$$n_0^{i} = \varepsilon_{n,0}^{i} \qquad \varepsilon_{n,0}^{i} \sim \mathrm{U}(\alpha,\ \ \beta) \tag{6-6}$$

where, $H_0^{i,down}$ is water stage at downstream of i th particle at time $t = 0$; $H_0^{obs,down}$ is observed water stage at downstream at time $t = 0$; $\varepsilon_{H,0}^{i}$ is the noise drawn from normal distribution; $Q_0^{i,in}$ is upstream discharge of i th particle at time $t = 0$; q_0 indicates the discharge calculated from the simple Manning equation by the uniform flow assumption where Manning's *n* is determined by 0.03 and the factors like slope and hydraulic radius are calculated from channel geomorphology at initial upstream water stage(H_0^{obs}); $\varepsilon_{Q,0}^{i}$ is the drawn from uniform distribution, of which upper limit($1.5q_0(H_0^{obs})$) and lower limit($0.5q_0(H_0^{obs})$) is determined by that Manning's *n* is

0.02 and 0.06, respectively. $Q_{lat,0}^{i}$ is lateral inflow which is assumed proportional to upstream discharge by the ratio of watershed area; $\varepsilon_{lat,0}^{i}$ is the noise of lateral inflow drawn from uniform distribution. The limit of noise is determined by 5% and 15% of inflow. n_0^i is Manning's *n* of *i* th particle at time *t*=0; article, α and β are determined by 0.02 to 0.04, 0.02 to 0.06 and 0.05 to 0.1 for main channel, flood plain, and vegetated area, respectively.

At the updating stage, Manning's *n* is evolved with the Eqs. (4-2) and (4-3). Then, downstream is disturbed with Eq. (6-7).

$$H_t^{i,down} = H_t^{obs,down} + \varepsilon_{H,t}^{i} \qquad \varepsilon_{H,t}^{i} \sim \mathrm{N}(0,\ 0.05^2) \tag{6-7}$$

Next, the lateral inflow is disturbed with Eqs.(6-8) and (6-9) to consider the assumptions that the lateral flow is proportional to the inflow.

$$Q_t^{i,lateral} = a_t^i + \varepsilon_{Q,t}^{i} \qquad \varepsilon_{Q,t}^{i} \sim \mathrm{N}(0,\ (0.2a_t^i)^2) \tag{6-8}$$

$$a_t^i = Q_t^{i,in} \frac{Q_{t-1}^{i,lateral}}{Q_{t-1}^{i,in}} \tag{6-9}$$

where, N indicates normal distribution; $Q_{t-1}^{i,lateral}$ is the lateral inflow at time *t* of particle *i*,

To evolve the discharge, the concept of rating curve following the power function is introduced. Until time *t* reaches 3 at the low flow, the inflow is generated by the $q_t\,(H_t^{obs})$ as below:

$$Q_t^i = q_t\,(H_t^{obs}) \frac{Q_{t-1}^i}{q_{t-1}(H_{t-1}^{obs})} + \varepsilon_{Q,t}^{i}, \varepsilon_{Q,t}^{i} \sim N(0, (0.1Q_t^i)^2) \tag{6-10}$$

After generating reference discharge to establish an artificial rating curve for each particle, $C_t^{i,1}$ and $C_t^{i,2}$ of Eq. (6-11) are set as the initial values using the least square method of the 3 particles obtained from *t*=1 to *t*=3. Thus the inflow of the particles are generated with the Eq.(6-11) and the evolutions of the index and the coefficient as shown in Eq. (6-12).

$$Q_t^{i,in} = a_t^i (H_t^{obs} - H_0^{cease})^{b_t^i} \tag{6-11}$$

$$a_t^i = a_{t-1}^i + \varepsilon_{a,t}^i \qquad \varepsilon_{a,t}^i \sim \mathrm{N}(0,\ 0.1^2) \tag{6-12}$$

$$b_t^i = b_{t-1}^i + \varepsilon_{b,t}^i \qquad \varepsilon_{b,t}^i \sim \mathrm{N}(0,\ 0.1^2) \tag{6-13}$$

where, H_0^{cease} is cease-to-flow level; a_t^i and b_t^i are the coefficient and index of the rating curve at time t of particle i.

6.2.2 Particle smoothing

Then particle smoothing is introduced to draw the samples from the whole history of the particles. Then sample realizations from the entire smoothing density $p(x_{1:t}|y_{1:T})$ are obtained by following factorization:

$$p(x_{1:T}\left|y_{1:T}\right.) = p(x_T\left|y_{1:T}\right.)\prod_{t=1}^{T-1} p(x_t\left|x_{t+1:T}, y_{1:T}\right.) \tag{6-14}$$

where, $p(x_t|x_{t+1:T}, y_{1:T})$ is proportional to $p(x_t|x_{1:t})f(x_{t+1}|x_t)$ using Markovian assumptions of the model. Then the equation is approximate by $\sum_{i=1}^{N} w_{t|t+1}^i \delta(x_t - x_t^i)$. Then the modified weights ($w_{t|t+1}^i$) are

$$w_{t|t+1}^{i} = \frac{w_t^i f(x_{t+1}|x_t^i)}{\sum_{j=1}^{N} w_t^j f(x_{t+1}|x_t^j)} \tag{6-15}$$

The modified weight is able to be used to generate states successively in the reverse-time direction. The algorithm proceeds as follows:

Table 6-1 Sample realizations

1. Choose $\tilde{x}_T = x_T^{(i)}$ with probability $w_T^{(i)}$

2. For $\mathrm{t} = \mathrm{T} - 1$ to 1:

   Calculate $w_{t|t+1}^{(i)} \propto w_t^{(i)} f(\tilde{x}_{t+1}|x_t^{(i)})$ for each $i = 1, \cdots, N$

   Choose $\tilde{x}_t = x_t^{(i)}$ with probability $w_{t|t+1}^{(i)}$

3. $\tilde{x}_{1:T} = (\tilde{x}_1, \tilde{x}_2, \cdots, \tilde{x}_T)$ is an approximate realization from $p(x_{1:T}|y_{1:T})$

6.3 Application results

6.3.1 Study area

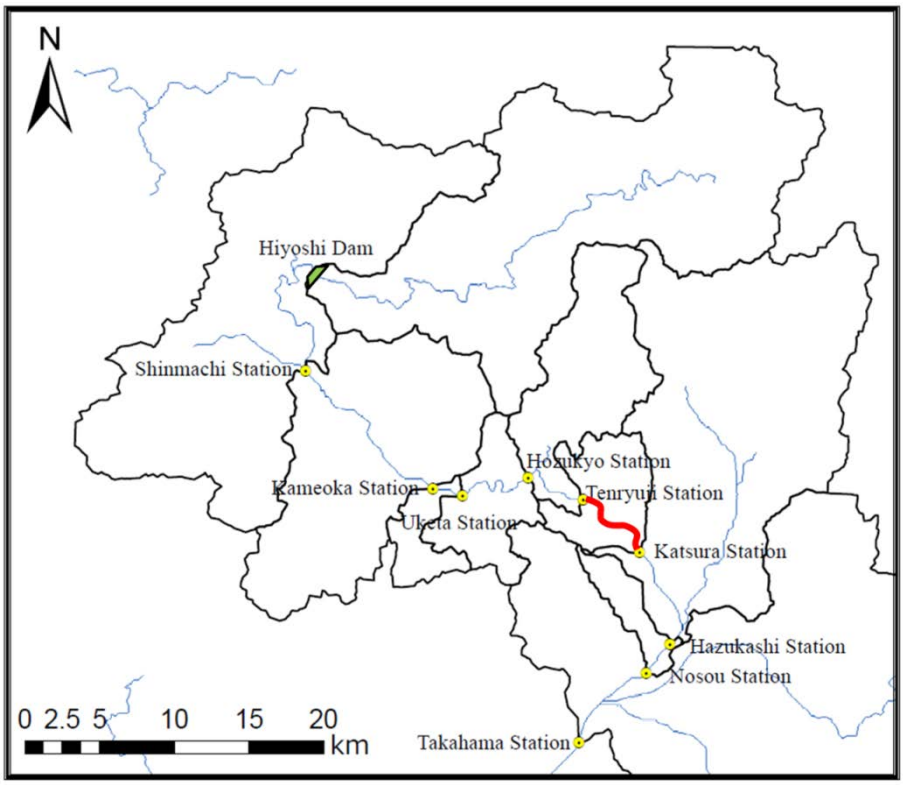

Figure 6-2 Study area and the objective channel reach, which is marked by red thick line.

The study area is the Katsura River located in Kyoto, Japan with the event occurred from 13:00 20th to 17:00 21st of October in 2004. Then the reach length is about 5.4km from Tentyuji station to Katsura station, and its calculation domain consists of 91 cross sections and 37 points on the each cross section as shown in Fig. 6-3.Water stage is continuously measured at both ends of the reach, and the channel geomorphology and aerial photo is measured at the interval of several years. Thus we could distinguish the distribution of the vegetation and hydraulic structure, and they are considered like Fig. 6-4.

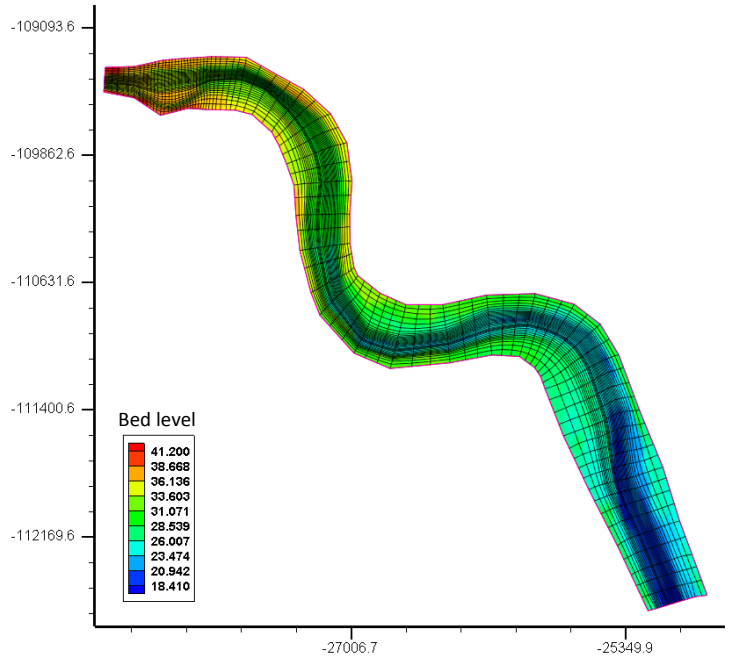

Figure 6-3 Calculation domain and bed level.

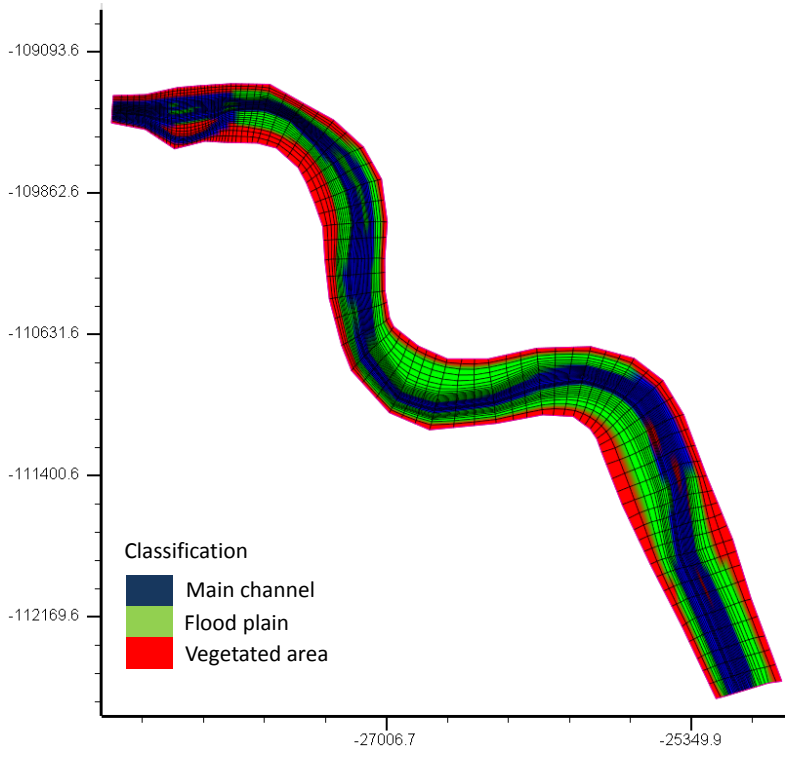

Figure 6-4 Classification of channel roughness in the calculation domain.

6.3.2 The results of PFs

For the simulations, 512 particles are utilized. The ratio of the number of the effective particles to the number of all particles is the criteria for the implementation of the resampling, and it is set by 0.8 in this application. In case that the ratio is lower than 0.8, resampling is implemented. Fig. 6-5 shows the comparison results between calculated water stage and observed water stage at the upstream end. As shown in the graph, the weight averaged water stage marked by “Est” is matched well with the observed water stage marked by “Obs”. The graph shows that the variation of water stage is quite large in comparison with the results of Chapter 3 to 5 because of the generic filters and the effect of the complex channel geomorphology, but we confirm that the variation of the water stage is reduced continuously and the performance is improved as process progresses. Thus smoothing is implemented to estimate the reasonable values for the whole time history based on the approximated distribution from the particles.

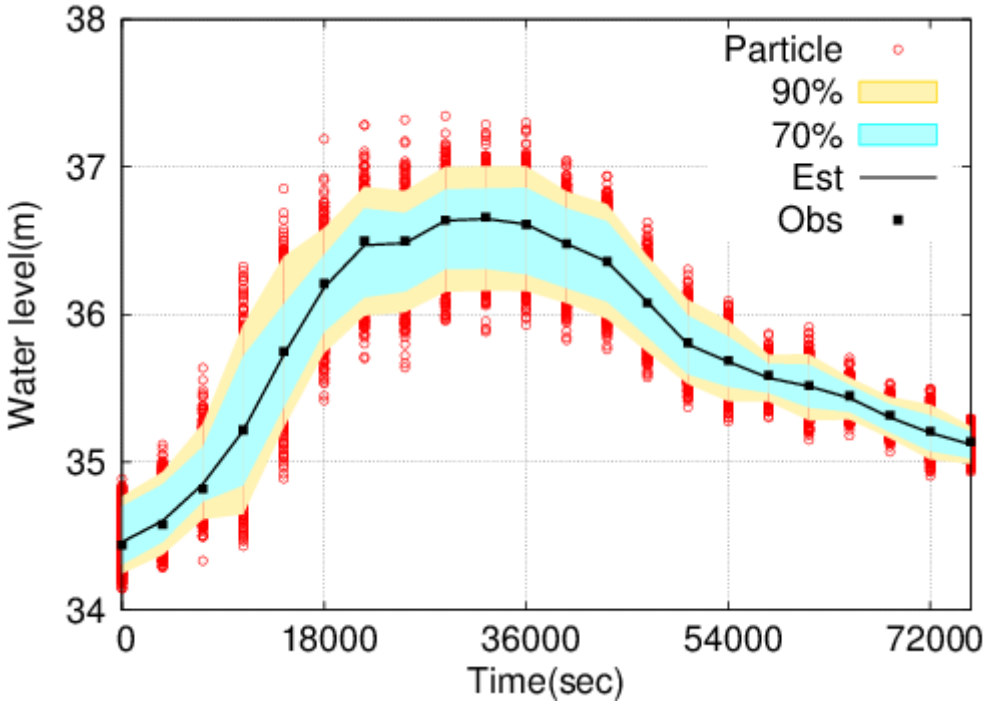

Figure 6-5 Comparison between the estimated and observed water at upstream.

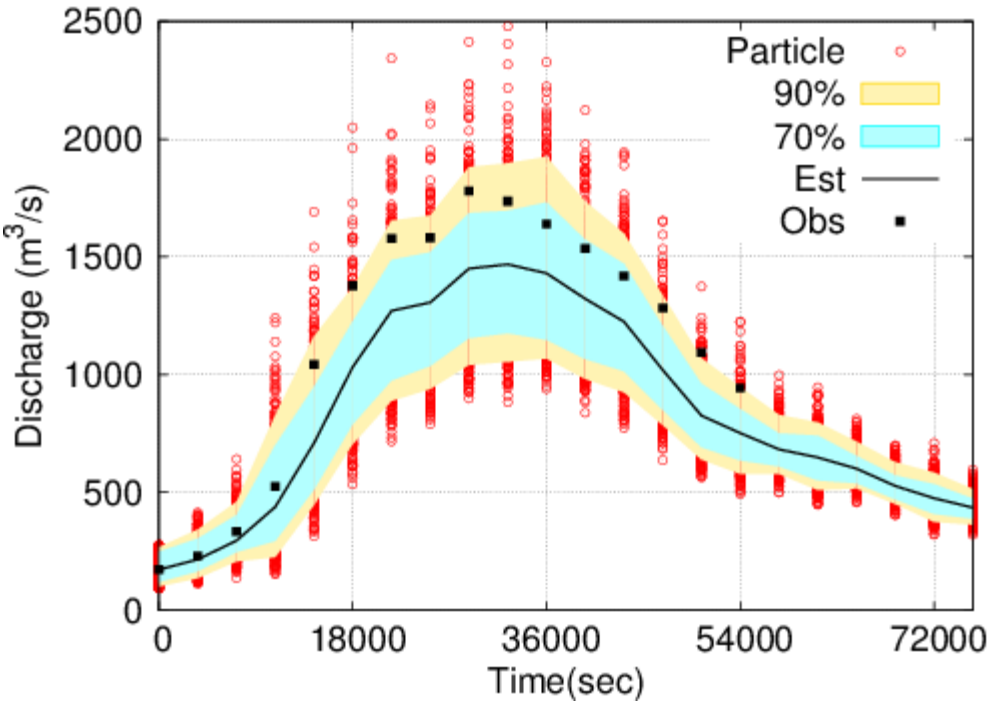

Figure 6-6 Comparison between the estimated and observed discharge at upstream.

Fig. 6-6 shows the comparison results between calculated upstream discharge and observed discharge. As shown in the graph, almost observed discharge data located within 90% interval, but the gap at the peak time is increased in comparison with the front part. The phenomenon is interpreted by the effect of the method to generate the inflow from the simple rating curve because there is a limitation to consider the unsteadiness of the river flow and the effect of the channel geomorphology.

The upstream discharge is generated from the artificial rating curve evolved with according to time. The index of the artificial rating curve following the power function is estimated, and the distributions at the certain time step are plotted in Fig. 6-7. Then the estimated coefficient of the rating curve is plotted also in Fig. 6-8. The index and coefficient represent the characteristics of the river channel in the rating curve. Thus only the distribution of the values is compared with results of Reitan and Petersen-Øverleir(2008).The distributions of the index of Figs. 6-7 shows similar pattern with Reitan and Petersen-Øverleir(2008), but the distributions of the coefficient

in Figs. 6-8 show the differences because of small noise to the coefficient.

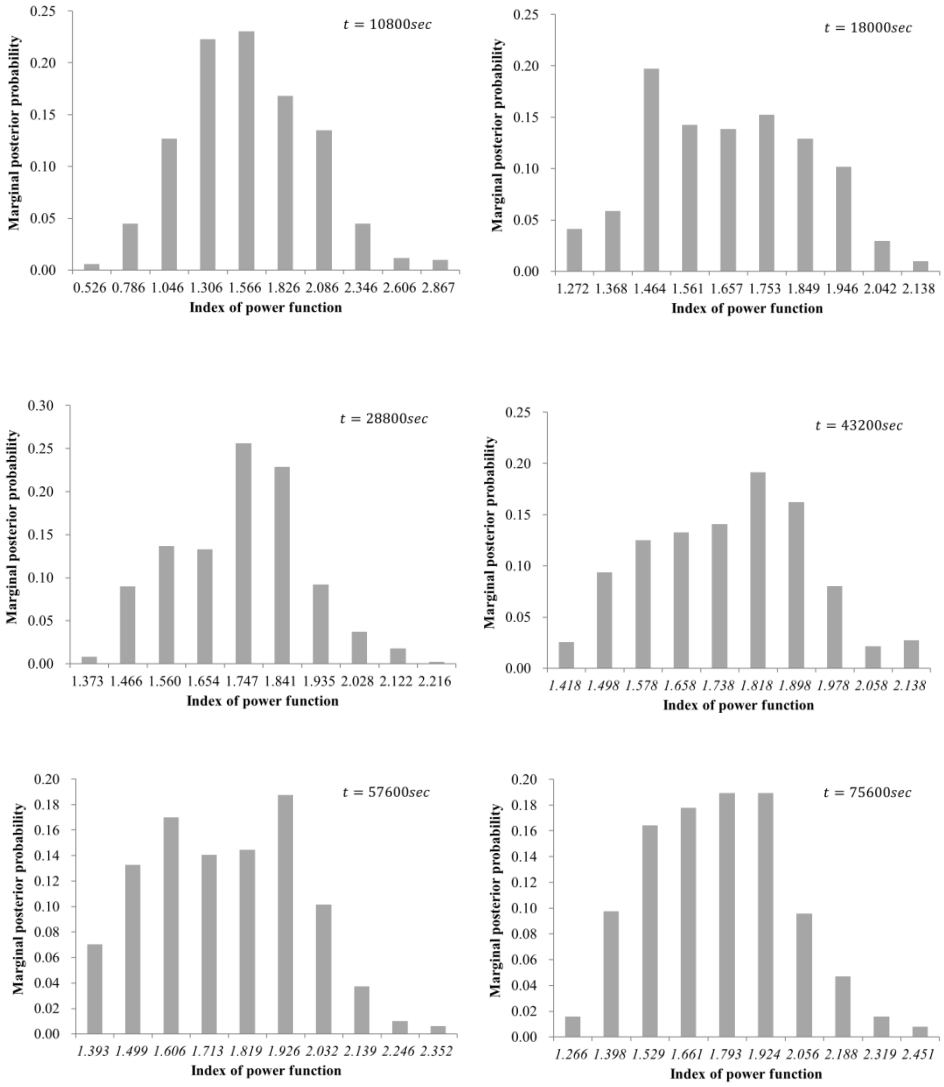

Figure 6-7 Estimated index of power function.

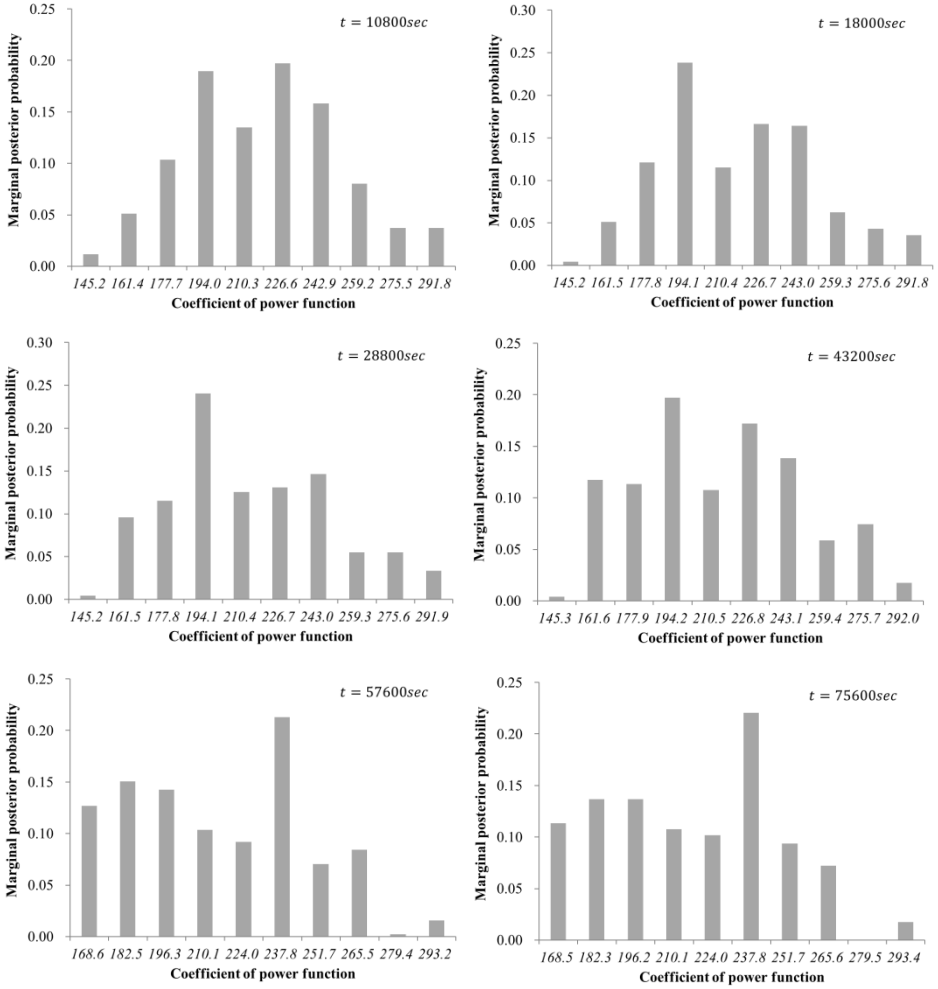

Figure 6-8 Estimated coefficient of power function

Fig. 6-9 shows the estimated Manning's *n* at the main channel. As described above, the purpose of the filtering step is to obtain the approximated distribution of the targeted values. With Fig. 6-9, we simply confirmed the estimated range, but it is difficult to identify the distribution of the particles. Thus Fig. 6-10 is plotted to understand the distributions of the variation of Manning's *n* at the main channel.

Fig. 6-11 shows the estimated results of Manning's *n* at the floodplain. The large uncertainties of Manning's *n* at the initial stage are maintained. Then unlike the distribution of Manning's *n* at the main channel shown in Fig. 6-10, Fig. 6-11 shows that the distribution of Manning's *n* is widely distributed. One of the reason is the

targeted variables are correlated closely. In previous studies (Kim et al., 2012(a); Kim et al., 2012(b); Kim et al., 2013), the flow of the study reach is only influenced by channel control, so continuous resampling could draw the reasonable distribution of the targeted values. However, this study reach is influenced by section control from the weir at the low flow and is influenced by channel control from the whole channel at the high flow. Thus it is very difficult to reflect in the proposed method with the form of simple rating curve. As a solution, we maintain the distribution of the particles and introduce the smoothing to consider the joint probability to estimate Manning's n and the index and the coefficient of an artificial rating curve, which are appropriate for the whole time series water stage.

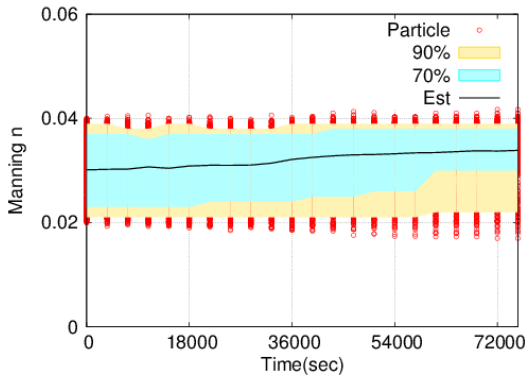

Figure 6-9 Estimated Manning's *n* at main channel.

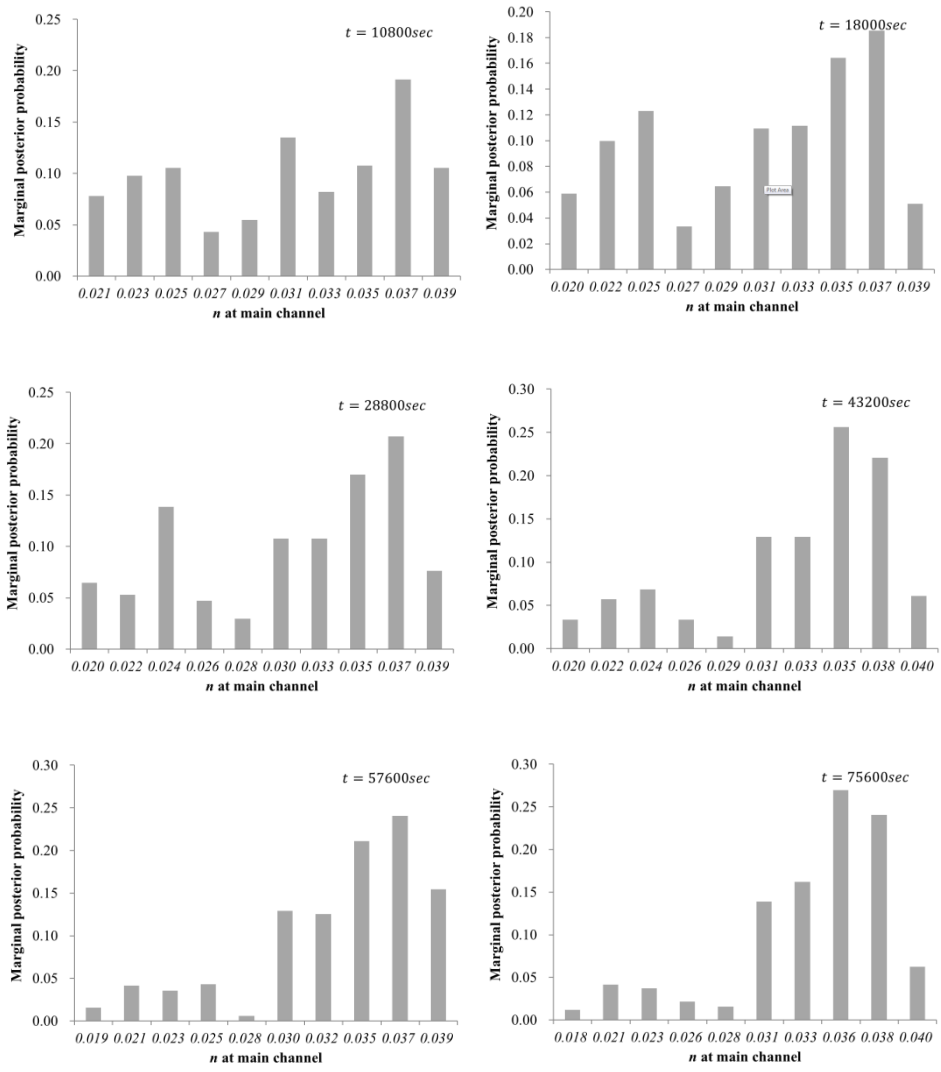

Figure 6-10 Change of distribution of Manning's *n* at main channel

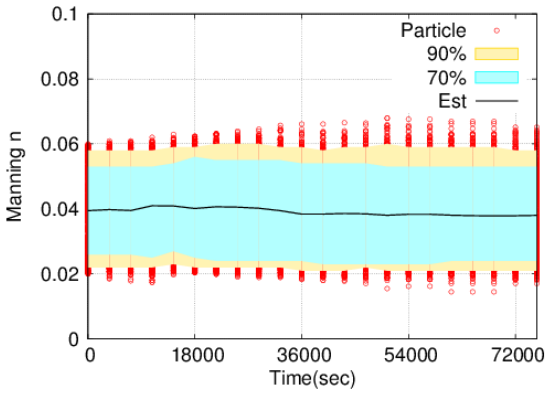

Figure 6-11 Estimated Manning's *n* at floodplain.

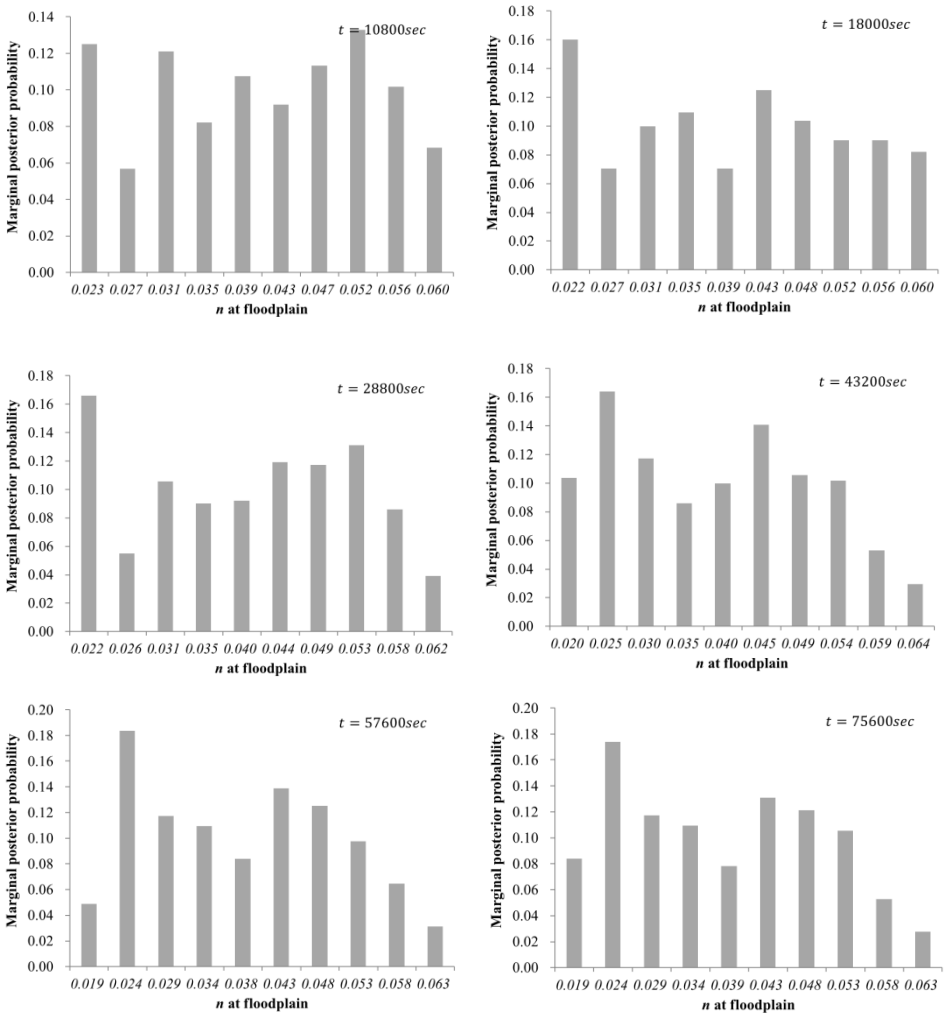

Figure 6-12 Change of distribution of Manning's *n* at floodplain

6.3.3 Results of trajectory tracking and smoothing

Original purpose of particle filters is to approximate the distribution of particle. Then particle smoothing is introduced for the estimation of the Manning's n and the index and the coefficient of a rating curve from the approximated distribution from the results of particle filters. The estimated values are able to be utilized for the practical use such as a design of the river management plan.

Although from Chapter 3 to Chapter 5, the river geomorphology is so simple that the estimated values with small variance can be utilized for practical use, the river geomorphology of the study area in Chapter 6 is so complex that only the approximated distribution of the particle can be obtained with the large variance because the river flow is governed by channel control or/and section control. To estimate them from the filtering results, two methods are able to be utilized. One is the sequential applications of the method as shown in Chapter 5. Then another is considering the whole time history to estimate the optimized values from the filtering results.

In this section, the whole time history is considered by introducing a smoothing density. Manning's *n* at floodplain and main channel and the index and the coefficient of the rating curve are estimated using particle smoothing, as shown in the section 6.2.2, based on trajectory tracking in the reverse time direction. Fig. 6-13 shows the results of trajectory tracking for 32 particles, which is selected by the systematic resampling at the last time step, in reverse time direction at the left side, and the estimated result considering the joint probability for the whole time history, smoothing density, at the right side.

The trajectories of 10 particles among the tracked 32 particles are plotted to check the movement of the particles more apparently at the left side of Fig. 6-13. The graphs at left side show the trajectories of the index of the artificial rating curve, the coefficient of the artificial rating curve, Manning's n at the main channel, and Manning's n at the floodplain in an order, respectively. As shown in the graphs, several particles are merged with other particles because the whole time history is considered in the reverse

time direction. In addition, the coefficient of the artificial rating curve is not disturbed so much, so the movement of the particle is limited because of small noise of the particle in comparison with the targeted values. Then in the third and fourth graph, the pattern is similar with the approximate distributions as shown in Fig. 6.11 and 6.12, so it shows that the trajectories can represent the distribution.

Based on the tracked trajectories and smoothing density, the figures at right side of Fig. 6-3 are plotted. In the figures, 'Smoothing' marked by a red line indicates the values considering the smoothing density, 'Filtering' marked by a blue line indicates the values estimated from the particle filters. Then 'Reverse' marked by a black line means that the values estimated from the smoothing density until current time step from the last time step of the simulation. At all figures at the right side of Fig. 6.13, the results of 'Smoothing' show the most consistent pattern for the whole time series, so it can be utilized for the practical use in establishing a simple rating curve in section 6.4. Then through the time varied pattern of 'Reverse', it is necessary to consider the multi-segment rating curve to represent the complex effect of channel geomorphology and river flow.

In addition, through the particle smoothing, the targeted values are determined. The index for the whole time series by smoothing is estimated by about 1.67, and its standard deviation is determined by about 0.17. Then, the coefficient is estimated by 228.92, and the standard deviation is determined by 32.98. They are utilized for establishing a rating curve at the next section. Next, the smoothed Manning's n for the main channel and the floodplain are 0.032 and 0.042, respectively. Finally, their standard deviations are determined by 0.0049 and 0.012, respectively.

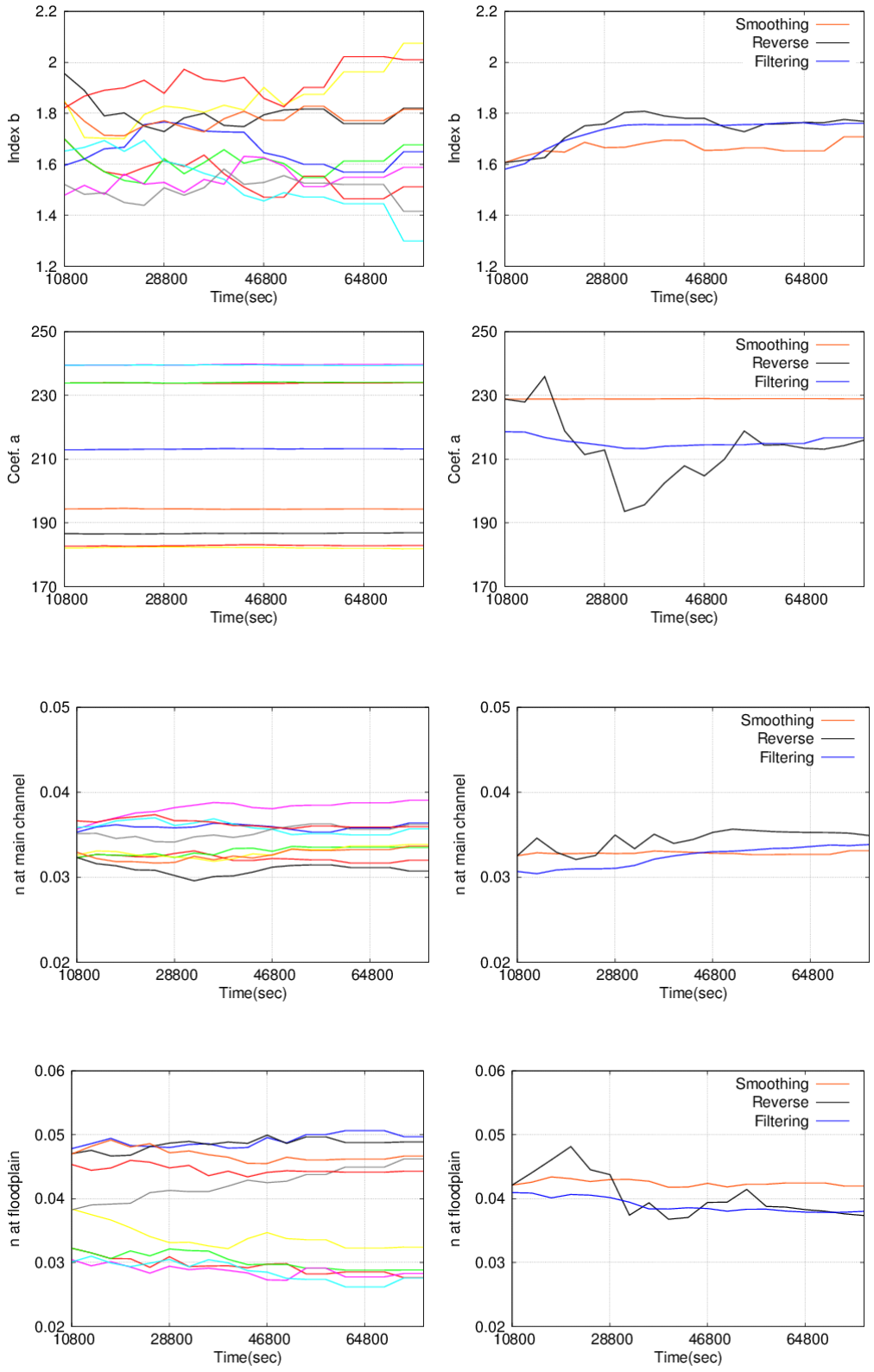

Figure 6-13 32 realizations of particle by trajectory tracking and smoothed values.

6.4 Establishment of rating curve based on filtering and smoothing

According to simulation, a rating curve is established as shown in Fig. 6-14. The black points indicate the observed discharge at the gauging station, upstream end of the river reach. Then the red points are the resampled particles at the filtering step. To establish the rating curve, the mean and the standard deviation of the index and the coefficient obtained from the particle smoothing is utilized. The distribution of the coefficient and the index is similar to the normal distribution as shown in Reitan and Petersen-Øverleir(2008). Thus the uncertain range of the rating curve is plotted by the line using the index and coefficient as $\mu - 2\sigma,\ \mu - \sigma, \mu,\ \mu + \sigma,\ \mu + 2\sigma$, respectively. $\mu \pm 2\sigma$ line is plotted by a broken line, and $\mu \pm \sigma$ line is plotted by a dotted line in Fig. 6-14. In addition, the black line is plotted by the μ of the coefficient and the index. The maximum absolute percentile error of the black line is 24% and the almost observed discharge data is within the black dotted lines. Moreover, the resampled particles are mainly located within the black dotted line, so we confirmed the simulations are implemented within the reasonable range.

Although the rating curve is not exactly matched with the observed values, we could provide the reasonable range of the discharge corresponding to the water stage without the discharge measurements.

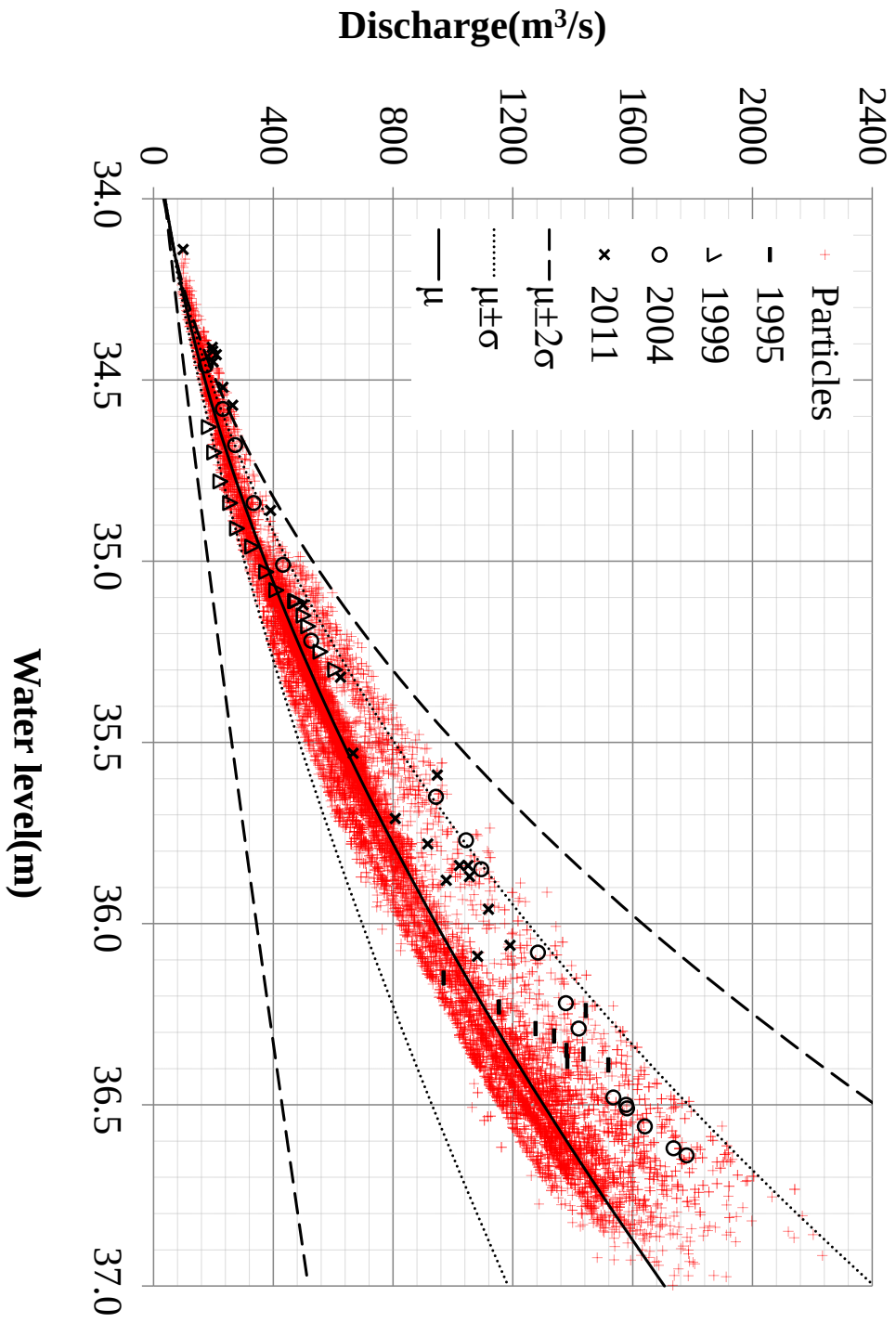

Figure 6-14 Established rating curve

6.5 Summary

The method to estimate the inflow without measuring discharge considering the uncertain characteristics of river channel is proposed. To estimate the uncertain characteristics of river channel and unknown inflow, particle filters are introduced into 2D dynamic wave model. The method is applied to complex geomorphology influenced by channel control or/and section control according to the water level. Thus to avoid the convergence to abnormal values due to the complex geomorphology, generic particle filters are introduced among the various particle filters. First, the distributions of particles are approximated by the particle filters, and the particle smoothing is implemented to estimate the Manning's n and the index and coefficient of the artificial rating curve. Using the index and the coefficient, the rating curve is established. The observed discharges are located within the estimated $\mu \pm \sigma$ line, and the resampled particles are mainly located within the range. Although the method does not use the measured discharge in establishing the rating curve, we could generate the reference discharge within a reasonable range of the rating curve.

Chapter 7. Concluding remarks

The findings from these experiments suggest that the stochastic approaches to a 2D dynamic wave model may improve the uncertain characteristics of the river channel. The point mass representations in particle filters make it possible to consider all feasible conditions together. Then the achievements of this thesis are as below:

1) Development of the stochastic approach to a 2D dynamic wave model to estimate inflow and the Manning roughness coefficient simultaneously.

2) Establishment of the alternative to construct and to improve a rating curve at certain cross sections within river's reach.

3) Construction of the basis to improve the hydrologic parameters and to enhance the water stage predictability.

Although the update of the water stage at upstream is generally utilized to enhance the estimation capability of discharge or Manning roughness coefficient in a hydraulic simulation, both of them are rarely considered together. Moreover, the applicable river reach was extremely limited, but it is also improved in this thesis.

In chapter 3, stochastic approaches are introduced to the 2D dynamic wave model to incorporate errors to consider the uncertainties of inflow and Manning roughness coefficient. As a stochastic approach, particle filters are utilized to deal with non-linear and non-Gaussian problems. In addition, the point mass representations in particle filters make it possible to consider all feasible conditions together. First, the proposed method is verified with the synthetic experiment to prevent unexpected exogenous disturbances. The estimated inflow and Manning roughness coefficient show good agreements with the artificial true value generated in the synthetic experiment. The availability as a water stage prediction model for a real event is checked. The estimated inflow show consistency with the observed discharge, but the gap between the predicted

water stage and observed value becomes lager according to the increase in leading time. Although the method showed good estimation capability, the consideration of Manning roughness coefficient as an uniform value limit the water stage predictability. In addition, the large variation of Manning's *n* in tracking the Manning's *n* changed according to the change of water depth induce the large variation in estimated water stage and upstream inflow.

In chapter 4, the two problems in chapter 3 are improved, and the availability to other events of the estimated inflow and Manning roughness coefficient from the proposed method is confirmed. One is the consideration of Manning roughness coefficient by a unique value all over the calculation domain. It degrades the predictability of water stage. As an alternative, the spatial distribution of Manning roughness coefficient is considered, and it is classified by the aerial photo. Another problem is large variation of the Manning roughness coefficient to track the Manning's n changed according to the water level. It induced too many uncertainties in the estimated water level and discharge. Thus a variation reduction factor is considered together with considering the spatial distribution of Manning's *n*. Then equifinality problems, which were induced by the combination of the Manning's *n* and the inflow in the resampling step, were solved by considering the variance reduction factor and the correction factor, an adequate number of particles and proper classification of the study area.

The proposed method was verified through an observed water stage and discharge data set. The proposed method enables the estimation of the inflow and the Manning's *n* simultaneously. Using the provided results from the method, the relationship between the water stage and the discharge at the water stage station can be constructed. The modified rating curve and Manning's *n* of each separated zone obtained from the proposed method was applied to another event to confirm the reproducibility. Through these verifications and application of the method, we confirm that it is a feasible alternative to the traditional method, in which the Manning's *n* estimated empirically

and the discharge converted from an existing curve are utilized.

In chapter 5, an estimation method using a 2D dynamic wave model and particles filters is introduced to estimate the discharge of the event occurring in September, 2011. Before estimating the discharge of the event, the uncertainties of the channel roughness for the main channel, flood plain, and inundation area are quantified by the sequential application of the method. With the quantified channel roughness, inflow to the upper boundary is also estimated from distributed hydrological model outputs. The discharge of the largest event is estimated by considering the uncertainties of roughness coefficients and upper boundary inflows. For the verification of the peak discharge, the highest water level of each particle is compared with flood marks. By the comparison with the flood marks, the peak discharge is estimated in the range from 22500m^3/s to 25500m^3/s. In addition, the rating curve established from the estimation process is compared to the currently updated rating curve.

In chapter 6, the method to estimate the inflow without measuring discharge considering the uncertain characteristics of river channel is proposed. To estimate the uncertain characteristics of river channel and unknown inflow, 2D dynamic wave model and particle filters are introduced. The method is applied to complex geomorphology influenced by channel control or section control according to the water level. To avoid the convergence to abnormal values due to the complex geomorphology, generic particle filters are introduced among the various particle filters. To estimate the reasonable inflow and Manning roughness coefficient from the results approximated by the particle filters, smoothing is implemented based on trajectory tracking in reverse time direction. Through smoothing, the index of the artificial rating curve and channel roughness was estimated. Using the index and the coefficient, the rating curve is established. The observed discharges are located within the estimated uncertain range, and the resampled particles are mainly located within the uncertain range. Although the method does not use the measured discharge in establishing the rating curve, we could provide the reasonable discharge within certain range by the rating curve.

Bibliography

ARDC, 2002. *ADRC 20th Century Asian Natural Disasters Data Book,* s.l.: Asian Disaster Reduction Center.

Aricò, C., Nasello, C. and Tucciarelli, T., 2009. Using unsteady-state water level data to estimate channel roughness and discharge hydrograph. *Adv. Wat. Res.*, Volume 32, pp. 1223-1240.

Arulampalam, M., Maskell, S., Gordon, N. and Clapp, T., 2002. A tutorial on particle filters for online nonlinear/non-Gaussian Bayesian tracking. *IEEE Transactions on Signal Processing*, 50(2), p. 174–188.

Barnes, H. H., 1967. *Roughness characteristics of natural channels,* Washington, DC: US Government Printing Office.

Barton, R. R., 2012. *Tutorial: Input uncertainty in outout analysis.*. In Simulation Conference (WSC), Proceedings of the 2012 Winter, IEEE.

Bentley, I. M., 1900. The synthetic experiment. *The American Journal of Psychology*, 11(3), pp. 405-425.

Boiten, W., 2000. *Hydrometry, IHE Delft lecture note series.* Rotterdam, Netherlands: A.A.Balkema.

Braca, G., 2008. *Stage-discharge relationships in open channels: Practices and problems,* s.l.: Università di Trento. Dipartimento di ingegneria civile e ambientale..

Bradely, P. C. N. G. P. N. a. D. S., 1992. A Monte Carlo Approach to Nonnormal and Nonlinear State-Space Modeling. *Journal of the American Statistical Association*, Volume 87, pp. 493-500.

Chow, V., 1959. *Open channel hydraulics.* New York: McGraw-Hill.

Coon, W. F., 1998. Estimation of roughness coefficients for natural stream channels with vegetated banks. In: *Water Supply Paper 2441*. s.l.:U.S. Geological Survey, pp. 1-133.

Crissman, R. et al., 1994. Uncertainties in Flow Modeling and Forecasting for Niagara River. *American Society of Civil Engineers Journal of Hydraulic Engineering*, Volume 119, p. 1231–1250.

DEFRA/EA, 2003. *Reducing Uncertainty in River Flood Conveyance, Roughness Review, R and D Technical Report to DEFRA / Environment Agency,* United Kingdom: HR Wallingford Ltd..

Di Baldassarre, G. and Montanari, A., 2009. Uncertainty in river discharge observations: a quantitative analysis. *Hydrol. Earth Syst. Sci.,* Volume 13, pp. 913-921.

Ding, Y., Jia, Y. and Wang, S., 2006. Identification of Manning's roughness coefficients in shallow water flows. *Journal of Hydraulic Engineering,* 130(6), pp. 501-510.

Domeneghetti, A. C. A. a. B. A., 2012. Assessing rating-curve uncertainty and its effects on hydraulic model calibration. *Hydrol. Earth Syst. Sci.,* Volume 16, pp. 1191-1202.

Dottori, F., Martina, M. L. V. and Todini, E., 2009. dynamic rating curve approach to indirect discharge measurement. *Hydrol. Earth Syst. Sci.,* 13(6), pp. 847-863.

Doucet, A., Godsill, S. and Andrieu, C., 2000. On sequential Monte Carlo sampling methods for Bayesian filtering. *Statist., Comput.,* 10(3), pp. 197-208.

Doucet, A. and Johansen, A. M., 2009. A tutorial on particle filtering and smoothing: Fifteen years later. *Handbook of Nonlinear Filtering,* Volume 12, pp. 656-704.

Fread, D., 1989. *Flood routing models and the Manning n.* Charlottesville, B.C. Yen, ed., pp. 699-708.

Giustarini, L. et al., 2011. Assimilating SAR-derived water level data into a hydraulic model: a case study. *Hydrol. Earth Syst. Sci.,* Volume 15, pp. 2349-2365.

Godsill, S. J., Doucet, A. and West, M., 2004. Monte Carlo smoothing for nonlinear time series. *Journal of the American Statistical Association,* 99(465), pp. 156-168.

Godsill, S. J., Doucet, A. and West, M., 2004. Monte Carlo smoothing for nonlinear time series. *Journal of the American Statistical Association,* 99(465).

Gonzalez-Castro, J. A. and Yen, B., 2000. *Applicability of the Hydraulic Performance Graph for Unsteady Flow Routing (HES 64),* s.l.: Univ. of Illinois at Urbana-Cahpaign.

Henderson, F. M., 1966. *open channel flow.* s.l.:Macmillan.

Hosoda, T. et al., 2010. Some considerations on computational method of flood flow without both upstream and downstream boundary conditions. *Annual Journal of*

Hydraulic Engineering, Volume 54, pp. 1159-1164.

Hosoda, T., Onda, S., Iwata, M. and Jacimovic, N., 2008. *Extension of flood flow simulation without upstream and downstream boundary conditions.* Cesme-Izmir, Turkey, In the Proceedings of the Int. Conference on Fluvial Hydraulics, pp. 655-659.

Hsu, M., Fu, J. and and Liu, W., 2006. Dynamic routing model with real time roughness updating for flood forecasting. *Journal of Hydraulic Engineering,* Volume 132, pp. 605-619.

Jones, B., 1916. *A method of correcting river discharge for a changing stage,* s.l.: US Government Printing Office.

Jones, B. E., 1915. *A method of correcting river discharge for a changing,* s.l.: U.S. Geological Survey Water Supply Paper,375-E.

Kim, S., 2006. *Stochastic real time flood forecasting using weather radar and a distributed hydrologic model,* PhD. dissertation: University of Kyoto at Engineering.

Kim, W., Kim, Y. and Woo, H., 1995. Estimation of channel roughness coefficients in the Han River using unsteady flow model. *Journal of Korea Water Resources Association,* 28(6), pp. 133-146.

Kim, Y. et al., 2012(a). Short term prediction of water level and discharge using 2D dynamic wave model with particle filters. *J Jpn Soc Civ Eng,* 68(4), pp. I_25-I_30.

Kim, Y. et al., 2013. Estimating the 2011 largest flood discharge at the Kumano river using a 2D dynamic wave model and particle filters. *J Jpn Soc Civ Eng,* 69(4), pp. I_163-I_168.

Kim, Y. et al., 2012(b). Simultaneous estimation of inflow and channel roughness using 2D hydraulic model and particle filters. *Journal of Flood Risk Management.*

Kitagawa, G., 1996. Non-Gaussian State-Space Modeling of Nonstationary Time Series. *Journal of the American Statistical Association,* Volume 82, pp. 1032-1063.

Le Coz, J., 2011. *A literature review of methods for estimating the uncertainty associated with stage-discharge relations,* s.l.: WMO report PO6a.

Lee, G., 2008. *Assessment of prediction uncertainty due to various sources involved in rainfall-runoff modeling,* PhD. dissertation: University of Kyoto at Engineering.

Mason, R. R. and Weiger, B. A., 1995. *Stream Gaging and Flood Forecasting : A Partnership of the U.S. Geological Survey and the National Weather Service,* s.l.: U.S. Dept. of the Interior, U.S. Geological Survey : National Oceanic and Atmospheric Administration, U.S. Dept. of Commerce.

Matgen, P. et al., 2010. Towards the sequential assimilation of SAR-derived water stages into hydraulic models using the particle filter: proof of concept. *Hydrol. Earth Syst. Sci.,* Volume 14, pp. 1773-1785.

Maybeck, P. S., 1982. *Stochastic models, estimation, and control.* s.l.:Academic press.

Meno, T. et al., 2012. *Analysus of the Kumano river flood by the Typhoon 12, 2011*. s.l., Proc. of the 67th Annual Conference of the JSCE.

Montanari, M. et al., 2009. Calibration and sequential updating of a coupled hydrologic model using remote sensing-derived water stage. *Hydrol. Earth Syst. Sci.,* Volume 13, pp. 367-380.

Moradkhani, H., Hsu, K. L. and Sorooshian, S., 2005. Uncertainty assessment of hydrologic model states and parameters: Sequential data assimilation using the particle filter. *Water Resour. Res.,* Volume 41, p. W05012.

Nagata, T., 2002. Hydraulics formulae: Hydraulics worked examples with CD-ROM. In: s.l.:Hydraulic committee,JSCE, pp. 16-19.

Nezu, I. and Nakagawa, H., 1993. *Turbulence in open channel flows.* IAHR Monograph ed. Rotterdam: Balkema.

Noh, S. J., 2012. *Sequential Monte Carlo methods for probabilistic forecasts and uncertainties assessment in hydrologic modeling,* PhD. dissertation: University of Kyoto at Engineering.

NRC, 1999. *Global Environmental Change: Research Pathways for the Next Decade,* Washington: The National Academies Press.

Onda, S., Hosoda, T., Uchida, T. and Jacimovic, N., 2006. Numerical simulation of unsteady flood flows with unknown boundary conditions. *Proc. of the 7th international conf. Hydroinformatics,* Volume 3, pp. 1619-1626.

Pelletier, M. P., 1987. Uncertainties in the determination of river discharge: a literature

review. *Can. J. Civ. Eng.*, Volume 15, p. 834–850.

Petersen-Øverleir, A., 2004. Accounting for heteroscedasticity in rating curve estimates. *Journal of Hydrology*, 292(1), pp. 173-181.

Petersen-Øverleir, A., 2005. *A hydraulics perspective on the power-law stage-discharge rating curve.* s.l.:Norges vassdrags-og energidirektorat.

Rantz, S., 1982. *Measurement and computation of streamflow: Volume 2. Computation of discharge, water supply paper 2175,* s.l.: U.S. Geological Survey.

Reitan, T. and Petersen-Øverleir, A., 2008. Bayesian Power-law Regression with a Location Parameter, with Applications for Construction of Discharge Rating Curves. *Stochastic Environmental Research and Risk Assessment,* 22(3), pp. 351-365.

Reitan, T. and Petersen-Øverleir, A., 2009. Bayesian Methods for Estimating Multi-segment Discharge Rating Curves. *Stochastic Environmental Research and Risk Assessment,* 23(5), pp. 627-642.

Reitan, T. and Petersen-Øverleir, A., 2011. ynamic Rating Curve Assessment in Unstable Rivers Using Ornstein-Uhlenbeck processes. *Water Resources Research,* Volume 47, p. W02524.

Rekleitis, I., 2004. *A Particle Filter Tutorial for Mobile Robot Localization. Technical Report TR-CIM-04-02*, Montreal, Quebec,Canada: Centre for Intelligent Machines, McGill University.

Rekleitis, I. M., 2004. *A Particle Filter Tutorial for Mobile Robot Localization. Technical Report TR-CIM-04-02*, Montreal, Quebec, Canada: Centre for Intelligent Machines, McGill University.

Ricci, S. et al., 2011. Correction of upstream flow and hydraulic state with data assimilation in the context of flood forecasting. *Hydrology and Earth System Sciences,* Volume 15, p. 3555–3575.

Ristic, B., Arulampalam, S. and and Gordon, N., 2004. *Beyond the Kalman Filter: Particle filters for tracking applications.* s.l.:Artech House.

Salamon, P. and Feyen, L., 2010. Disentangling uncertainties in distributed hydrological modelling using multiplicative error models and sequential data assimilation. *Water*

Resour. Res., 46(12).

Schaffranek, R. W., Baltzer, R. A. and Goldberg, D. E., 1981. *A model for simulation of flow in singular and interconnected channels,* s.l.: US Government Printing Office.

Schmidt, A. R., 2002. *Analysis of stage-discharge relations for open-channel flows and their associated uncertainties,* PhD Thesis: University of Illinois at Urbana-Champaign.

Shiiba, M., Laurenson, X. and and Tachikawa, Y., 2000. Real-time stage and discharge estimation by a stochastic-dynamic flood routing model. *Hydrological Process,* Volume 14, pp. 481-495.

Smith, P. J., Beven, K. and Tawn, J. A., 2008. Detection of structural inadequacy in process‐based hydrological models: A particle‐filtering approach. *Water resources research,* 44(1), p. W01410.

Tachikawa, Y. et al., 2011. Development of a real-time rivers stage forecasting method using particle filter. *Annual Journal of Hydraulic Engineering, JSCE,* Volume 55, pp. 511-516.

Thirel, G. et al., 2010(a). A past discharges assimilation system for ensemble streamflow forecasts over France–Part 1: Description and validation of the assimilation system. *Hydrol. Earth Syst. Sci.*, Volume 14, pp. 1623-1637.

Thirel, G. et al., 2010(b). A past discharge assimilation system for ensemble streamflow forecasts over France–Part 2: Impact on the ensemble streamflow forecasts. *Hydrol. Earth Syst. Sci.*, Volume 14, pp. 1639-1653.

Tillaart, S., 2010. *Influence of uncertainties in discharge determination on the parameter estimation and performance of a HBV model in Meuse sub basins,* Master dissertation: University of Twente.

Vrugt, J. A. et al., 2008. Treatment of input uncertainty in hydrologic modeling: Doing hydrology backward with Markov chain Monte Carlo simulation. *Water Resources Research,* 44(12).

WMO, 2010a. *Mannual on stream gauging: Vol. 1, fieldwork,* s.l.: WMO.

WMO, 2010b. *Mannual on stream gauging: Vol. 2, computation of discharge,* s.l.:

WMO.